Processing and characterisation of electrospun nanofibrous membranes : influence of polymer Rheology , structuration of fiber network and its mechanical properties

Khula Ganhi Jahsim Aljaber

UNIVERSITÉ GRENOBLE ALPES

THESIS

To obtain the degree of

DOCTOR OF UNIVERSITY OF GRENOBLE ALPES

Specialty : **2MGE : matériaux, mécanique, génie civil, électrochimie**

Arrêté ministériel : 25 mai 2016

Presented by

Khawla KANI JASIM AL JABER

Thesis directed by **Frédéric BOSSARD**

Prepared in the **Laboratoire Rhéologie et Procédés**
In the Doctoral School Ingénierie-Matériaux, Mécanique, Energétique, Environnement, Procédés, Production **I-MEP²**

Processing and Characterisation of electrospun nanofibrous membranes: influence of polymer Rheology, structuration of fiber network and its mechanical properties.

Thesis defended publically on **21.06.2017**

In front of the esteemed jury comprised of:

M. Benjamin NOTTELET McF HDR à l'IBMM, Université de Montpellier	Reviewer
M.Guy SCHLATTER Pr.à l'ICPEES, Université de Strasbourg	Reviewer
Mme. Nadia El KISSI DR CNRS au LRP, Université Grenoble Alpes	Examiner
M. Frédéric BOSSARD Pr. au LRP Université Grenoble Alpes	Director

TABLE OF CONTENTS

CHAPTER III Part 2: Mechanical Properties of Electrospun Membranes

This thesis work is dedicated to

My husband Razzaq, and all my beloved family memberes, who have been constant encouragement and support during on the course of this thesis.

AKNOWLEDGEMENTS

I would like to thank (Allah) for the strength and hope that allowed me to complete this thesis through one of the most challenging and interesting times in my life.

I vividly remember the day I received the news of the acceptance of PhD scholarship from higher education in Iraq and still recall all the mixed feelings; the joy of stretching out my wings and the sorrow of leaving loved ones behind.

Today, I am all again filled with emotions; the excitement of accomplishment and the bliss of contentment. Iam certainly blessed to be surrounded by mentors, supervisors, supporters, friends and family who enlightened my educational development towards growth path and disclosed new horizons ahead. I am grateful and in depth with them all, specially:

Prof. Frederic Bossard, my PhD main supervisor for giving me a great opportunity to work under his day to day guidance and support. Besides the advice, valuable suggestion and encouragement, he provides me a great and wonderful scientific research experience on the topic.

I would like to thank my jury committee: **Prof. Guy Schlatter** and **McF HDR Benjamin Nottelet** for approving my PhD work, and together with **Dr.Nadia El Kissi** and my supervisor: **Prof. Frédéric Bossard** for acknowledging me a degree of Doctor of University of Grenoble. France.

This dissertation could not have been completed without a kind support of **Iraqi Government**. I am gratefully to forward my gratitude to the **Government of Iraq** for the financial support and to have this great opportunity to study and to accomplish my research work in France.

My heartfelt thanks to my home-laboratory Rheologie et Procedes and its present director **Dr.Nadia el Kissi**, for welcoming me in their facilities. I would also extend my special thanks to the researchers, engineers, and technicians for their contribution to this work, their assistance and helpful instructions. **Hélène Galliard, Rachel Martin, Frédéric Hugenell, Didier Blésès, Mohamed Karrouch, Éric Faivre, Sylvie Garofalo, Francois Bergerot, Louise Infuso.**

I have created bonds with my fellow lab members in the Rheologie et Procedes lab that I will never forget. It is rare to find a group that fit so well, I truly consider myself blessed to have had the opportunity to work with all of them. My heartfelt thanks to my close friends:

Dr.louiza Achab, Dr.Solomon Mengistu Lemma, Dr.Gabriel Landazuri.

I am grateful to all of my colleagues at Rheologie et Procedes lab in France specifically **Dr.Abdulgadir Ahmed, Hanan Ali, Amara Amar&Ferial, Candice Rey, Alexis Mauray, Dr.Carhel Dassi , Dr.Fiacre Ahongui Dr.Noriyuki Isobé, Ayoub Barchouchi , William Chevremont , Dr. Chourouk Mathlouthi, Moctar Gueye , Gary Massoni , B.Ouattara, Dr. Nabil Ali , Hugues Mondesert, Essa Ahmed , Ahlem Romdhane , Sihem Ben Haj, Dr.Monika Bravo, Dr. Anica Lancuski, Dr Benjamin Vuillemey, Dr. Maxime Rosello, Dr.Etienne Ghiringhelli, Dr.N. Malladi , Dr. Fanny Rasschaert, Dr. J. Patarin.**

Thank you to all the professors in Al-Muthanna University and my friends in Iraq that have supported and encouraged me: **Dr.Moslem Abed Mohammed Alkadier, Dr.Zaman Sahb Mehdi, Dr.Yassir Dakheel Kremsh ALAsadiy, M.Mohamed jaber Farhan, Dr.Neran Ali Thamer, Dr.Sukaina Hussein Kadhim , Mme.Hala Hassan, Miss.Raqqiat Kazim Nasir, Dr.Noorance Al-Mukaram, Dr.Ibtehaj Raheem Ali, Dr.Maysaa ALhar.**

I would also like to thank my family in Iraq- **my beloved parents, my brothers and sisters** for their eternal caring, supporting, loving and praying me during my PhD study. **Razzaq**, my love, husband, best friend, and encourager, who his charm made it possible throughout the tough times. Thank you so much for your love, support and understanding to keep me on the accomplishment of this research.

Abbreviations

AFD*– Average Beads Connecter Fiber Diameter

AFD – Average Fiber Diameter

AFM – Atomic Force Microscopy

ASTM – American Society Testing and Materials

CTA – cellulose triacetate

DCM – dichloromethane

DNA – deoxyribonucleic acid

DMF – N, N-dimethylformamide

DSC – differential scanning calorimetry

DTAB – dodecyl (trimethylammonium bromide)

FDA – Food and Drug Administration

FDD – fiber diameter Distribution

FEG – Field Effect Canon

HFP– hexa (fluoropropylene)

HMS – Houwink–Mark–Sakurada equation

Mw – weight-average molecular weight

Me_{soln} – entanglement molecular weight

Me_{melt} – entanglement molecular weight melt

MEK – methyl (ethyl ketone)

NaCl – Sodium chloride

NaH2PO4 – Sodium dihydrogen phosphate

NGP– nerve growth precursor

PAA – poly (acrylic acid)

PAH – poly (allyl amine hydrochloride)

PAN – poly (acrylonitrile)

PCL – poly (ε-caprolactone)

PDO – Poly (dyoxanone)

PEO – poly (ethylene oxide)

PHBV – poly (b-hydroxybutyrate-co-hydroxyvalerate)

PLA – poly (lactic acid)

PLAGA – poly (lactide acid-co-glycolide acid)

PLLA – poly (L-lactic acid)

PLGA – poly (D, L-lactide-co-glycolide)

PVA – poly (vinyl alcohol)

PVDF– poly (vinylidene fluoride)

PVP– poly (vinylpyrrolidone)

PVC– poly (vinyl chloride)

PMMA – poly (methyl methacrylate)

PGA – poly (glycolic acid)

PU – polyurethane

PS – polystyrene

PSBMA – poly (sulfobetainemethacrylate)

PTT– Poly (trimethylene terephthalate)

SEM – scanning electron microscope

SiO_2 – Silicon dioxide

TBAC – tetra (butyl ammonium chloride)

TCD – distance between the needle tip and collector

TEM– transmission electron microscopy

THF – tetrahydrofuran

LiCl – Lithium chloride

V2O5 –Vanadium pentoxide

WXRD – wideX-ray diffraction

KH2PO4 – Potassium dihydrogen phosphate

Introduction

Introduction

Electrospinning is technique that use to spinning polymers solution electrically for production of nano-scale fibers and beads. The working principle of electrospinning is based on the stretching of spray polymer solution induced by electrical charges to produce fibers diameter ranging from a few tens of nanometers to micrometers[1]. This techniques has attracted great interest because of its unique capability to produce material having high surface area to volume ratio and nonwoven fibrous structures[2]. As dated back in the beginning of the 20th century, Preciselyin 1902, the use of electrospinning started and documented[3]. In the course of the 1990s, the process of electrospinning was well reused for manufacturing fibrous structures[2]Subsequently, the last two decades researches have been done a lot for the improvement of both the technique and characteristics of produced structures. The advancement of characteristics of structures, small size pores, and easy to used making electrospinning is a good candidate for the production of nanomaterials in wide range of applications[4-7]. These produced micro/ nanofibers can be used in a variety of purposes such as wound dressings, filtration, drug delivery, protective clothing for the military, scaffolds for tissue engineering and drug delivery devices, in nano composites, sensors, magneto-responsive fibers, and super hydrophobic membranes[7-13]. In recent years, some industrial companies started to use electrospinning to produce structured nanofibrous materials for tissue engineering. These nano structured matrices were obtained using various polymers such as polylactic acid, polyurethane, silk, collagen, and cellulose[14].

However, the technique can be highly affected by solution properties and processing parameters to produce beads, beaded fibers and free fibers[15]. Optimizing these parameters allows to obtain different morphological arrangement of fibers specifically bead free structures. In addition, the polymers intrinsic properties and environmental factors also determine the electrospun fibers morphology for specific intended applications.

The solution properties are one of the influencing factors to produce electrospun nanofibrous structures[16, 17]. Among from solution properties, concentration and rheology are the most dominant parameters in electrospinning. These solution properties are also related with molecular characteristics of the polymer such as molear weight, polydispersity, degree of branching and types solvents[15, 16]. In the electrospinning, these molecular properties play a vital role in determining fiber initiation and stabilization. Several investigators have tried to establish the optimum ranges for concentration and molecular weight in order to insure stable fiber formation[15-19]. The viscosity of a polymer solution is generally known to increase with

polymer molecular weight tends to increase electrospun fiber diameters[20, 21]. High viscosity solutions have greater resistance to the electric field-induced drawing force as the solution emerges from the spinneret. Additionally, higher viscosity solutions undergo less bending instabilities before contacting the collector surface, thus reducing the distance and time under which the drawing (elongation) force acts[21]. Additionally, the effect of viscosity is more fundamentally associated with the presence (or absence) of the polymer chain entanglement network in the solution[16, 17, 22]. Entanglements in a solution or melt occur as a result of physical interlocking of two or more chains due to overlapping[16]. Initially, at low polymer concentrations, the jet tends to break up entanglement into small droplets due to the effect of surface tension, which tends to minimize the surface area of the solution[16]. This cause to form beads instead of fibers. The critical amount of chain entanglements offer high resistance to the jet break up consequently instability is subdued. This results in continuous fibers formation. In the contrary, when the entanglements are present, but the extent of chain overlap is below the critical value and also the instability is not completely eliminated. This leads to the formation of fibers with beaded morphologies[16, 17]. In addition to these, solution viscosity has been found to influence fiber diameter[20], initiating droplet shape, formation of Tylor cone and the jet trajectory[23]. Solution surface tension and electrostatic forces have also synergetic effect on the structure and morphology of the final product. In general, the development of bead free fiberous structure for different applications requires a thorough knowledge of controlling the dominant affecting parameters of the electrospinning process and their effect on fiber diameters, morphology and properties of electrospun nanofibers.

This PhD thesis study was carried out using electrospinning as a main focus of the title. Typically, the study aimed at the development of poly (ethylene oxide) PEO architectural membranes by electrospinning. In addition to this main goal, the study addressed the control of the morphology of the networks obtained by using microstructure collectors. Further, the rheological properties of the polymer in solution under elongational flow were characterized, as well as the morphological analyses of the membranes were also investigated using scanning electron microscopy (SEM) and their mechanical properties.

Structure of the thesis:

Chapter one discusses the relevant information on the introduction of electrospinning, production and its significance affecting parameters together with detail review of electrospinning process and its applications. Chapter two present the materials methods used, and detail production and characterization techniques performed in the production of PEO nanofibrous structures. Chapter three, part I: describes the results concerning the effect of parameters that govern the electrospinning of investigation of the effect of variation of the governing parameters on the electrospinning of PEO. In addition, this chapter examined the influence of viscosity, concentration, porosity, and surface tension of PEO solutions on the obtained fibers. Chapter three, part II: explains the influence of the morphology of the fiber network on the mechanical properties of scaffolds and their biomimetic character that could favor the colonization and growth of the cells of the host tissue. The control of this structure has been achieved through the development of collectors. Finally, chapter four summarized the general conclusions of this work.

CHAPTER I

Literature Review

I- Literature Review

1.1Nanofibers

In general, the definition of nano is one millionth ($1/10^6$) of a millimeter or 10^{-9} meter. When the term is applied to technology, nanotechnology, the common definition is the precise manipulation of individual atoms and molecules. For the polymeric nanofibers the smallest practical size is approximately 50 nm as a polyester crystallite has dimensions in the order of 40 nm so structures approaching this size would begin to become an ordered array of atoms and would not have typical fiber morphology[24]. Similar to the nature's design, polymeric nanofibers and their composites can provide fundamental building blocks for the construction of devices and structures. Drug delivery systems, scaffolds for tissue engineering; wires, capacitors, transistors and diodes for information technology; systems for energy transport; conversion and storage such as batteries and fuel cells, and structural composites for aerospace applications are expected to be impacted by the development of nanofibers[25].

Polymeric nanofibers can be produced by an electrospinning process. Electrospinning is a process that spins fibers of diameters ranging from 10 nm to several hundred nanometers. This method has been known since 1934 when the first patent on electrospinning was filed. Fiber properties depend on the electric field properties, polymer viscosity and TCD (distance between the needle tip and collector)[26]. Scanning electron microscopy (SEM) allows us to explore the structure and morphology of electrospun nanofibers.

1.2 Nanofibers Formation Techniques

A variety of techniques can be used for creating polymeric Nanofibers such as drawing[27], template synthesis[28], self-assembly[29], phase separation[30], electro blowing, centrifugal and electrospinning[31]. A Brief description of each processing technique is presented in this chapter.

1.2.1 Centrifugal Spinning Technique

Centrifugal spinning method is similar to the cotton-candy spinning method. In a cotton candy machine, sugars are melted by heating and extruded by centrifugal spinning through nozzles, resulting in sucrose fibers randomly distributed in the free space near the spinneret. Recently, the fabricated sucrose fibers have been used as a mold for porous polymer forming[32]. This process has been patented by Huang in 2007[33]. Centrifugal production method is quite similar to centrifugal electrospinning. But, in this method no electrical charge is used. Instead, it consists of dropping of a polymer solution onto a typical spin coater followed by a very fast rotating spinneret. Moreover, the spinning procedure offers many technologically relevant opportunities, such as yielding hollow polymer beads, and being applicable to different types of polymers[34].

Recently, a company named Fiberio has improved a new technique called Forcespinning TM (Figure I.1) for the production of nanofiber. Forcespinning TM is applicable for solutions and molten materials via centrifugal force. Because Forcespinning TM uses less solvent or no solvent at all, it is more productive in terms of cost when compared to electrospinning. No heated air jets or no heating make it more cost effective than melt blown[35]. A spinneret with a reservoir containing liquid material is rotated centrifugally on an axis at high rpm. While the spinneret rotates, liquid material is pushed to the outer wall through an orifice. In this process, centrifugal and hydrostatic forces together initiate the jet[35].

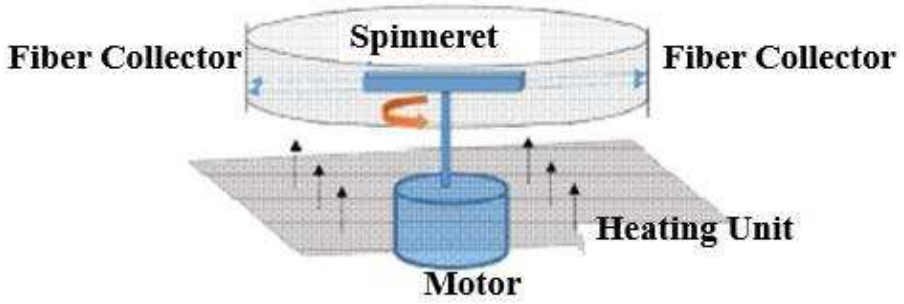

Figure I.1: Forcespinning TM[35]

1.2.2 Self-Assembly

The molecular self-assembly techniques are inspired by the natural driving force of bio macromolecules to form functional structures in living beings. Bio macromolecules such as proteins can arrange themselves into different configurations through non-covalent bonding such as hydrogen bonding, van der Waals and hydrophobic interactions. Control of the chemistry behind the natural arrangement of bio macromolecular has resulted in the formation of nanofibers[33]. For example, residues of peptides have been chemically modified to produce nanofibers with a hydrophobic interior and hydrophilic exterior having a diameter of 5 to 8 nm[36].

Advantages and disadvantages of the different techniques to produce ultrafine fibers are taken into account for selection purposes. Although drawing is the simplest approach for forming long fibers, it has a low throughput since fibers are produced one at a time. Template synthesis, which needs a nanoporous membrane to form fibrils, cannot produce single continuous long nanofibers. The phase separation and self-assembly techniques could be applied to create nanofibers, but the preparation time is longer than the other methods[33].

1.2.3 Fiber Drawing Technique

The drawing technique provides simple and cost effective photonic wire manufacturing. But a steady temperature distribution is needed in the drawing zone and the lengths of the fabricated wires are limited to tens of millimeters. PTT nanofibers with diameters down to 60 nm and lengths up to 500 mm can be fabricated by the drawing process, as described in (Figure I.2). PTT is retracted at a speed of 0.1–1 m/s. The extended PTT wire is quickly cooled in air and finally an unclad amorphous PTT nanofiber is created[37]. Fibers fabricated by this technique not only show low optical losses but also offer good flexibility[38].

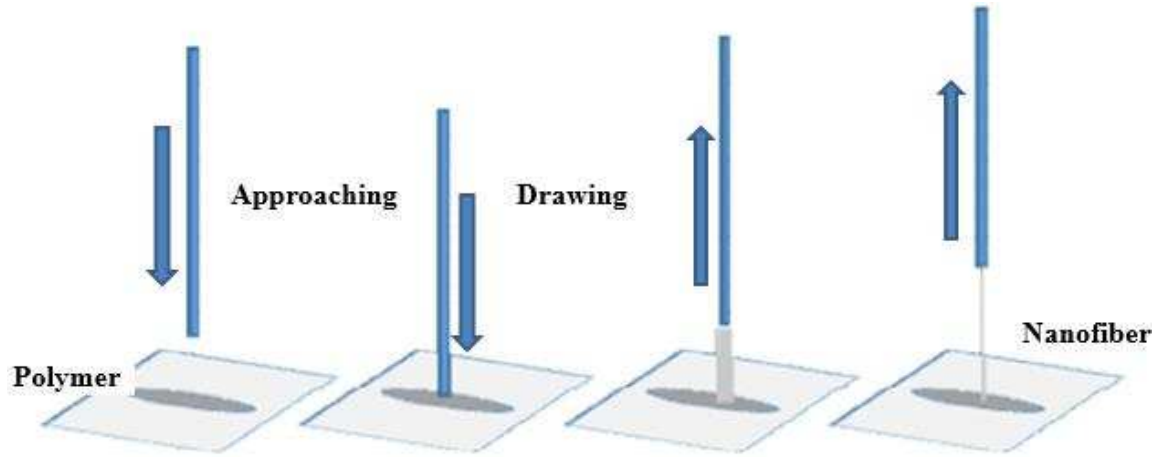

Figure I.2: Drawing process

Ondarçuhu and Joachim[39] described a nano-fiber drawing technique from a micro droplet or a micro-pipette of a polymer solution in a continuous manner over precisely defined period of time. Each fiber is pulled at the threshold of solidification. When they used long polymer chains entangled in the solution, fibers with micron diameters could be obtained. When shorter unentangled molecules are used, sub micron fibers are collected. Even though generating nano-sized fibers, this process is strongly limited by the size of the droplet as well as by the time of solvent evaporation.

1.2.4 Template Synthesis

Template synthesis is a method for preparing nanostructures (nanotubes or nanowires) by directly synthesizing a desired material within the pores of a porous template-membrane[40]. Common membranes, used for template synthesis, include anodic aluminium oxide and mesoporous silica. Depending of the type of the membrane, pores could be inter-connected or isolated. When anodic alumina membranes are used, solid material is formed inside the isolated pores[41, 42]. In the case of mesoporous silica template, nanowires or nanotubes are inter - connected by the porous silica wall. Sol-gel chemistry,[43, 44] electrochemistry[45]or in-situ polymerization[46] methods could be used for depositing a material inside the pores of such membranes. Finally, nano-fibrils or nano-tubules are formed within each pore of a membrane.

Template synthesis generates aligned fibers with well-defined fiber's size and interfibrous distance. However, this technique strongly depends on the size of the template adopted. Nevertheless, by carefully choosing the template and polymer for molding, various

materials ‘architectures could be easily attained, serving as a sensitive gravimetric apparatus for detecting ammonia gas or as biodegradable extracellular matrices[47].

1.2.5 Phase Separation Technique

In phase separation, a polymer is firstly mixed with a solvent before undergoing gelation. The main mechanism in this process is (as the name suggests) the separation of phases due to physical incompatibility. One of the phases which is the solvent is extracted resulting in leaving behind the other remaining phase[31]. In other words, the process can be described subsequently as: dissolution of polymer, liquid-liquid phase separation, polymer gelation, extraction of solvent from gel and quenching, respectively[48].

1.2.6 Electrospinning Technique

The manufacturing process of electrospinning was first reported by Formhals[26] in 1934, the experimental setup and procedure of which has been explained in the sections to come. Since then, the process of electrospinning has caught the attention of many researchers and many reports, publications and patents in this field ascertain this. Gibson et al.[7] describes electrospinning as a process in which high voltage is used to produce an interconnected membrane like web of small fibers. This method provides the capacity to lace together many types of polymers, fibers, and particles to produce ultra-thin layers.

The principle of electrospinning is to use an electric field to draw a charged polymer solution from an orifice to a collector. This creates a jet of solution from the orifice to the grounded collection device. The jet emerges at the base from the nozzle, which has a geometry of a cone (Taylor cone, see Figure I.3). Then it travels and get stretched befor reaching the collector. However, splaying is a misnomer as researchers have observed a rapidly rotating spiral jet[49, 50], which is indistinguishable from splaying phenomenon to the naked eye. The fiber is eventually collected on a grounded metal screen.

In the electrospinning process, a high voltage is used to create an electrically charged jet of polymer solution or melt, which dries or solidifies to leave a polymer fiber[26, 51]. One electrode is placed into the spinning solution/melt and the other attached to a collector. Electric field is subjected to the end of a capillary tube that contains the polymer fluid held by its surface

tension. This induces a charge on the surface of the liquid. Mutual charge repulsion causes a force directly opposite to the surface tension[52]. As the intensity of the electric field is increased, the hemispherical surface of the fluid at the tip of the capillary tube elongates to form a conical shape known as the Taylor cone[53], see Figure I.3. With increasing field, a critical value is attained when the repulsive electrostatic force overcomes the surface tension and a charged jet of fluid is ejected from the tip of the Taylor cone. The name "Taylor Cone" simply represents the conical shape formed at the needle tip (see Figure I.3). This cone was described by Sir Geoffrey Ingram Taylor in 1964[53] as a continuation of the work of Zeleny in 1917[53] on the formation of a cone-jet of glycerine exposed to high electric fields. Several others continued researching this area, including Wilson & Taylor (1925), Nolan (1926), and Macky (1931)[53]. However, it was Taylor who looked further into the reactions between droplets and electric fields.

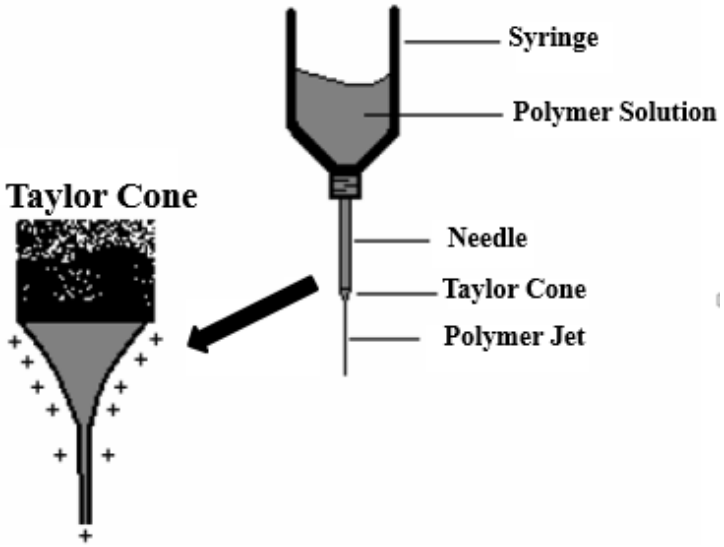

Figure I.3: Illustration of Taylor Cone formation from the Syringe Needle Tip

Taylor's derivation is based on two assumptions:

1. The surface of the cone is an equipotential surface.
2. The cone exists in a steady state equilibrium.

Once discharged and the Taylor cone activated, the polymer jet undergoes a whipping process[54] where in the solvent evaporates, leaving behind a charged polymer fiber, which lays itself randomly on a grounded collecting metal screen. In the case of the melt the discharged jet solidifies when it travels in the air and is collected on the grounded metal screen[53]. An example of our experimental set up used for electrospinning is shown in (Figure I.4).

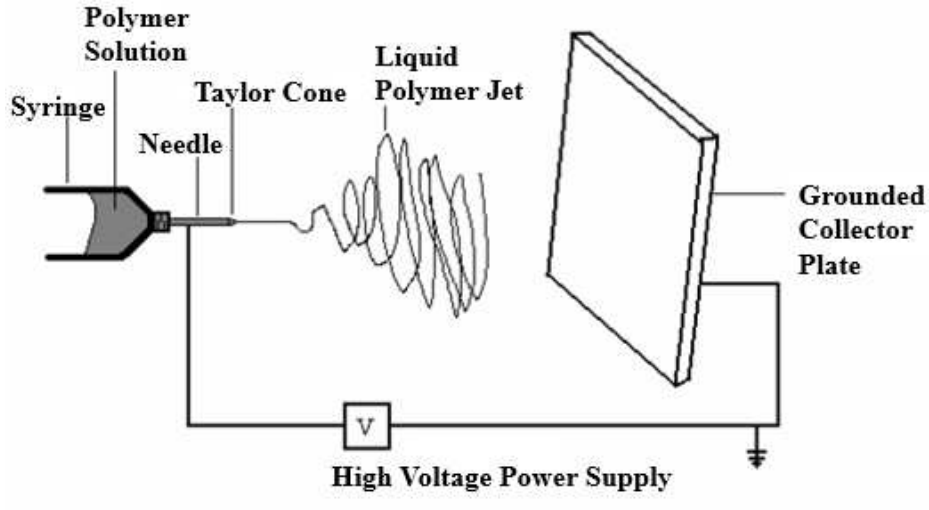

Figure I.4: General Electrospinning schematic

The polymer solution or melt is contained in a syringe. A metering pump attached to the plunger of the syringe generates a constant pressure and flow of the fluid through the pipette. The driving force is provided by a high voltage source that is attached to the needle. The high voltage source can generate up to 30 kV, and the setup can be run on either positive or negative polarity. Adjusting the flow of the fluid and the magnitude of the electric field controls the spinning rate. Using electrical forces alone, the electrospinning process can produce fibers with nanometer diameters. Because of their small diameters, electrospun fibers have larger surface-to-volume ratios, which enable them to absorb more liquids than do fibers having large diameters. The principle of electrospinning now being introduced, it is necessary to study the parameters that will influence this process and the morphology and diameter of the fibers.

1. 3 Parameters of the Electrospinning Process

Although most of the fibers that are produced through electrospinning are circular solid filaments, there are occasions when tubes, ribbons, coils, and beaded structures can be generated. There are a number of factors, which affect the production of electrospun fibers during the electrospinning process: (a) The polymer solution properties, such as viscosity, elasticity, conductivity, and surface tension; (b) The process parameters, such as the gap distance between the capillary tip and the collector, applied voltage, and hydrostatic pressure in the solution container; and (c) The Environmental effects, such as temperature, humidity, and air flow.

By using a suitable theoretical model of the electrospinning process, the effects of parameters on the fiber diameter can be evaluated. The models should indicate which parameters have the greatest influence on the fiber diameters. Hence, these parameters are the ones to focus on in the empirical studies[55].

The two major properties of the fibers are, on the one hand, the diameter and on the other hand, the presence of beads connected by fibers. These beads have an undesirable phenomenon for our application (Figure I.5).

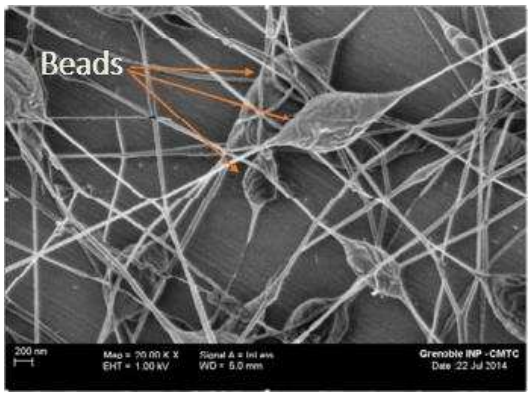

Figure I.5: SEM of poly (Ethylene Oxide) nanofibers Electrospum from aqueous solution 2.9% M_w: (1.0 x 10^6) g/mol

1.3.1 Solution Parameters:

A) Molar Weight of the Polymer and Viscosity of the Solution

This influence of viscosity is more fundamentally associated with the presence (or absence) of entangled network of polymer chain into the solution[16, 17, 22]. Entanglements in a solution or melt occur as a result of physical interlocking of two or more chains due to overlapping[16] Initially, at low solution concentrations, the jet tends to break up into small droplets due to the effect of surface tension, which tends to minimize the surface area of the solution. This phenomenon is known as Rayleigh instability[16]. Beads form primarily due to this break up. The critical amount of chain entanglements offer high resistance to the jet break up and the Rayleigh instability is subdued. This results in continuous fiber formation. If the entanglements are present, but the extent of chain overlap is below the critical value, Rayleigh instability is not completely eliminated. This leads to the formation of fibers with beaded morphologies[16, 17].

Shenoy et al.[16] performed a semi-empirical analysis to quantify the minimum requirement of the degree of chain entanglements that produced uniform bead-free nanofibers. They expressed the entanglement density in terms of the entanglement number '' defined as : $(\eta e)_{soln}=Mw/(M_e)_{soln}=\varphi_p Mw/(M_e)_{melt}$.

Whereas, Mw is the weight average molar weight of the polymer, φ_p is the volume fraction of the polymer in the solution, $(Me)_{soln}$ and $(Me)_{melt}$ are the entanglement molecular weights for solution and melt, respectively.

It has been shown by Bueche[56] that the onset of entanglements occurs at $(\eta e)_{soln} \sim 2$. However, Shenoy et al. showed that the fiber formation started at this value but the fibers possessed beaded morphologies[16].They demonstrated that the entanglement number of at least 3.5 was required in order to form fibers without beads for a number of polymer solvent systems [PS in THF; PLA in DMF, dichloromethane (DCM), chloroform, and 1, 1, 2, 2-tetrachloroethane; and PVP in ethanol] they used in their study. This is illustrated in Figure I.6 for the PLA solution in DMF or DCM for two different molecular weights as an example[16].

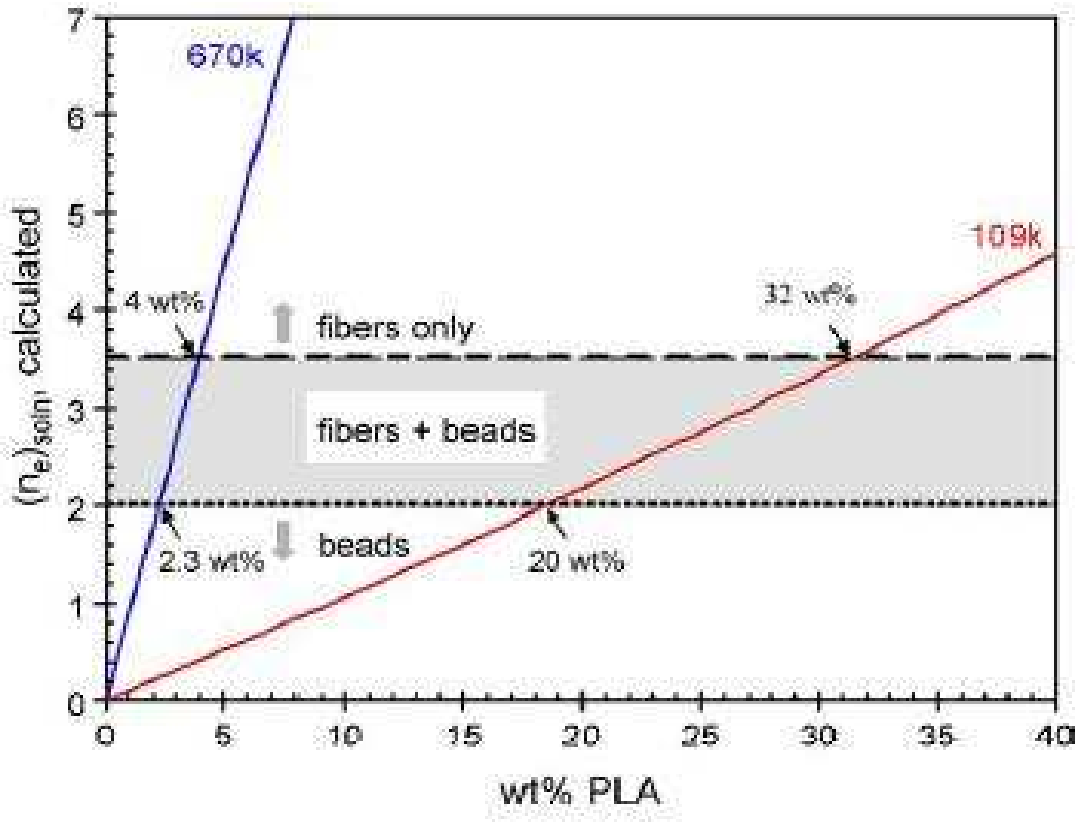

Figure I.6: Plot of calculated entanglement number versus solution concentration[16]

Shenoy et al.[16] further demonstrated that based on the entanglement number of 3.5, the required solution concentration to form uniform fibers can be calculated using the equation given above. This is shown in (Figure 1.6) for PLA spinning. The authors, however, indicated that the approach is valid only for the systems in which there is no specific polymer-polymer interaction, e.g., hydrogen bonding between polymer chains in polyamides.

If the viscosity of the polymer solution is too high, it is difficult for the polymer to traverse the needle and properly eject as a jet when an electric field is applied. The surface tension forces are too strong to be overcome by the electrostatic forces. Additionally, at a high viscosity, polymer solutions tend to exhibit longer stress relaxation times, which is suggested to prevent the fracturing of the jet during electrospinning, and create continuous fibers[57]. For the aforementioned reason, a low viscosity would reflect shorter stress relaxation times, and result in disturbances of the jet. These disturbances of the polymer jet will result in non-continuous fibers, as well as non-uniform fibers with "beads."

Aqueous solution from poly (vinyl alcohol) (PVA) with the same concentration, beaded fibers were obtained when electrospinning low molar weight (Mw 9000-10,000 g/mol) PVA, while uniform bead free fibers were obtained when electrospinning high molar weight (M_w 13,000-23,000 g/mol) PVA[58].

The elongational viscosity (not shear viscosity) is most frequently used to describe the rheological properties of the polymer solution/melt as it is more akin to the deformations being applied during fiber spinning[16]. Since electrospinning is analogous to conventional fiber spinning, the use of elongational viscosity is more appropriate than zero shear viscosity, and in fact, has been recently done by Feng[59]. However, both zero shear and elongational viscosities are a function of the number of chain entanglements (among other factors)[16]. Only under the influence of a shear stress or elongational flow, as is the case for electrospinning, does there exist a critical strain rate(greater than the disentanglement or reputation time), above which the entanglements or physical junctions act as mechanical effective junctions on short time scales (>τ_D(disentanglement time))[60].The shear mode measurements, however, in general are insufficient to shed light on the rheological behavior of the same non-Newtonian fluid in elongational flows. For example, a high elongational viscosity (formally identical to shear thickening) of a suspension can delay the capillary breakup of its thread and can therefore pose

a major challenge in applications relying on droplet generation of such suspensions, even though the latter exhibit shear thinning. Measurement of elongational properties of different Newtonian and non-Newtonian liquids can be made employing capillary self-thinning of liquid threads formed between two solid plates[61].The role of such fundamental fluid properties as shear viscosity and presence of entanglements in setting the morphology of the fibers produced in electrospinning has been discussed in the article of McKee et al.[17].

Solution viscosity is one of the most influential factors that affect the nanofiber formation. It is directly controlled by the molecular weight (fixed concentration) or the solution concentration (fixed molecular weight). Empirical evidence reported by number of authors indicates that by increasing the solution concentration, transitions occur from beads to beaded fibers to homogeneous fibers[62]. As an example, Fong et al. in one of the earlier studies showed that by varying the viscosity of polyethylene oxide (PEO) (MW: 9×10^5 g/mol) in water from 13 to 1250 cP by increasing the solution concentration from 1 to 4 wt%, transitions from beads to uniform nanofibers could be effectively achieved (Figure I.7).

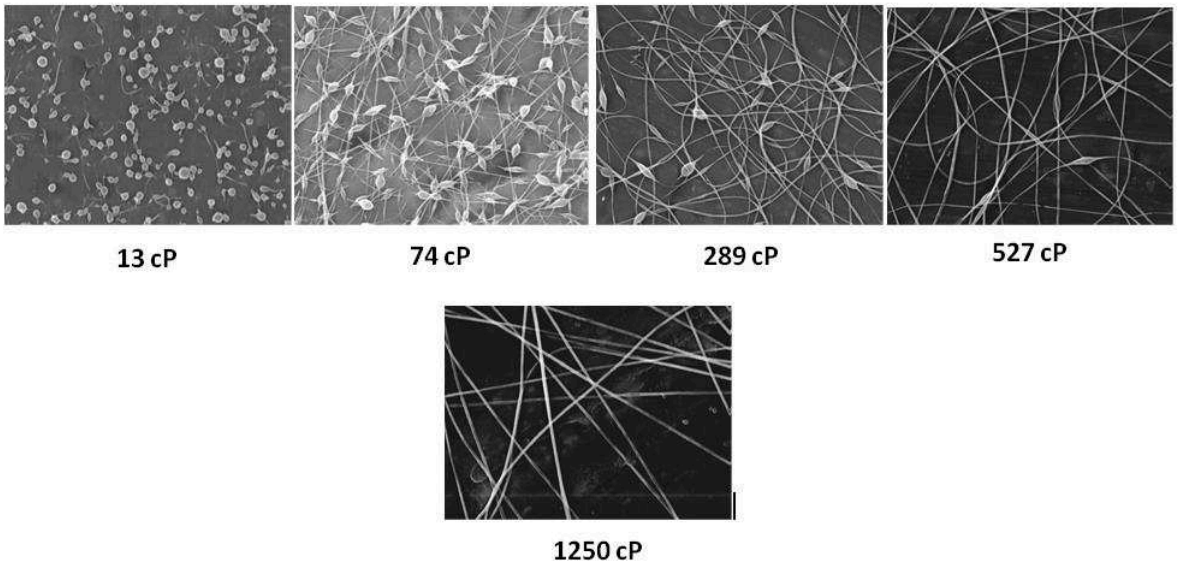

Figure I.7: Effect of solution viscosity on the fiber morphology[20]

Bolgen et al.[63] conducted a systematic study of deposition poly-ε-caprolactone (PCL) (Mw = 80000 g mol^{-1}) dissolved in chloroform / dimethylformamide (DMF) 30/70 volume ratio. By varying the concentration of PCL, they showed that from 13% by mass the fibers obtained do not contain little or more beads. Jointly, the diameter of the deposited fibers was measured and it shows that it increases with the concentration. This observation is supported for a large number of polymer[64]. Indeed, when a viscous solution is electrospinning; the viscoelastic

resistance of the solution is higher, so the charges will be more difficult to stretch the jet thereby producing larger diameter fibers.

Fong[20] recognized that higher polymer concentration resulted in fewer beads. At higher concentration, the bead diameter, if any, was larger. The shape of the beads changed from spherical to spindle like, when the polymer concentration varied from low to high levels. (Figure I.8)

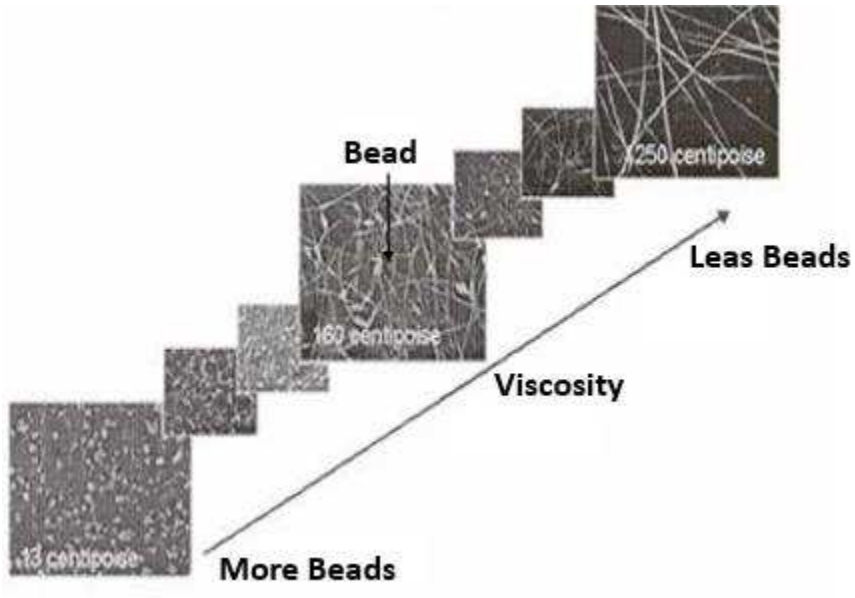

Figure I.8: SEM images of electrospun nanofibers with beads from different polymer concentration solutions[20]

B) Evaporation of Solvent

The evaporation rate of the solvent is primarily responsible for formation pore in the micro- or nano fibers. During the electrospinning, the solvent will evaporate as the flying jet accelerates toward the collector. If the most of the solvent evaporates before the jet reaches the surface of the collector, well defined fibers will be formed. However, if the solvent used has a high boiling temperature, its evaporation process might not be complete when the flying jet arrives to the collector, and instead of fibers, a thin polymer film would be collected[65].

Solvent evaporation rate plays an important role on fiber morphology. By using volatile solvent, porous fibers can be obtained. For example, Porous cellulose triacetate (CTA) fibers with circular shape pores in the range of 50–100 nm were electrospun from methylene chloride[66].The mechanism of pore formation during electrospinning is complicated. Phase

separation due to fast solvent evaporation may be responsible for the pore formation[67].During electrospinning; the volatile solvent evaporates fast, which causes original miscible polymer solution to separate into two phases: polymer-rich and solvent-rich phases. Once the fiber solidifies, the polymer-rich phase forms the fiber matrix while solvent-rich phase gives rise to the pores.

Bognitzki et al.[67] used highly volatile solvents to produce PLLA fibers and obtained electrospun fibers with pore sizes of 100 nm in width and 250 nm in length along the fiber axis. Lee et al.[68] studied the effect of volume ratio of the solvent on the fiber diameter and morphology of PVC fibers. They found that as the amount of DMF in the THF/DMF mixed solvent increased, the average fiber diameter decreased.

Vapor concentration of solvent and temperature affects evaporation and solidification of the jet[69]. Most investigations were carried out in an open atmosphere without controlling the vapor concentration of solvent. No systematic study was conducted on the influence of evaporation and solidification of the jet.

Evaporation and solidification affected the fiber diameter and morphology. Fiber diameter became smaller when evaporation and solidification happened more slowly because of the higher vapor concentration of solvent. For poly (ethylene oxide) in water, the linear decrease in the diameters of electrospum fibers with increasing humidity provides an effective process control parameter. Beaded fibers were formed when jet diameter was very thin and the charge per unit area was smaller. The size of the beads and the length of fibers between them changed systematically as the relative humidity increased[70].

Other physical and rheological parameters of the solution used can influence the fiber morphology as:

C) Surface tension

Surface tension of the polymer solution has been closely associated with its tendency to form beads or beaded fibers when all other parameters are unchanged[16, 71, 72]. This is because, when the jet forms from the solution, the surface tension tends to reduce the specific surface area of the jet by breaking it up into spherical droplets thus giving rise to the so called axisymmetric Rayleigh instability (Figure I.9)[16, 71]. This causes bead formation.

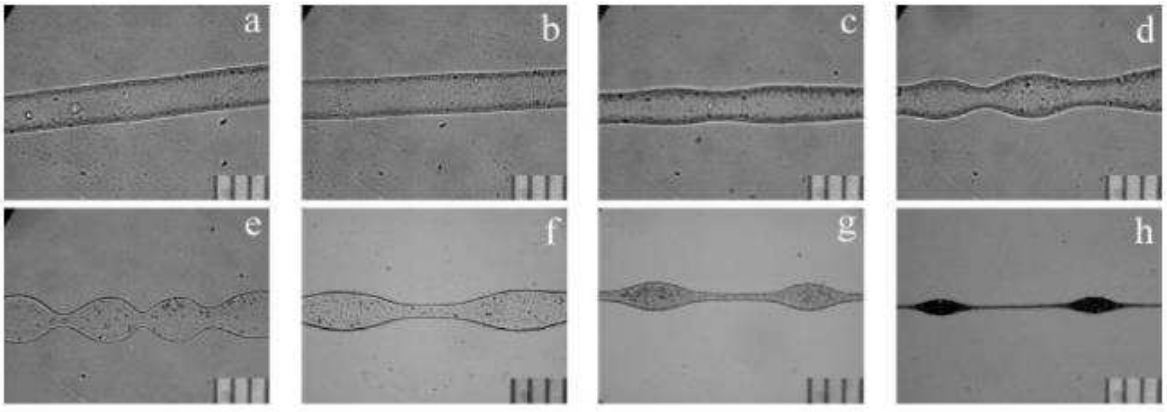

Figure I.9: Onset of axisymmetric instability causing bead formation in the fibers. The pictures taken at different distances from the needle. a. 1 cm, b. 3cm, c. 5cm, d. 7cm, e. 9cm,f. 12cm, g. 15cm, h. 30 cm

The surface tension of a polymer solution is a characteristic dependent majority of the solvent. This property of the solution plays a critical role in the process by electro statically spinning. Indeed, it is surpassing the component that opposes to the formation of charge jet, which distorts the drop of solution at the tip of the needle to permit spinning. Different solvents may contribute to the surface tension thereby facilitating spinning. In general, a high surface tension suppresses electrospinning process, causes instabilities in the solution jet and causes the appearance of beaded filaments. Conversely, a low surface tension of the solution of polymer allows spinning with a smaller electric field while limiting training "pearls" polymer in the nonwoven[(73)]. If you consider all the other constant spinning parameters, that is the surface tension, which determines the upper limits, and lower spin ability window[(74)].

The surface tension can be lowered by using a low surface tension solvent[(63)]or by the addition of surfactant[(75)]. For example, the addition of 40 g ethanol into 57 g water lowered the surface tension of PEO/water solution from 76 to 51 mN/m and fibers with fewer beads were obtained [(63)]. A high critical voltage was needed for electrospinning PVA/water solution since water had surface tension of 73 mN/m[(32)]. With the addition of a small amount of surfactant (Triton X-100) into water, the surface tension decreased, which lowered the critical voltage for electrospinning, and PVA fibers were subsequently obtained.

Zuo et al. observed that by increasing the surface tension of the solution while keeping all other parameters constant such as conductivity, applied voltage, and flow rate, the resultant fibers possessed beaded morphologies[(71)].Yao et al., on the other hand, used Triton X-100 nonionic

surfactant to reduce the surface tension of the PVA solution in water. They found that at least 0.3% v/w of surfactant was necessary to achieve complete fiber formation from aqueous PVA solutions[75].The actual value of the surface tension required, however, was not reported. Overall, although not quantified, it has been suggested in the literature that the surface tension of the solution should be as low as possible for optimum spinning.

1.3.2 Process Conditions

The processing parameters encompass the applied electric field, tip to collector distance, and flow rate or ejection rate of the polymer solution. By properly manipulating any of the parameters listed above, the morphology and fiber diameter of the electrospun fibers can be controlled.

A) Applied Voltage

In electrospinning, the applied electrical voltage affects the jet stability and the fiber morphology to a remarkable degree. In general, an increase in the applied voltage causes high deposition rate due to large amount of mass flow from the needle tip. For the polyethylene oxide-water system, it was observed that the fiber morphology changed from a defect free fiber at an electrical potential of 5.5 kV to a highly beaded structure at 9.0 kV[76].

Megelski et al.[64] determined the dependence of the fiber diameter of polystyrene fibers on voltage, and showed that the fiber size decreased more or less from 20 m to 10 m without a dramatic change in the pore size distribution when the voltage was increased from 5 kV to 12 kV.

Zuo et al. studied the effect of applied voltage on the bead formation[71]. They found that by increasing voltage as 10 to 20, and 26 kV, the bead size in the PHBV fibers reduced as 14 to 10, and 8 μm. A voltage of 30 kV produced completely bead-free fibers[71].

Deitzel et al., on the other hand, observed that higher voltage than that minimally required to obtain bead-free fibers caused bead formation in the fibers (Figure I.10)[76].The authors attributed this result to the change in the shape of the liquid surface at the needle tip, which reflected the mass imbalance due to higher voltage. This imbalance occurred as the solution

was removed at higher rate than that of the delivery. This introduced instability in the initial part of the jet, which correlated, with the beaded morphology in the fibers[76].

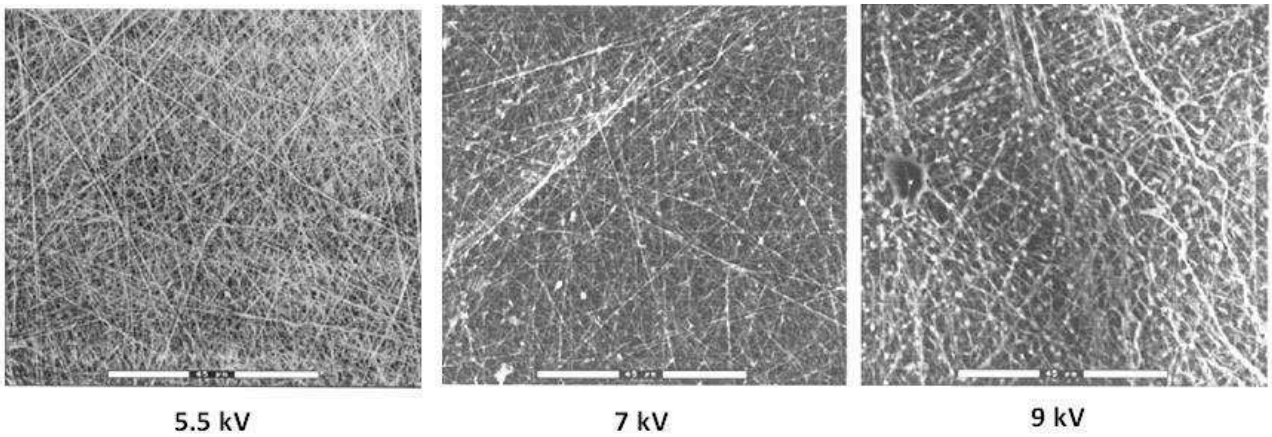

Figure I.10: Bead formation at higher voltage[76]

It was proven quite early in the history of contemporary spin that the shape of the initial drop depends on the process parameters, but today there are two different views on the role of the applied voltage. Reneker et al.[2] have shown in their research on the PEO that the electric field does not influence the diameter of the nanowires. Zhang et al.[74] have demonstrated that when the applied voltage is large, it ejects a larger amount of polymer solution, which has the effect of producing filaments of large diameter.

Other authors[64, 74, 50, 76, 77] have reported that the increase in spinning tension increases the repulsive electrostatic force to the jet of solution that contributes to shrinkage of the diameter of the filaments. In most cases reported in the literature, the authors report that a larger electric field, causes a greater stretching of the jet through more intense coulombic forces and therefore of the filaments of smaller diameter. In return for this reduction in diameter, the authors stress that the probability of formation of beaded filaments also increases with increasing electric field strength.

Jacobs et al. studied the effects of applied voltage on the morphology of electrospun fibers using a polyethylene oxide (PEO) solution[78]. The group noted that with a low applied voltage of 5kV, there would be an irregular formation of fibers, bead like structures, a thicker fiber diameter, and a proper Taylor cone would not form[78]. The same research group found that an applied voltage of 20 kV would decrease the fiber diameter and offer more uniformity throughout the electrospun fibers. When the voltage was increased to above 25 kV, the beads

that formed at 5 kV were present again[78]. With the increase in voltage to above 25 kV, the polymer solution droplet that would form at the end of the spinneret would recede completely. As a result the jet was initiated from within the capillary, without the formation of a Taylor cone. A similar observation was found by Larrondo et al., who also demonstrated that the fiber diameter would decrease by nearly half when the applied voltage was doubled[79]. Additionally, the group noticed that the aforementioned statement only held true up to a certain voltage, and that when the voltage was increased too high, there was a greater probability for large beads to form throughout the fibers.

Figure I.11 below shows the effect of tension applied to the form of the Taylor cone with a constant feed rate.

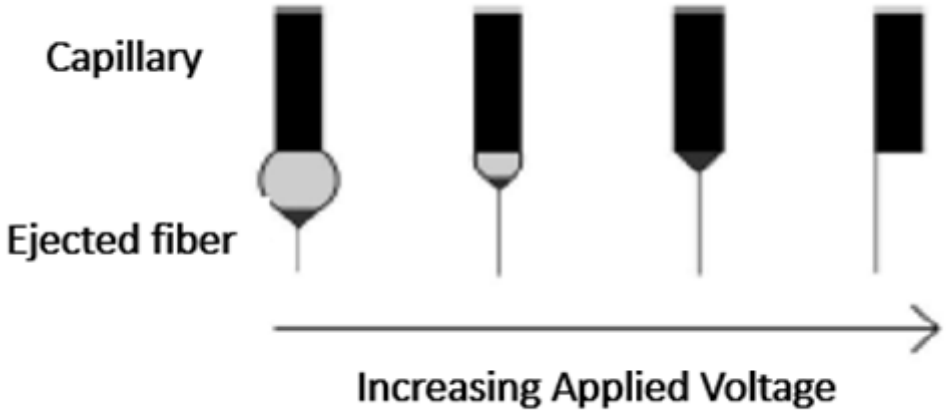

Figure I.11: Taylor cone according to the voltage to a constant flow of solution.

When the applied voltage is increased (left to right), the volume of Taylor cone decreases. If the voltage is further increased, without being offset by an increase in solution flow rate, the Taylor cone is missing which generates a jet of discontinuity leading to an increase in the number of beads in the non-woven membrane.

B) Solution Flow Rate

The flow rate or feed rate of the polymer solution from the syringe is a critical parameter that affects the jet velocity, Taylor Cone formation, and material transfer rate. It is important to strike a balance between the applied voltage and flow rate. Fundamentally, the applied voltage

is stretching or pulling the polymer solution toward the collector, while the syringe pump is ejecting the polymer solution toward the collector. Hence, it is important that an optimal balance is found so that a Taylor cone is formed and uniform fibers are produced. A lower feed rate is more desirable as the solvent will get enough time for evaporation, and result in a smaller and more consistent fiber diameter[80]. Wannatong et al. studied the effect of flow rate on electrospinning as well, and found that when the flow rate is too high, the fibers form large beads, as there was not enough time for the solvent to dry prior to reaching the collector[81].

C) Distance Collector /Needle

Another component to the electrospinning process is the gap distance – the distance the grounded collector is placed from the tip of the spinneret. The space between the two offers the solvent time to evaporate before the polymer becomes dry and aggregates on the collector. The influence this parameter has on fiber morphology is not as significant as the other parameters discussed above. Zhang et al. studied the effects of this parameter while electrospinning poly vinyl alcohol (PVA) and found no noticeable trends with the gap distance parameter[74]. However, it has been suggested that flatter fibers are produced at closer gap distances, and that at larger gap distances the fibers tend to be more rounded[82]. Moreover, as discussed earlier it is important to find an optimal gap distance that allows the solvent enough time to evaporate before the polymer reaches the collector.

The distance between the collector and the needle jet is related to the time of flight and strength resulting electrostatic. When the distance is small and the voltage is constant, the time flight is lower, the jet is less stretched and deposited fibers are larger diameters. However, the latter observation is based on the solution properties. Demir et al.[83] have shown that for a polyurethane-urea solution in DMF, increasing the distance of testimony or the decrease in the value of the field results in a decrease in the density of beads formed.

D) Temperature

Mit-Uppathameta1.have studied the effect of temperature on electrospinning of polyamide-6fibersin formic acid ranging from 25 to 60 ° C inside the spinning device, and discovered that an increase in temperature reduced the fiber diameter[21]. The group suggested that since there is an inverse relationship between temperature and viscosity, the increased

temperature would decrease the viscosity of the polymer solutions, and as a result lead to smaller fiber diameter sizes[84].

The authors observed that certain physical properties (viscosity, surface tension and conductivity) decrease with increasing temperature. They explain that the temperature rise reduces degree of entanglement between polymer chains thereby reducing the viscosity. The small reduction in viscosity is the factor that explains the decrease in diameter.

E) Humidity

The change in humidity is also an important environmental factor. In general, the spinning standard devices do not control humidity. Researchers also evaluated the impact of this parameter on the electrostatic spinning.

Casper et al. investigated the influence of the ambient parameter humidity on electrospun polystyrene solutions. The research group found that an increase in the humidity resulted in the appearance of small circular pores on the surface of the fibers, and that further increasing the humidity would lead to pores that would coalesce[84]. At allow humidity, the evaporation rate of the solvent would be faster, which could clog the spinneret within minutes. It is important to have an ambient humidity that will be conducive to the evaporation of the solvent as the polymer solution leaves the tip of the spinneret to the collector. Moreover, it is important to remain aware that the ambient parameters can also influence the electrospinning process.

Effect of humidity on the morphology of electrospun PS/THF fibers was studied. When humidity was less than 25 %, no pores were visible in the fibers. With increasing humidity level, the number of pores increased significantly and the pore size ranged from 50 to 280 nm.

Breath figure theory[85] was used to explain this phenomenon. Breath figures form when evaporative cooling occurs as a result of rapid solvent evaporation during jet travel. The jet surface cools down and the moisture from air condenses on the fiber surface. When the fiber dries, the water droplet regions form pores.

All of the parameters discussed in the sections above influence the final fabrication product, the electrospun fiber. Since there are so many variables that can affect the process, it is important to be mindful of each parameter and find a balance. Typically, through trial and error, many groups have succeeded in creating electrospum fibers that are consistent, uniform, and effectively enable cellular interactions for tissue engineering applications[57, 84, 86, 87, 88].

1.4 Different Types of Collectors

Although the morphology of the nanofibers can be controlled, to some extent, electrospinning can only lead to nonwovens arranged without order or structure. This random structure of filaments excluded conventional electrospinning for applications requiring structural organization. It was therefore necessary to obtain structures dimensional, two-dimensional fibers obtained by process. The following sections describe the different types of collector developed forget these new fiber architectures.

1.4.1 Static Collector

A) Conductive Pattern Manifold

The control of the jet during the electrospinning through the design of new electrodes may be used to make more arrangements complex. Figure I.12 shows different patterns to two collectors and photos SEM nanofibers electrospun.

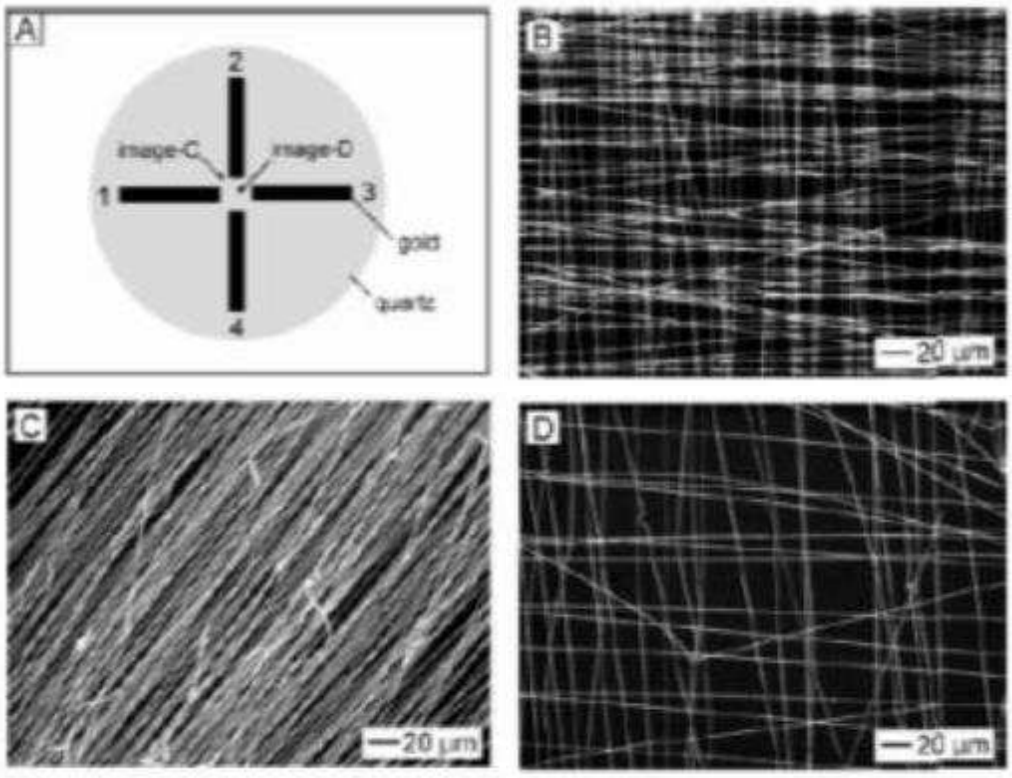

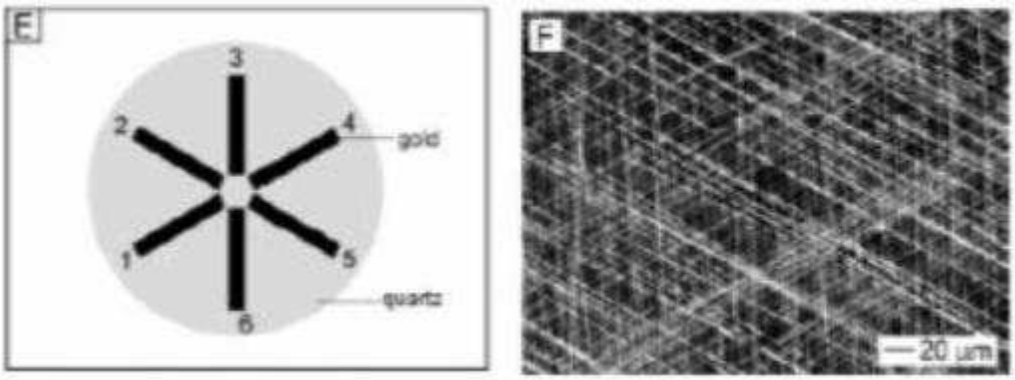

Figure I.12: Diagrams collectors patterned cross with 4 branches (A) and 6 branches (E) and SEM photos of nanofibers obtained in different zones (B, C, D and F)

By varying the position and on the electric field and different patterns of collectors, it is possible to obtain three-dimensional structures of filaments (3D) at 90° or at 60°, thus increasing the complexity of the materials and opening nanofibers other Applications[89].

B) Microstructure Collector

Recent research has used rapid prototyping engineering[89] to design and manufacture micro-structured collectors. A variety of models (sine, saw tooth, hexagonal ...) was manufactured with sizes (width and height) units ranging from 100 to 1000 microns. Subsequently, they examined the adhesion of fibroblast cell membranes of poly (D, L-lactide-co-glycolide) (PLGA), harvested on these manifolds. They found that the fiber distribution reflects the topography of the collector. Fiber diameters are uniform for the sinusoidal model and hexagonal. A small reduction in the diameter to the model saw too this observed between the top and the portion around it.

1.4.2 Cylindrical Collector

This is the most common elementary form after the non-woven random; it gives birth to a filamentary shape aligned. It was through a cylindrical rotating collector at a speed of several thousand revolutions per minute (r / min), it is possible to obtain a proper alignment of the nanofibers. Figure I.13 shows cylindrical collection device rotary used to obtain non-woven aligned with respect to each other.

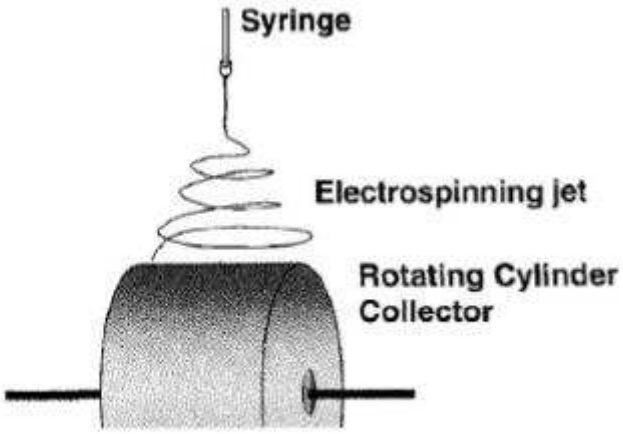

Figure I.13: Rotating cylindrical collector for the unidirectional aligned nanofibers in the direction of rotation

Boland et al., Using this technology, managed to produce filaments aligned glycolic acid poly (PGA)[90] (1000 r / min) and collagen[91] type I (4500 r / min). Figure I.15 Shows two SEM pictures of non-woven collagen (Figure I.14A) and PGA (Figure I.14B) aligned collected on a rotating cylindrical device.

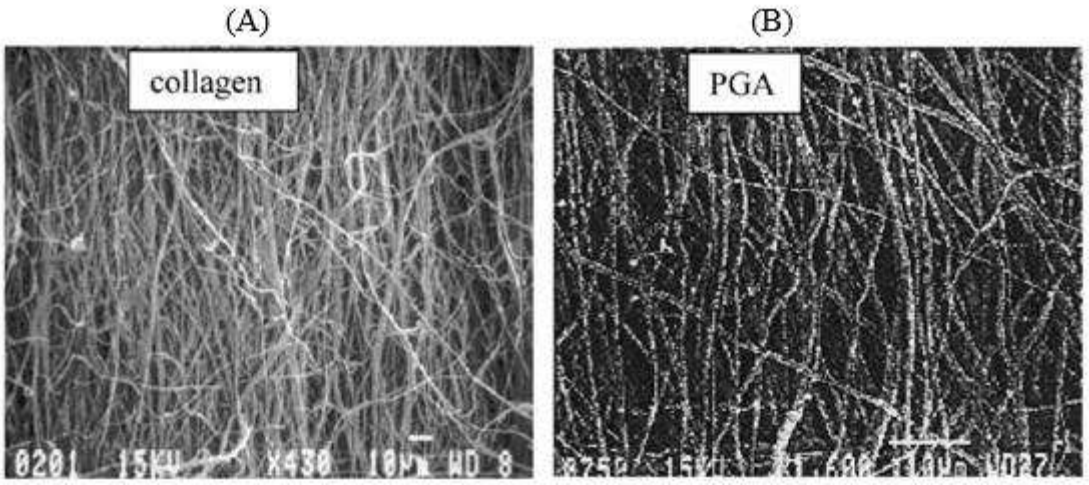

Figure I.14: Aligned nanowires collagen and PGA

Although a clear alignment of the fibers is obtained, the degree of alignment is not optimal because there are still a significant number of non-aligned fibers, which are collected. In electrospinning, the jet is traveling at a very high speed. Accordingly, to align the fibers around a mandrel, it is necessary that the mandrel rotate at a speed very high. Such speed can be called alignment speed. If the rotation of the mandrel is lower than the speed of alignment, the deposited fibers are randomly oriented.

1.4.3 Sharpened Collector

Using a sharpened rotary disk, it is also possible to orient the fields and the electrostatic coupling at a high rotational speed; it allows to obtain alignment of nanofibers [92]. Due to the concentration of the field lines towards the top of the disc, the jet will tend to follow the direction of the field lines converge and towards the blade disc. Permanent rotation of the disk causes the fibers along the blade by imposing an alignment.

Theron et al.[92] were among the first to align the fibers of PEO, using a sharpened rotary disk 15 cm in diameter and 0.5 mm thick. Due to concentration of the field lines toward the perimeter of the disk, the jet will tend to follow the direction of the field lines converge towards the periphery of the disc. The rotation Permanent disk causes the fibers along the perimeter by imposing an alignment. It has been shown that PEO nanofibers, having a diameter ranging from 100 to 400 nm with a spacing of 1 to 2 µm can be aligned on the circumference of the disc. Figure I.15 describes the device spinning using a rotary disk for manifold.

Zussman et al. used a tapering wheel-like disk as the grounding collector to generate aligned nanofibers[92]. Aligned fibers were found to be deposited on the sharpened edge of the wheel collector. These authors believe that the sharpened edge of the wheel could greatly increase the local electrical field strength so that the charged fibers were wound on the edge preferentially. It is also possible that the fibers were further arrayed by the repulsive interaction between these charged nanofibers.

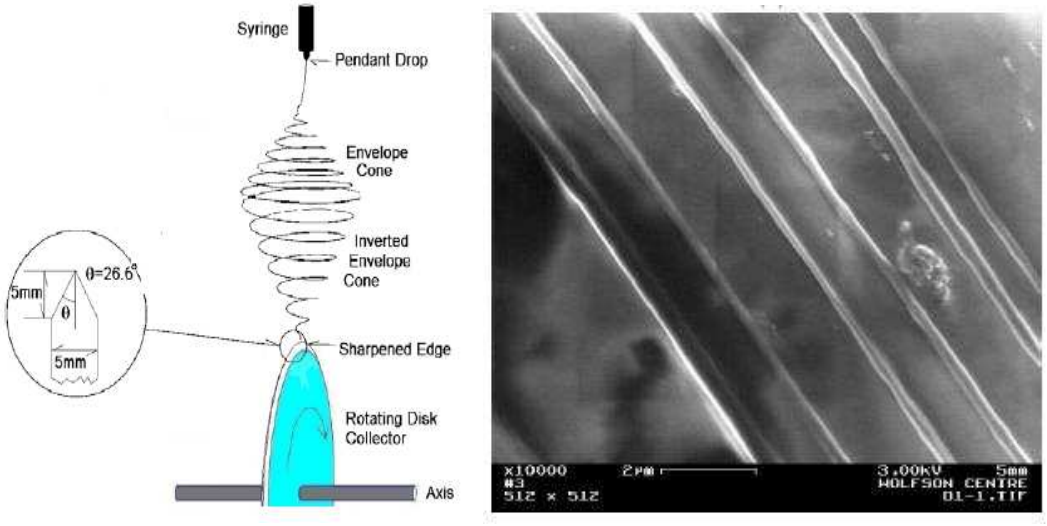

Figure I.15: Diagram of the rotary circular collector device and PEO filament obtained by this method

The right photo is a SEM photo of filaments aligned PEO obtained by this spinning method. The typical speed of the disk to get aligned fibers about 1000 RPM, equal to a linear velocity of 10.46 ms^{-1}. The use of a cylinder also possible to deposit aligned fibers[92]. A manifold cylindrical diameter of 4 cm, rotating at a speed equal to 2.6 ms^{-1}, allows obtaining a proper alignment of the nanofibers.

1.4.4 Slotted Collector, Parallel Collector

Previous methods described allow obtaining aligned fibers involving the use of a mechanical rotation of a disc or a mandrel. The method collectors slots or parallel collectors that operate on the same principle, allow electrospun fiber alignment only by the behavior of jets in a field electrostatic. When two parallel conductive electrodes are placed under the needle with a space there between as, the electric field lines in the adjacent parallel electrodes are divided into two portions pointing towards the edges of the gap along the electrodes[93].

Xia's group developed another grounding collector design to obtain an array of nanofibers as shown in (Figure I.16a)[89].The collector is composed of two pieces of conductive Si wafers separated by an insulating gap, and the well-aligned nanofibers can be obtained across the insulating gap (Figure I.16b). This type of nanofiber array is believed to be caused by two types of electrostatic interactions[89]. One is the electrostatic attraction between the positively charged

fibers and the negatively charged Si wafers that can stretch the fibers to align themselves along the direction perpendicular to the edges of the conductive Si wafers. Another one is the electrostatic repulsion between deposited fibers that can further enhance the degree of alignment.

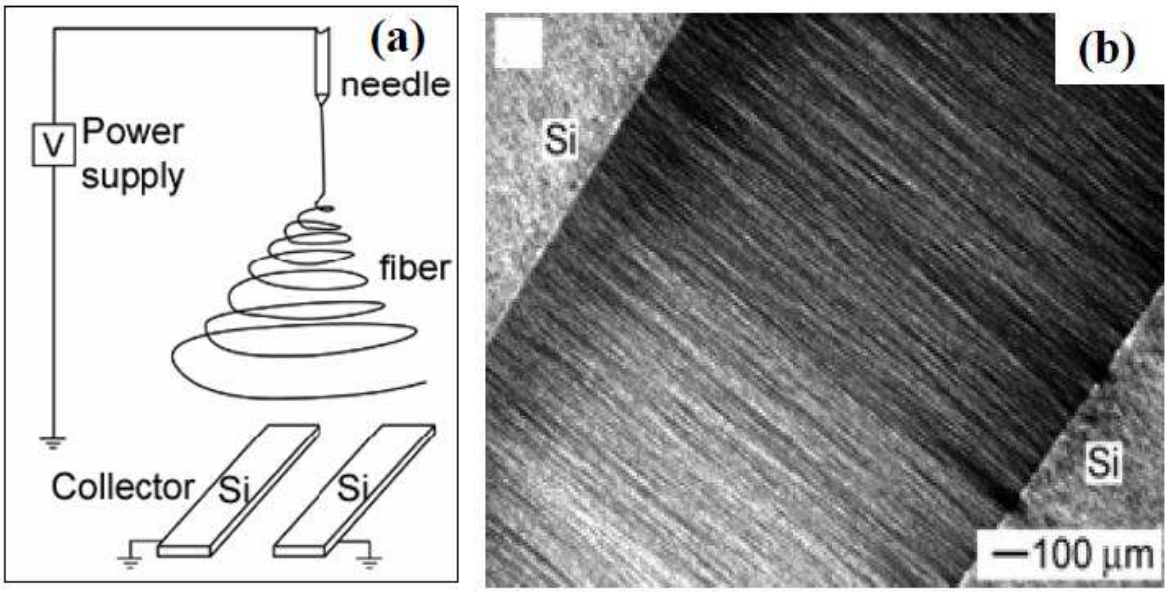

Figure1.16 :(a) Schematic illustration of the grounding collector to obtain arrayed fibers across the insulating gap. (b) SEM image of the arrayed PVP fibers. Adapted from ref.[89]

1.5 Electrospun Fibers Characteristics

The process of electrospinning results in sub micrometer size fibers, which are laid as an extremely fine, randomly oriented, average pore size membrane. This explains the need to study the fiber characteristics of electrospun fiber web. The property of having large surface area of the web enhances the interest. We want to explain about the techniques of fiber characterization, namely and fiber diameter distribution.

The characterization of electrospun nanofibers is difficult to achieve. The size of the materials being handled makes any complicated manipulation and possibility of obtaining an individual filament is very low if not impossible. For a good understanding and eventually a better master the electrostatic spinning, it is necessary to evaluate all the intrinsic parameters of the process, the polymer solution properties Mechanical nanofilaments. Generally, about electrospinning, there are three pillars characterizations of nanofilaments:

Physical and structural, mechanical and chemical[94]. Currently, scientists are interested in nanofibers and more specifically to their morphological properties micro and nano and their ability to form three-dimensional networks. For this, many studies look to the influence of the spinning parameters on the morphology and characteristics of nanofibers.

1.5.1 Objectives of Characterization

Analyzing the electrospun webs yield results and information, which will help researchers in improving the quality and predicting the overall performance of the electrospun web. Some of the reasons for characterization may be process control, process development and product or quality control[95].

1.5.2 Shapes of Electrospun Fibers

It has been observed under scanning electron microscope that electrospinning a polymer solution can yield in addition to round nanofibers, a wide variety of cross-sectional shapes, which includes branched fibers, flat ribbons, ribbons with other shapes, and fibers that were split longitudinally from larger fibers[96].

Jaeger et al.[97, 98] observed beaded electrospun fibers obtained from aqueous solution of Poly (ethylene oxide) and they reported that the bead diameter and spacing depended on the fiber diameter i.e., thinner the fiber, shorter the distance between the beads and smaller the diameter of the beads. They explained that the formation of beads is the draw resonance phenomenon, which occurs if fibers are drawn to high draw ratio.Yarin[99] and Entov et al.[100] developed a mathematical model for the break-up of jets of polymer solutions and they reported that the beaded electrospun fibers are related to the instability of the jet.
Fong et al.[20] carried out experiments on aqueous PEO and reported that the formation of the beaded structures can be considered as the capillary breakup of the jets by surface tension altered by the presence of electrical forces. They found four reasons for the bead formation, viscosity, net charge density, surface tension, charges on the jets and gave solutions namely, as the viscosity is increased, beads become bigger, the average distance between beads longer, and the shape of the beads changes from spherical to spindle-like.

The beads become smaller and more spindle-like when the net charge density is increased. Decreasing the surface tension results in bead disappearance and neutralization of the charge affects, the formation of beads.

As Koombhongse says, 'this may be due to many reasons including, the ejection of smaller jet from the surface of primary jet, separation of primary jet into smaller jets, and electrically driven bending instability of the jet. The elongation of the jet and the evaporation of the solvent change the shape and the charge per unit area carried by the jet'. These shapes can be used as guides for the extension of existent models for the electrospinning process.

1.5.3 Porosity

A pore can be defined as a portion of space bounded by solid surfaces and by planes erected where the hydraulic radius of the space exhibits a minima[102]. The local minima define an arbitrary pore size. The hydraulic radius of a capillary of uniform cross-section is the ratio of volume of the capillary to the surface area of a capillary.

Pore characteristic is one of the main tools for evaluating the performance of any nonwoven fabric and it applies to electrospun web too. The size and shape of the pore can influence permeability and filtration properties[103]. Pore orientation reflects fiber orientation and pore placement indicates the structure uniformity and hence both have effects on fabric mechanical properties such as strength and elongation. The increasing success and demand for nonwoven webs in various areas and applications have led to the development of more effective and accurate methods for measurement of pore size, shape and other pore characteristics.

Porosity, 'ϕ' is the fraction of the bulk volume of the porous media (Ub) that is occupied by void or pore space (Up). The void volumes include the blind pores, the closed pores and the through pores[104]. The porosity for a solid material like metals will be close to zero while that of the highly porous medium like filters will be high. Depending on the type of porous medium the porosity of the material will vary from zero to almost unity. The porosity of a material depends on the mode of packing and compaction of solid particles in a consolidated material, whereas on the other hand it depends on the packing of the particles, their shape, size and arrangement in an unconsolidated material[105].

The measurement of porosity is dependent on the measurement of two of the three volumes of porous material, namely, the bulk volume, the volume of the solid matrix, and the volume of the pore space. There are various methods for the measurement of porosity and some of them are mercury injection method, imbibition method, optical method, gas expansion method, and density method.

The pore size and its distribution are determined by two main techniques, namely intrusion and extrusion types. Mercury porosimetry is an example of intrusion type while the bubble point method is of extrusion type[106]. Both types are based on the principle of capillary flow, which states that a porous material will allow a fluid to pass when the pressure applied on the system exceeds the capillary force of attraction of the fluid in the largest pore[107].

1.5.4 Structure

Depending on the process and material variables the diameter of the fibers produced by electrospinning vary and it ranges from a couple of hundred of nanometers to a couple of micrometer fibers. The arrangement of fibers collected is usually random, with a slight bias to the machine direction. This is probably due to two main reasons, namely the movement of the collector and the air drag/suction. The variation in the length of the fibers has still not been quantified, but for sure, there is lot of variation in the length because of high speed splaying of fibers, charged jet and air current. During the electrospinning process, the polymer in the spinneret is subjected to various external conditions/variables. These variables can be broadly classified into control and process variables. The control variables mainly include the temperature and pressure of the polymer.

The process variables and material used to produce the electrospun web effects the structure and properties of the web. The processing variables are classified into online variables and offline variables[108].

The online variables have been defined as those that can be altered during the production of the web, and offline variables are those, which cannot be altered during the operation of the process. The online processing variables in general include electric voltage, the distance between the spinneret and the collector, the polymer concentration. The offline processing variables in general includes the diameter of the spinneret and design parameters. Although the concept the electrospinning dates back to many years now, not much of characterization has been done in

this field. The demand of these electrospun fibers in wide variety applications has influenced to develop the characterization and testing techniques for the webs produced.

1.5.5 Fiber Diameter and its Distribution

One of the foremost roles of the electrospinning process is to produce thin fibers. Almost everybody who have done electrospinning experiments have reported that the fibers spun through this process have fiber diameters in the range of a few nanometers to a couple of microns.

Fibers spun through different polymer solutions did not make much of a difference in the fiber diameter. The measurement of fiber diameter in the electrospun webs that have been reported in the literature is based using various techniques. The instruments for measuring the fiber diameter and the analysis have been done using various instruments, mainly scanning electron microscope, transmission electron microscope and atomic force microscopes.

The analyses have been done by capturing of images through these devices called the micrographs. Fiber diameter distribution in nonwovens was done by Pourdeyhimi and Dent[109] through Image analysis techniques. The method uses a binary image to create a distance map of the image, which records the distance from each pixel to the background, and from the distance map, the fiber diameter at any pixel location could be determined.

The distance transform applied to a binary image is accomplished by scanning the image twice in opposite directions. The image capturing and segmentation is done as explained by Pourdeyhimi and Dent[110]. The algorithm for determining fiber diameter uses the skeleton, a distance-transformed image, and the skeleton acts as a guide for tracking the distance-transformed image by recording the intensities to compute the diameter at all points along the skeleton. But, both the distance-transform and the skeletonizing procedures result in slight deviations at the corners. Since the measurements do not distinguish between true variations in diameter and variations caused by multiple fibers, being joined together, this causes the skewing of the distribution. There is no standard technique to measure the fiber diameter and analyze its distribution.

To eliminate all possible errors, the ideal case of measuring the fiber diameter of electrospun webs would be to produce a good image of the web at a suitable magnification using the electron microscopy techniques and then analyze the image manually using suitable calibration scale.

The manual analysis usually consists of the following steps, determining the length of a pixel of the image, identifying the edges of the fibers in the image and counting the number of pixels between two edges of the fiber.

1.5.6 Geometrical Characteristics

These properties include fiber properties such as length, cross-sectional area, shape and crimp. Fiber length uniformity, cross-sectional area of the fiber (fiber diameter) and fiber fineness affects processing efficiency and the quality of the final product. As the fibers become finer, the number of fibers in the cross section of a yarn will increase creating more regularity. Crimp describes the waviness or longitudinal shape of the fiber. Conventional textile manufacturing equipments require some degree of fiber crimp. All natural fibers are crimped; however, synthetic fibers must be crimped artificially to be processed into spun yarns. It is very difficult to control the length; fineness and crimp of natural fibers and the economic value of these fibers are mostly dependent on the uniformity of these properties. In terms of synthetic fibers, the length can be set to almost any desired value and their uniformity can be easily controlled. It is necessary to use techniques such as scanning electron microscopy (SEM), microscopy transmission electron (TEM) and more recently the Atomic Force Microscopy (AFM)[111].

1.5.7 Mechanical Characterizations

The three most commonly reported mechanical properties are Young's modulus, tensile strength, and elongation to break[112]. These properties are determined from a stress-strain curve obtained by pulling the sample at a known rate and measuring the resulting resistance force until the specimen breaks. The testing rate and specimen size are determined based on the material and the testing station; the American Society for Testing and Materials, (ASTM) has published guidelines for appropriate testing procedures. The Young's modulus, a measure of the stiffness or elasticity of a material, is the slope at low strain. The break point defines the elongation and tensile strength.

Mechanical testing of thin polymer films is covered by ASTM spec D882, Standard Test Method for Tensile Properties of Thin Plastic Sheeting[113]. The specimens are cut into rectangular shapes. The guidelines for strain rate account for the elongation of the material being tested, with faster rates given for materials with a large elongation to break.

Many basic mechanical properties can be obtained from the tensile test. The first is the modulus of elasticity, defined by Hooke's law. It is analogous to the spring constant, k, in the following equation:

$$F = -kx \qquad \text{eq. (1)}$$

Where F is the applied force and x is the displacement. Equation 1-1 illustrates the linear relationship between the applied force and displacement. Similarly, the stress (σ) and strain (ε) are defined. The amount of stress applied is proportional to the amount of strain on an object. The elastic modulus is the constant of proportionality between stress and strain, as shown in equation (1-2).

$$\sigma = E\varepsilon \qquad \text{eq. (2)}$$

Where σ and E have dimensions of force per unit area, (Nm^{-2}or Pa) and ε is dimensionless (m/m).

A material tested in this region of the stress-strain curve is referred to as linear elastic. If a sample is loaded and unloaded in this region, it will return to its original length and cross-sectional area. More importantly, permanent deformation has not occurred. Hooke's law is only valid for small deformations. Any large deformation usually becomes non-linear, and this law does not apply.

The point at which the slope changes from linearity is called the yield point. At this point, the material is being strained beyond its elastic region. Any deformation after this point is plastic, meaning once unloaded, the sample will not return to its original length.

The yield stress or strain can be rather ambiguous due to the nature of the data. The ASTM has a convention for American structural design defining the yield strength as 0.2% offset from the linear slope of the data. This point of the data was chosen because a definite amount of permanent deformation has occurred . The ASTM standard D3822 is referenced to define the yield strength as a horizontal line connecting a point from where the initial slope begins to

deviate from a straight line and the vertical axis. Yield strain is the vertical line drawn from the deviation from linearity to the strain axis.

In order to test the strength of a material, the tensile loading will continue until a sample ruptures. For metals, the stress-strain curve will reach a peak before rupture. This point is the largest load the sample can withstand before necking occurs. The maximum load defines the ultimate tensile strength, or loosely known as strength.

$$\sigma_{UTS} = \frac{P_{MAX}}{A_0} \qquad \text{eq. (3)}$$

Where $\mathbf{P_{MAX}}$ is the maximum load and $\mathbf{A_o}$ is the original cross-sectional area Percent elongation is defined as:

$$\varepsilon = \frac{(l - l_0)}{l_0} * \mathbf{100} \qquad \text{eq. (4)}$$

Where **lo** is the initial sample length and **1** is the length in tension. Strain is a figure of merit for the ductility of a material.

1.6 Applications of Polymeric Nanofibers

The special geometry of electrospun nanofibers makes them attractive options for various applications in the field of nanostructured materials and design. Figure I.17 illustrates the potential applications of polymer nanofibers in different fields.

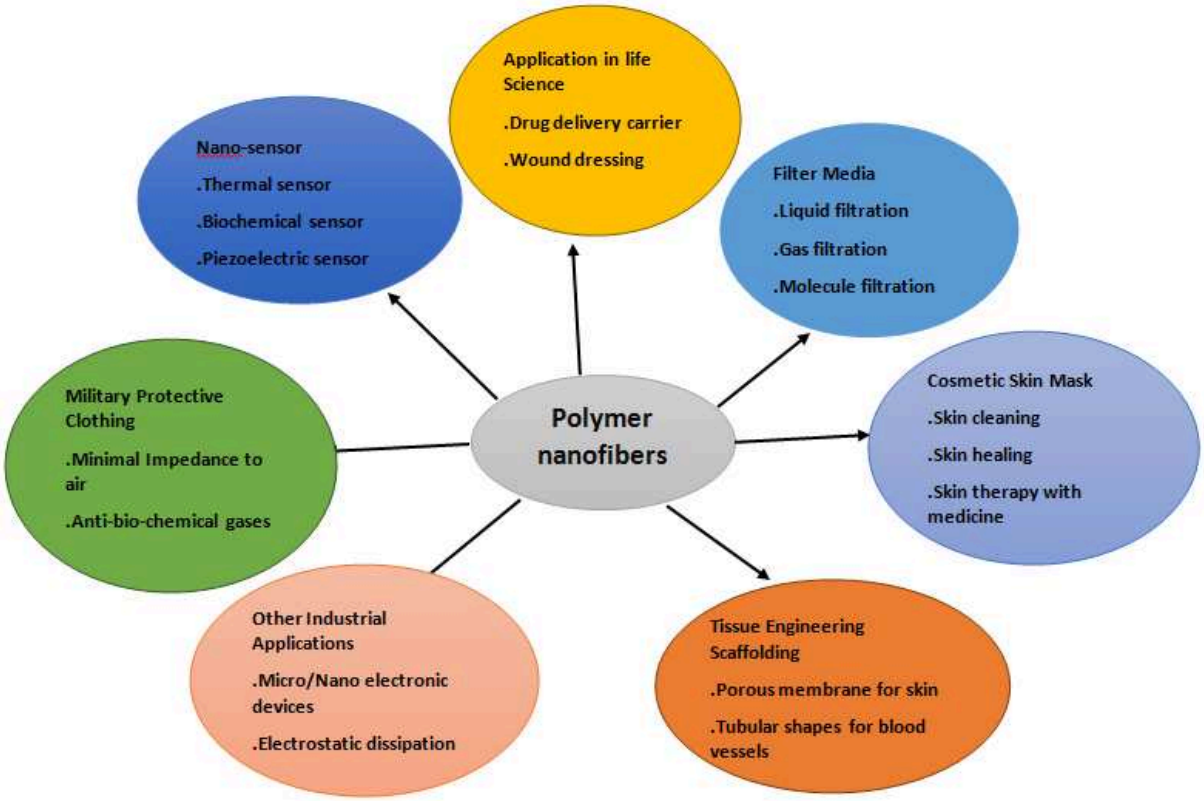

Figure I.17: The diversity of application areas proposed for electrospun nanofibers[114]

Nano fibrous mats have a high surface area to mass ratio (40-100 m^2/g). This unique characteristic is ideal for various membranes applications such as:

- Chemical membranes for removal of toxic products.
- Protective clothing against chemical, biological or environmental attacks.
- Ultrafine filters for air filtration in medicine, military devices, food processing and electronic industries to absorb tiny particles.
- Highly breathable membranes due to high absorption capability and high porosity.

About 30% of U.S. patents published on nanofibers are related to biological and medical applications. However, the first completely industrialized application of nanofibers was introduced in filtration due to its huge market. Nanofibers are also attractive materials for nano sensor applications because their high specific area provides the ability to absorb or react rapidly with low levels of chemical.

1.6.1Membranes Filtration

Membrane filters have been developed to enable the purification of molecules on the molecular weight or size, rather than on the physicochemical properties or biological functions. Filtration is required in many fields of engineering. The fibrous materials used for filters, provide advantages like efficiency high filtration low air resistance[115]. Filtration efficiency is closely associated with fiber diameters that make up the membrane leaving or not spend particles on steric selection. Figure I.18 shows schematically the relationship between the diameter of the filaments and the filtered particles.

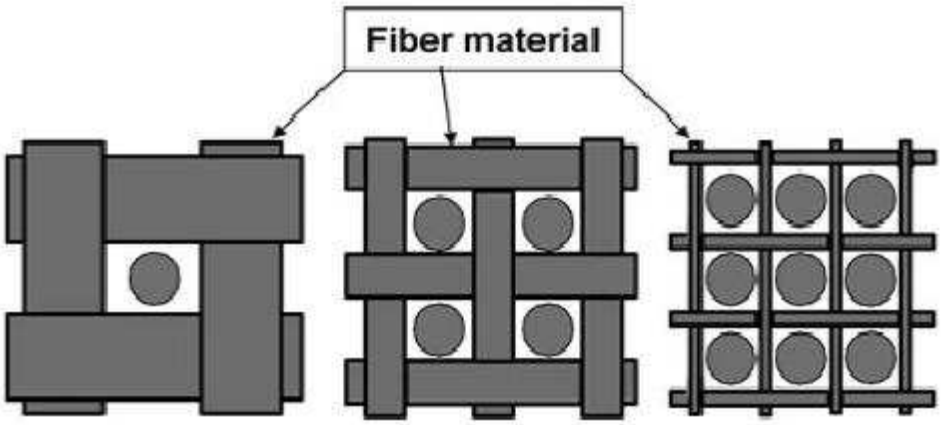

Figure I.18: Scheme of the relationship in principle between the diameter of the filaments and the filtered particles

Since the channels and the structural elements of a filter must be adapted to scale particles or droplets that must be collected in the filter, in a manner direct develop effective ultra filtration membranes is to use size fibers nanometer in the filter structure[116]. In general, because of the very large surface area with respect to volume, the nanofiber membranes have a strong cohesion. Of minute particles of about 500 nm can be easily trapped in the filters electrospun. In the field of global filtration, Freudenberg Nonwovens was the first and largest producer and seller of electrospun membrane filters for markets filtration of ultra-high efficiency since more than 30 years[117]. This is one of the first commercial enterprises recognized in the domain of electrospinning.

Filtration efficiency or capture efficiency of filter media has been shown to be inversely proportional to the diameters of the fibers in filters. Because of the very high surface area-to-volume ratio and the resulting high surface cohesion of nano fibers, particles on the order of

less than 0.5 micrometer are easily trapped in the nano fiber mats. Electrospun nano fibers on substrates such as glass, polyester and nylon have also proved to enhance the life of filters in pulse-clean cartridges for dust collection and increase the efficiency of filters used in cabin air filtration of mining vehicles. Polymer nanofiber mats can also be electrostatically charged to provide them the ability to capture particles by electrostatic attraction without an increase in pressure drop, leading to improve the filtration efficiency[118].

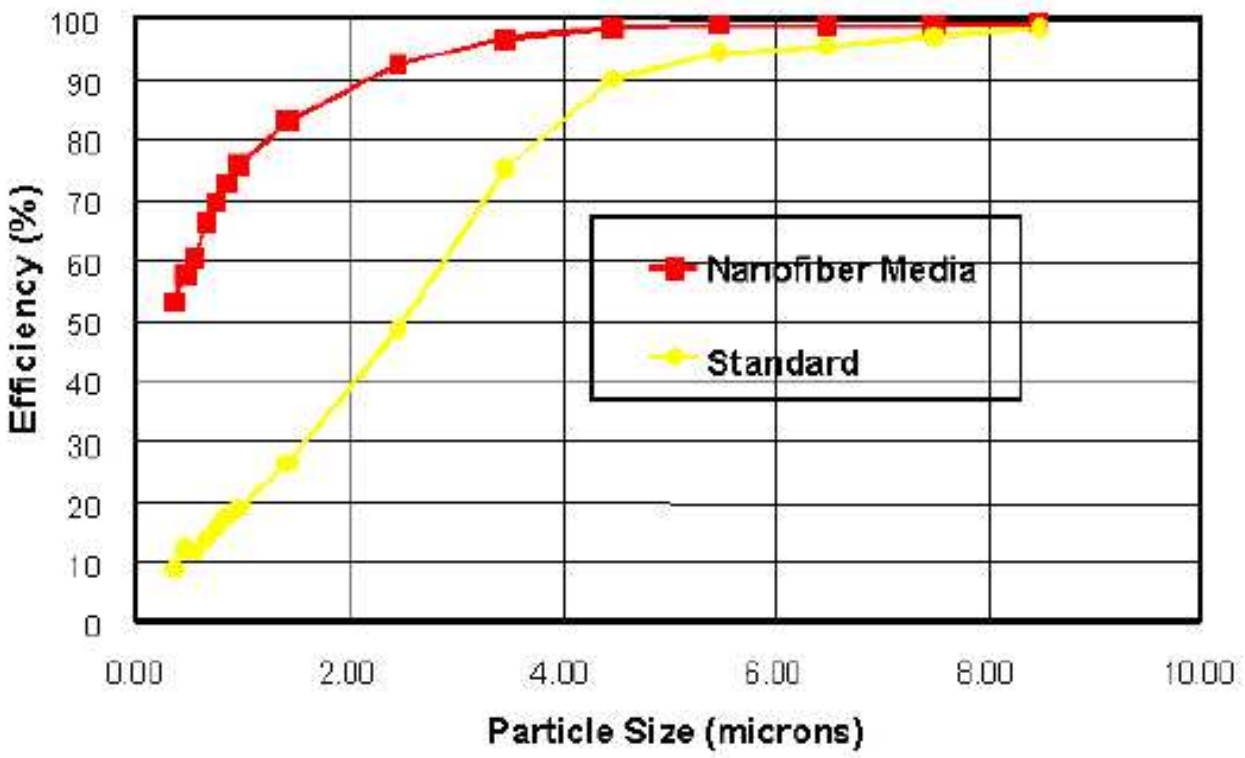

Figure 1.19: Fractional efficiency (Filtration Efficiency versus particle size) for a standard cellulose media and nanofiber filter media[119]

1.6.2 Biomedical Applications

From the biological viewpoint, almost all of human tissues and organs are deposited in Nano fibrous forms or structures. Examples include bone, dentin, collagen, cartilage, and skin. All of them are characterized by well-organized hierarchical fibrous structures realigning in nanometer scale. Because of this analogous behavior, it can be seen that nanofiber webs have a promising potential in various biomedical areas[114].

Researchers have tried to convert biopolymers into nano fiber mats that mimic biological structures [118]. It was also shown that electrospun biocompatible polymer nanofibers can also

be deposited as a thin porous film onto a hard tissue prosthetic device designed to be implanted into the human body. This coating film with gradient fibrous structure works as an interphase between the prosthetic device and the host tissues, and is expected to efficiently reduce the stiffness mismatch at the tissue/device interphase and hence prevent the device failure after the implantation[114]. As another biomedical application, polymer nanofibers can be used for the treatment of wounds or burns of a human skin, as well as designed for haemostatic devices with some unique characteristics.

With the aid of electric field, fine fibers of biodegradable polymers can be directly sprayed/spun onto the injured location of skin to form a fibrous mat dressing, which can let wounds heal by encouraging the formation of normal skin growth and eliminate the formation of scar tissue, which would occur in a traditional treatment Drug delivery with nanofiber capsules is another promising biomedical application of nanofibers. It is based on the principle that dissolution rate of a particulate drug increases with increasing surface area of both the drug and the corresponding carrier if needed.

Drug delivery method and, generally, pharmaceutical applications make use of drug-containing electrospun fibers. A drug is introduced into the polymer solution for electrospinning and transformed into fibers that transport and simultaneously release active substances. Fabrication of core/shell fibrous structures has added to the versatility of these nonwovens affording a wider range of molecules to be released in a controlled manner[120].

.

Hu et al.[121] made use of emulsion electrospinning to successfully electrospin both hydrophilic and hydrophobic drugs into the poly (L-lactic –co-glycolic acid) (PLGA)/gelatin fibrous mats. The core /shell fibers structure where core carries a drug and shell, consisting of PLGA/gelatin polymer blend, enabled constant and sustainable release of Cefradine drug.

Mickova et al.[122]used coaxial electrospinning setup to obtain liposome loaded PVA/PCL core/shell fibers (Figure I.20).Coaxial electrospinning was reported to preserve enzymatic activity of horseradish peroxidase encapsulated in the liposome, while monoaxial electrospinning setup caused the liposomes to break and release their encapsulated material.

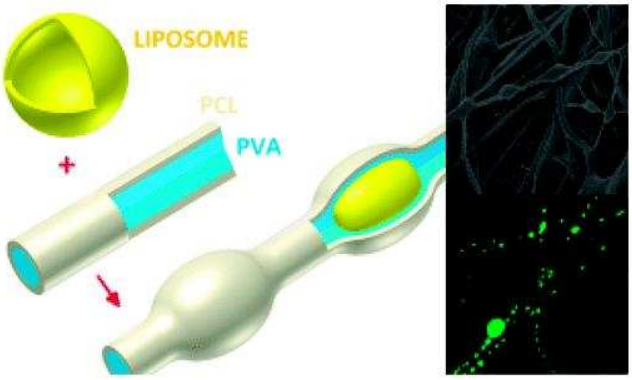

Figure1.20: Schematic representation of the PVA/PCL core/shell fibers loaded with liposome and their SEM and confocal microscopy images[122]

The efficacy of the core /shell fibers containing protein-loaded liposomes was tested in a cell culture study of mesenchymal stem cells and showed to stimulate the cell proliferation.

Polyesters, having a slow degradation rate have been used as contraceptive devices. Dasaratha Dhanaraju et al.[123] incorporated contraceptive steroids into PCL microspheres. Two water – insoluble steroids were encapsulated into PCL microspheres by double emulsion – solvent evaporation process. In vitro drug–release tests showed prolonged diffusion of these molecules, promoting PCL microspheres as promising devices for controlled delivery of contraceptive steroids[124].

1.6.3 Protective Clothing

Because of their great surface area, nanofiber fabrics are capable of the neutralization of chemical agents and without impedance of the air and water vapor permeability to the clothing. Preliminary investigations have indicated that compared to conventional textiles the electrospun nanofibers present both minimal impedance to moisture vapor diffusion and extremely efficiency in trapping aerosol particles, as well as show strong promises as ideal protective clothing[114]. Researchers, developing polymer nanofibers for various protective clothing applications, have found that compared with conventional textiles, electrospun nanofibers mats provide minimum impedance to moisture vapor diffusion and maximum efficiency in trapping aerosol particles[118].

1.6.4 Sensors

Results of studies on sensors indicate that the sensitivities of nanofiber films to detect ferric and mercury ions, and a nitro compound are two to three orders of magnitude higher than that obtained from thin film sensors. Polymeric nanofibers could also be used in developing functional sensors with the high surface area of nanofibers to facilitate the sensitivity. Poly (lactic acid co glycolic acid) (PLAGA) nanofiber films were employed as a new sensing interface for developing chemical and biochemical sensor applications[119].

1.7 The Future of Tissue Engineering Scaffolds

Research in tissue engineering can be dated back to 1933 when Bisceglie implanted mouse tumor cells that were encased in a polymer membrane into the abdomen of chick embryos and showed the survival of these cells. Tissue engineering has since evolved into a highly interdisciplinary field in which almost every tissue and organ structure is actively being studied. However, few products have entered clinical trials and even fewer have been approved be the FDA for clinical use in humans.

A major obstacle in the engineering of organs is the ability to organize cells in the proper manner and deliver nutrients to and from the system. Strategies for increased vascularization of the engineered tissue include release of growth factors such as vascular endothelial growth factor from the scaffold. Cell organization has also been enhanced by new scaffold processing techniques, which allow for a much more controlled fabrication of the scaffold architecture and morphology to acquire the appropriate tissue architecture. Scaffolds in the future will not only provide the correct microenvironment for the cells to reside in, but also supply the appropriate physiological stresses and soluble signals for functional tissue development. Advances in scaffold design will ultimately lead us closer to the goal of engineering fully functional tissues to restore, maintain or enhance tissues and organs.

CHAPTER II

Materials and experimental procedures

Materials and experimental procedures

Introduction:

The primary task involved in this research was the development of architected membranes of Poly (ethylene oxide), PEO, by a spinning process under intense electric field. The control of the networks morphology is achieved through the design and the realization of microstructure collectors.

In this chapter, we present details about the polymer used to draw membranes. Poly (ethylene oxide) (PEO) has been extensively studied due to its unique behavior in aqueous media and its important industrial application. PEO has a wide range of applications in adhesives, drag reducers, additives, effective flocculants for finely dispersed solids in water, and packaging materials for insecticides and pesticides.

After that, we expose the methods and materials used to measure the properties of the polymer, in particular the viscosity, viscoelasticity , elongation flow, surface tension, , and the electrospinning process parameters, such as the applied voltage, flow rate and the gap distance. Electrospinning was used to produce uniform nanofibers by system which is a spinning device electrostatic entirely designed to "Laboratoire Rhéologíe et Procédés". The deposit of fibers was made on two types of collectors: a) Aluminum foil, b) micro-structured collector (dimension 3 × 3 cm).

Scanning Electron Microscope (SEM) was used for determining and characterizing the morphology of electrospun fibers and fiber webs. Fiber diameter and its distribution were assessed using the image analysis software Image (J).

We provide the method concerning the study of the mechanical properties of PEO based composites for both fiber mat and short fiber forms by tensile tests, tests were performed at ambient temperature. The details of various materials used and experiments performed in this research are given below.

2.1 Materials

Among the polymers that have been investigated in electrospinning research, PEO is the one that has been most well characterized due to its unique properties that endow its ease for electrospinning. The chemical structure of PEO is presented in (Figure II.1). The extreme water solubility of PEO is of special interest compared to the degree of solubility in water of other polymers such as Poly (methylene oxide), polyacetaldehyde, higher molecular weight (greater than about 1000) Poly (propylene oxide), and Poly (trimethylene oxide)[125]. PEO is also soluble in many common solvents such as acetonitrile, dichloromethane, carbon tetrachloride, tetrahydrofuran and benzene at room temperature[125].

PEO-aqueous interaction mostly influenced by the temperature. The increasing of temperature is responsible for the decrease of its solubility due to breaking of hydrogen bond. On the other hands, at room temperature its water solubility is found to be dependent on its concentration. Indeed, water is a good solvent at low concentration and high temperature while it becomes a bad solvent at intermediate concentration, close to the critical concentration[126].

PEO is a linear polymer that consists of ethylene and ether segments [-CH2CH2O-] n. The ether oxygen allows this polymer to interact with other hydrophilic species, while the ethylene part participates in hydrophobic interactions. Due to its amphiphilic nature, PEO is soluble in water by forming hydrogen bonding between the oxygen of the PEO ether group and the hydrogen of water molecules[127]. In addition, the oxygen-oxygen inter distance on the PEO backbone matches the distance of the oxygen atoms (2.8 A°) in the water molecules, which is believed to be important in making the polymer soluble in water. This theory supports the fact that homologues of PEO such as Poly (methyl ethylene) and Poly (propyl ethylene) are not water soluble due to the mismatch oxygen-oxygen inter distance with that of water[128].

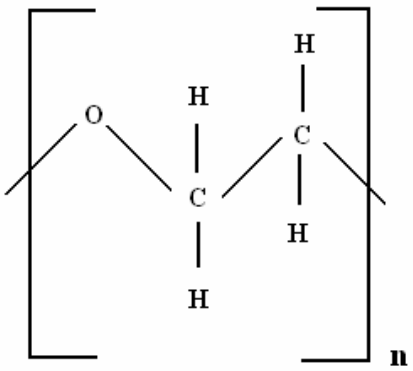

Figure II.1: Chemical structure of PEO

Due to its water solubility, non-toxicity and electrospin ability, PEO has been used as an additive in biopolymer solutions to enable the formation of electrospun fibers.
Different molecular weights Poly (ethylene oxide) polymers were used for the production of nano fiber structure (Sigma-Aldrich), (1.0×10^5, 3.0×10^5, 1.0×10^6, and 5.0×10^6 g/mol). Various solution concentrations used for each polymer.

2.1.1 Preparation of Solutions

The polymer concentrations were prepared as dry weight percentages in deionized water and then stirring at 125 RPM at 30 mm amplitude by using a laboratory Shaker (SM 30 Edmund Bühler GmbH, German). Solution mixing was performed at room temperature for 4 days to ensure complete dissolution of the polymers and obtain homogeneous solutions.

The dispersion time of 1 month is the upper limit beyond which natural degradation arises, leading to the decrease of rheological properties of PEO-water solutions. The homogeneous state of polymer solution has been appreciated visually by checking the uniform natural light scattering of each sample, and it was confirmed by the reproducibility of rheological measurement for various samples from the same batch. Samples have been prepared and stored in darkness to prevent photo oxidation of polymer solution.

2.2 Rheological Behavior

Rheology is defined as the science of flow and deformation of materials. To determine the rheological consistency of a material both its viscosity and elasticity parameters must be studied. The viscosity of a material according to the rate at which it is sheared, provides important information about processing and performance. This can be important in production where stirring, dispensing and pumping of the product will subject it to a variety of shear rates. Low shear rate behavior can be related to storage conditions of materials: sedimentation, phase separation, and structure retention. Single point viscosity information does not profile the material across a spectrum of shear rates. The elasticity of an aqueous solution of high molecular weight PEO has been attributed to its linear and flexible chain structure that is conducive for the formation of uniform fibers during electrospinning[84].

A) Viscosity

One of the three major physical characteristics of a solution that would determine the spin ability of a solution in an electrospinning trial is the viscosity of the solution. The Physic ARG2 Rheometer from TA Instruments (New Castle, DE, USA) was used to characterize rheological behavior of polymer solutions under shear in order to define the zero-shear rate viscosity η_0. The cone plate geometry (diameter = 50 mm, cone angle = 2°, truncation = 60 μm) was used for this purpose. Small amount of polymer solution was poured between the plates the gap between which was maintained at 0.5 mm. The temperature of the plates was kept constant at (25 ± 0.1) °C. The top plate was rotated at a controlled rate to apply shear force on the solution. The shear rate was increased gradually to obtain a plot of viscosity against the shear rate. The value of viscosity was then estimated from the data. Data were collected using a step shear rate procedure, a sufficient time was allowed at every shear rate value so that the shear stress reaches an equilibrium value. Viscosity was calculated as the ratio on the stress of equilibrium and the imposed shear value. In order to prevent rapid evaporation the solvents (specially chloroform), a small amount from a solvent was put around the sample during measurements.

B) Viscoelasticity

Small amplitude oscillatory shear experiments were carried out using a DHR3rheometer (TA InstrumentsUSA) equipped with cone plate geometry (diameter d = 60 mm, cone angle α = 0.01 rad) at T = 25°C using a water thermostat. Experiments were done in the linear response regime covering a frequency range from 0.0001 to 1000 rad/s of the sample around 3.0 mL. The instrument operates in a strain-controlled mode and amplitude sweeps at ω = 1 rad/s were performed prior to each frequency sweep in order to identify the linear viscoelastic response regime. All frequency sweeps were done at strain amplitudes γ_0<100% to assure linear response.

C) Elongation Flow

Characterization of elongational flow properties was done with a CaBER1 rheometer (ThermoHaake). A small quantity (0.5 mL) of sample filled the millimetric gap between two circular plates. The top plate was rapidly separated from the bottom plate at 2.0×10^{-1} mm/s speed, resulting in the formation of a filament between the two plates. After stretching, the fluid was squeezed by the capillary force imposing an extensional strain on the fluid. A laser micrometer monitors the midpoint diameter of the thinning fluid filament as a function of time.

2.3 Surface tension Measurements

The principle of electrospinning is to overcome the surface tension with electrostatic forces induced by the intensity of the electrical field. In order to determine the relationship between the spinnability of the solutions and any existing correlations between the fiber diameter and the solvent ratio, the surface tension was used as a common factor for comparison. The surface tension at the air-liquid interface were measured by the pendant drop technique.

- **Test Protocol**
- **1- Hanging drop method**

The so-called hanging drop technique gives access to the surface tension of liquids from the shape taken by the drops just before their expulsion of a capillary tube. The calculation is based on measuring the parameters of a drop of liquid freely suspended at the end of a capillary, as shown schematically in Figure II.2. Two form factors are introduced:

$$S = \frac{\Delta\rho.g.de^2}{\eta} \qquad \text{eq. (1)}$$

$$S = \frac{(\rho_l - \rho_v)g.de^2}{H} \qquad \text{eq. (2)}$$

With S the surface surface tension, Δρ the difference of volumic mass density of the liquid and gas, g acceleration of gravity, de the equatorial diameter, and H the distance between end of needle and the top of the drop. The characteristic dimensions of the drop describe above were determined from the capture of drop shape.

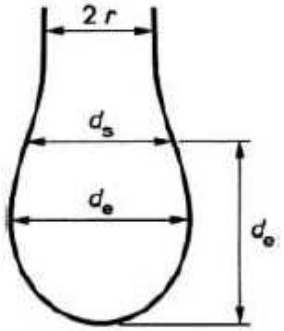

Figure II.2: Profile of a pendant drop, according to B. Neindre in the K475 Technical Engineer [129]

This method has the advantage of requiring a small amount of liquid. It is also particularly suitable for surface tension measurements in the presence of surface-active agents.

The measurements were made by (GBX Digi drop, France). The PEO solution samples were dropped and hanged at the tip of the 0.81 mm internal diameter needle. Subsequently, the pictures of this hanged drop were taken for further image analyses to obtain the surface tension. The last 10 images were chosen to the maximum size of the drop before to fall. Further, the density of the PEO solution (0.7% PEO – 1.001 g/mL, 1.0% PEO – 1.002 g/mL , 4.0% PEO – 1.008 g/mL, 4.3% PEO – 1.009 g/mL, 5.35% PEO – 1.011 g/mL, 9.2% PEO – 1.01 g/mL, 10.3% PEO – 1.02 g/mL, and 25% PEO – 1.05 g/mL) were taken to determine the final values of the surface tension. All the experiments were carried out at room temperature. A snapshot series was presented in (Figure II.3).

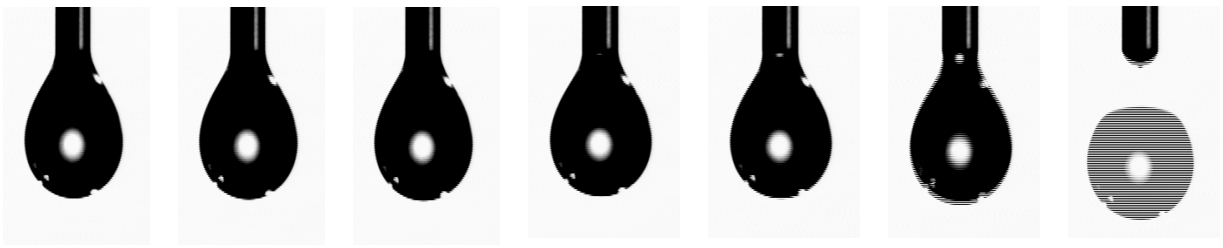

Figure II.3: Photographs used for the calculation, 40ms between each shot rightmost corresponds to ejection: not exploitable

2.4 Membrane Production Process (Electrospinning)

The nanofiber produced with homemade electrospinning in designed to « Laboratoire Rheologíe et Procédés »in team of Prof. Frédéric Bossard. This system consists of a syringe of 5mL which delivers the solution polymer to the tip of the needle (0.51mm) with a diameter of 400 to 700 microns located vertically manifold and a syringe pump (KDS Legato 200, KD Scientific, Holliston, MA, USA) outdoor adjustable flow the spinning apparatus itself. The spinning system is vertical (taking into account forces of gravity). High voltage source was used to charge the solution by attaching the emitted electrode of positive polarity to the nozzle, and the grounding to the collector.

The system was isolated by a wall of Plexiglas to avoid external interferes electrical phenomena, as well as any airflow disturbance. A precise adjustment of the tip to collector distance is made possible by usingcomputer system control. The range of variation was between 2.0 and 50 cm. The density distribution nanofilaments on the receiving plate would be defined not only by the production time, but also by the manner in which the filaments are deposited on the support. The rate of spinning was from 0.02 to 0.1 mL/min after adjusted the flow rate and the distance between the tip of the needle and the collector, we studied two fibers deposition patterns; the first deposition on a sheet of Aluminum (Figure II.4) and the second was performed on a micro-structured manifold Copper dimension 3 × 3 cm with 1mm spacing between spots (Figure II.5). An electrical potential of 25kV was applied across a distance of 27cm between the tip of the needle and the outer surface of the collector.

All experiments were done at room temperature. The relative humidity noted was between 30% and 50%. A visualization of the distribution of the fibers by SEM scanning electron microscopy was carried out after checking the absence of beads and the continuity of the fibers by the

optical microscope(Zeiss ultra 55 SEM FEG, Oberkochen, Germany)operated at 1 kV. Prior to SEM imaging the PEO nanofibers were coated with 1 nm gold/palladium layer for 10 s.

Figure II.4: Machine electrospinning with the aluminum foil collector

Figure II.5: Machine electrospinning with the static collector

Collector used:
We have used two collector types:

1- An aluminum foil collector
2-Micro-structured collector

Different micro-structures can be used to obtain a uniform distribution of a membrane .This study showed that it is possible to have a distribution of fiber forming a very uniform primitive cell in a network. Cupper made of microstructure Collector used in "Laboratoire Rheologíe et Procédés" with the dimension 3 × 3 cm (made of Cupper) see (Figure II.6).

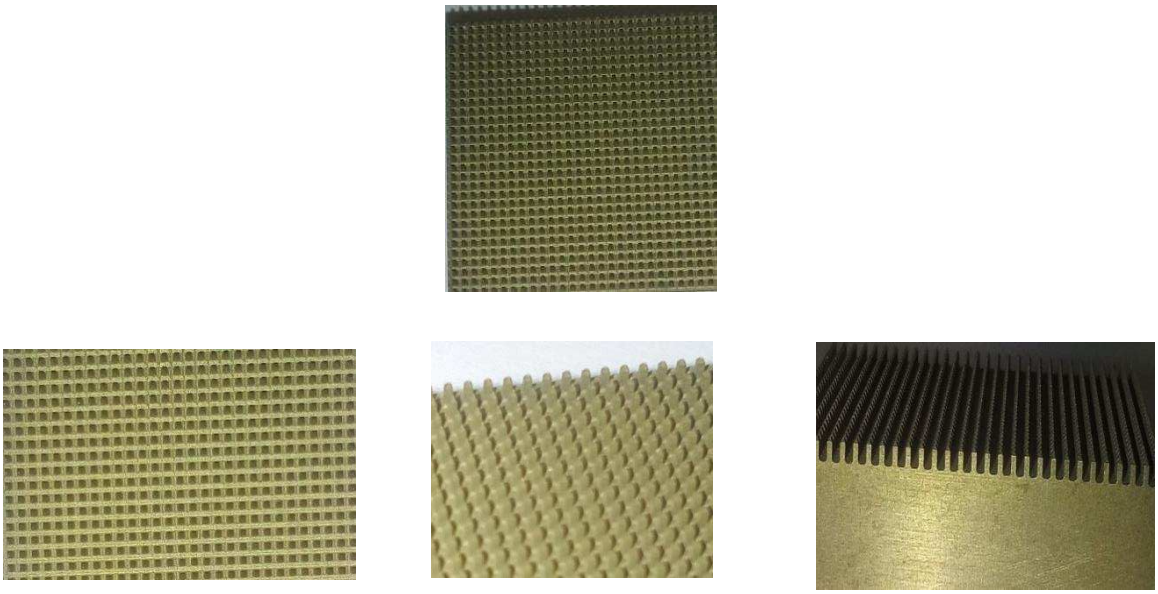

Figure II.6: The micro-structured collector used

2.4.1 Operating Parameters of Electrospinning

The relevant operating parameters are flow rate, electric field strength, and electric current flow between the needle tip and collector. The volumetric flow rate is closely controlled through the use of a syringe pump. Field strength may be varied by changing either the applied voltage or the distance over which the voltage drop to ground occurs. Both variables were studied.

2.4.2 Characterization of Nanofibers

Scanning electron microscopy (SEM) and fiber diameter Distribution (FDD) were used to address the morphology change of the nanofibers structures.

A) Structural of Nanofibrous

SEM was a primary technique used for determining and characterizing the morphology of fibers. In scanning electron microscopy, a fine beam of electrons was scanned across the surface of a specimen to which a light conducting film has been applied. Secondary electrons emitted when the beam hits the specimen are collected to provide a signal used to modulate the intensity of the electron beam in a television tube to form an image that corresponds to the small

raster and information, pixel by pixel, emanating from the specimen surface, scanning in synchronism with the microscope beam[130].

The SEM is used to quantify the diameters of the nanofibers and the distribution in size and the overall direction of the nonwoven. That is the observation technique more commonly used in the field because it is very easy and quick to perform and does not require large amounts of material. Fiber morphology was observed at CMTC-INP Grenoble, France, by the SEM field emission gun whose characteristics are Field Effect Canon (FEG) Schottky; High vacuum mode; Accelerating voltage: 100 V to 30 kV; Resolution secondary electron: 1 nm to 15 nm and 1.7 kV to 1 kV. Its principle is based on the scanning of a very thin electron beam, mono kinetic, the surface of a sample, which occur interactions detected by a sensor that controls the brightness of a cathode-ray oscilloscope whose sweep is synchronized with that of electron beam; it is thus possible to compare the SEM of a CRT system.

The principle of a field emission gun is to use an advanced form very thin metal cathode and applying a voltage of about 2000-7000 volts between the tip and the anode. This produces, by "burst effect", a very intense electrical field, of the order of 10^7 V.cm^{-1}, at the end of the cathode. The electrons are then extracted from the tunneling tip. The nanofibers of PEO solutions 1.0×10^5, 3.0×10^5, 1.0×10^6, and 5.0×10^6 g/mol are observed. Average fiber diameters of the electrospun fibers were obtained as a mean value of 150 different diameters measured by Image J software.

B) Fiber Diameter Distribution by Image Analysis

Fiber diameter and its distribution were assessed using the image analysis software ‘Image J’ developed by (National Institutes of Health, USA). The image pixels were calibrated using the pixel length of a magnification bar (in nanometers) generated on the image in SEM. To measure the fiber diameter, a line was drawn on the fiber perpendicular to its axis. The length of the line was automatically converted into nanometers by the software. This gave a value of fiber diameter at that point. Hundred fifty readings were taken from each image to calculate the average value of the fiber diameter and the standard deviation of the diameter values. Using at least eight different images of each type of electrospun nanofibrous mats, inter-fiber distances, F_d, were calculated using the empirical model[131].

$$F_d = 0.5\sqrt{\frac{A}{N}} \qquad eq.(3)$$

Where
N = Number of fibers, and A = Viewing area

2.5 Mechanical Test

A tensile test is a method for determining the mechanical behavior of materials under axial loading. In order to investigate the mechanical behavior of the membranes produced, Mechanical properties of the electrospunNanofibrous membranes were measured with the rheometer equipped (ARESG2-TA Instruments) pulling jaw at the drawing speed of 0.25 mm / s. The fiber membrane was placed between the tension jaw (Figure II.7), after recording its weight and its initial surface. The force was related to the sample section to find the Young's modulus.

All samples were prepared in the form of rectangular shape with dimensions of 30 x 10 mm from the electrospun fibrous membranes (Figure II.8). The thicknesses of samples were measured with a digital micrometer. At least five samples were tested for each type of electrospun fibrous membranes.

The Young's modulus from tensile testing (E) is defined in the following equation[132].

$$E = \sigma / \varepsilon \qquad \text{eq. (4)}$$

Where,

σ :is the maximum flexural tensile stress at break (Pa).

σ=F/S

ε: is the deformation

σ=F/S

F: is the force (N)

S: is the surface area of the membrane (m^2) given by:

Surface area of the membrane (S) = (LW)

L: is the length of specimen (mm) ≈ (30) mm and W is the width of specimen (10) mm.

Figure II.7: Device for the mechanic (ARESG2) with camera

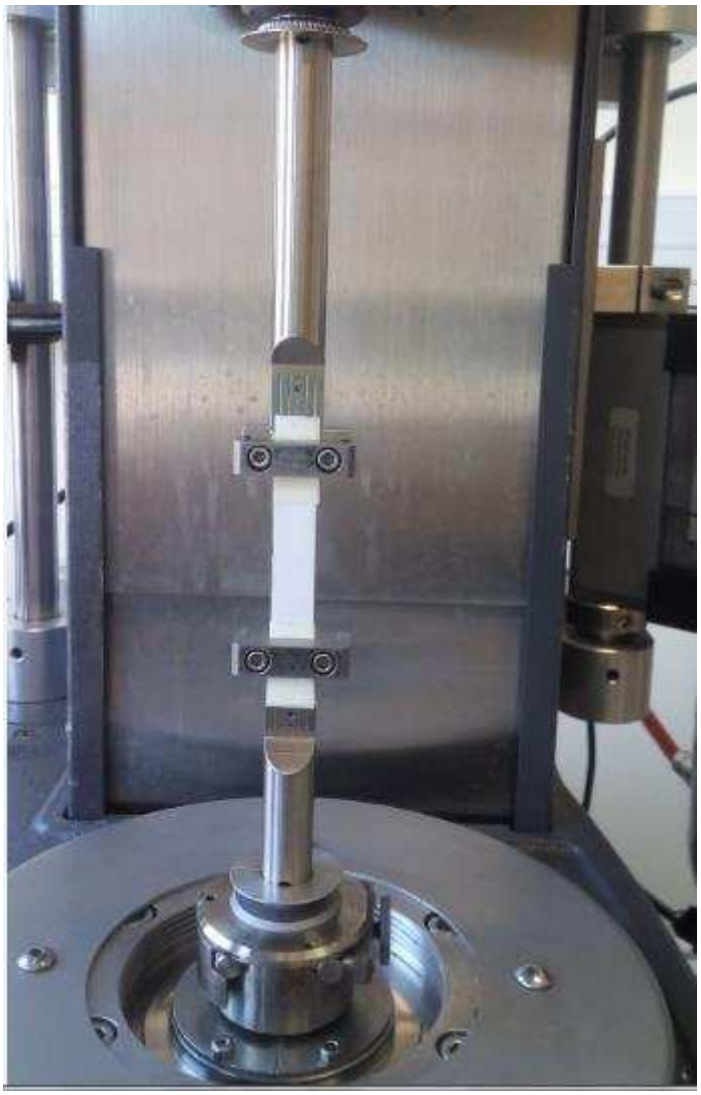

Figure II.8: Sample was prepared in the form of rectangular shape with dimensions of 30 x 10 mm from the electrospun fibrous membranes

CHAPTER III

Part I: Rheological Properties of PEO Solutions

Introduction:

In this study, one of the most important properties of the spinning solution is the viscosity, so it is necessary to study the rheological behavior of these polymer solutions to establish relations between the parameters of the spinning process and the physical properties and mechanics of materials obtained.

Electrospun-affecting factors had been evaluated for the production of Nanofibrous structure from PEO. The factors are categorized into two that is processing parameters and solution properties. Processing parameters comprised, applied voltage, collector distance, flow rate. Whereas, the solution properties include polymer concentration and viscosity. As the results confirm the average fiber diameter has direct correlation with increasing the concentration as shown in Table III.1.2.

This section gives details of the results obtained and explanations of the possible reasons behind the findings. The main objective of this work was to develop architected membranes of Polyoxyethylene PEO by electrospinning. Control of the morphology of the networks will be achieved through the design and realization of microstructure collectors.
In this chapter split into two parts, are grouped various research carried out in this work.
1. The rheological study of the polymer solutions for the spinning.
2. Characterization the morphology of the fibers by the scanning electron microscope SEM.

3.1.1 Rheological Properties of PEO Solutions

Rheological behavior of PEO solutions examined repeatedly for studying the interactions between solvent and polymer as depicted in Figure III.1.1. The viscosity increased with increment of concentration of the same molar weight of PEO. Figure III.1.1 shows the rheological behavior of PEO solutions with in the range of concentrations from 1.0 wt% to 50.0 wt%, at molecular weight of PEO (Mw ~ 1.0×10^5 g/mol). As the results confirmed the viscosity is nearly stable in the range of high shear rates. There similar evidence reported that by increasing the solution concentration, transitions occur from beads to beaded fibers then to homogeneous fibers[133]. The same processing conditions, the PEO solutions of 1.0, 2.0, 6.0 and 8.0 wt% concentration, the values of viscosity were maintained constantly around 22.0×10^{-4}, 38.0×10^{-4}, 110.0×10^{-4} and 357.0×10^{-4} Pas, respectively. In the same case, solution concentration increased from 12.0, 14.0, 30.0, 40.0 to 50.0 wt% the viscosity become 21.0×10^{-2}, 4.0×10^{-1}, 20.2×10^{0}, 95.0×10^{0} to 498.0×10^{0} Pas, respectively. The solutions with higher concentrations showed higher viscosities, as might be expected increment of total PEO weight in the solution. The decrease of shear viscosity against shear rate is known to due to entangled chain networks in polymer solution[134]. If a particular solution has a high viscosity, then solvent molecules spread more evenly over the entangled polymer. Therefore, a higher solution viscosity results in more polymer entanglement, which serves to maintain a continuous jet during electrospinning.

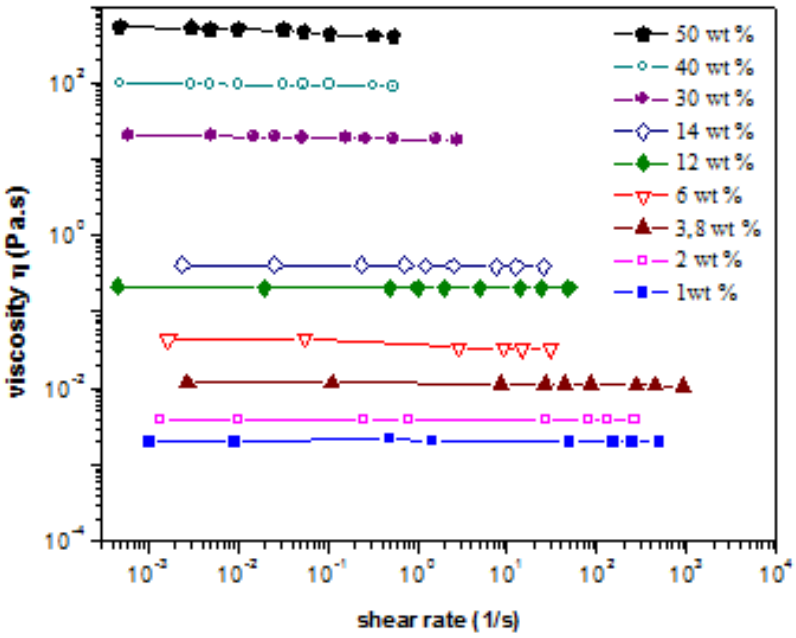

Figure III.1.1: The viscosity of PEO polymer solutions (1.0×10^5 g/mole) as a function of shear rate at different the concentrations

Figure (III.1.2A, B) shows the rheological behavior of PEO solutions at $\eta/\eta_0 = 1$ and concentrated regime. With different concentration (17.5, 6.0, 2.9 and 0.5 wt%) at molecular weight (1.0×10^5, 3.0×10^5, 1.0×10^6, 5.0×10^6) g/mole, respectively. The results show that in the Figure III.1.2A, B zero shear viscosity plotted against shear rate. Figure (III.1.3A, B) shows the rheological behavior of PEO solutions at $\eta_0 = 1$ and concentrated regime. With different concentration (25.0, 9.2, 2.9 and 0.7 wt%) at molecular weight (1.0×10^5, 3.0×10^5, 1.0×10^6, 5.0×10^6) g/mole, respectively. The results show that in the Figure (III.1.3A, B) zero shear viscosity plotted against shear rate. We found Whenever least molecular weight polymer becomes more resistant that the value of any viscosity remains constant, such as the concentration of 25.0 wt%, which has the molecular weight of 1.0×10^5 g/mole reverse the concentrations of high molecular weights have few viscosity.

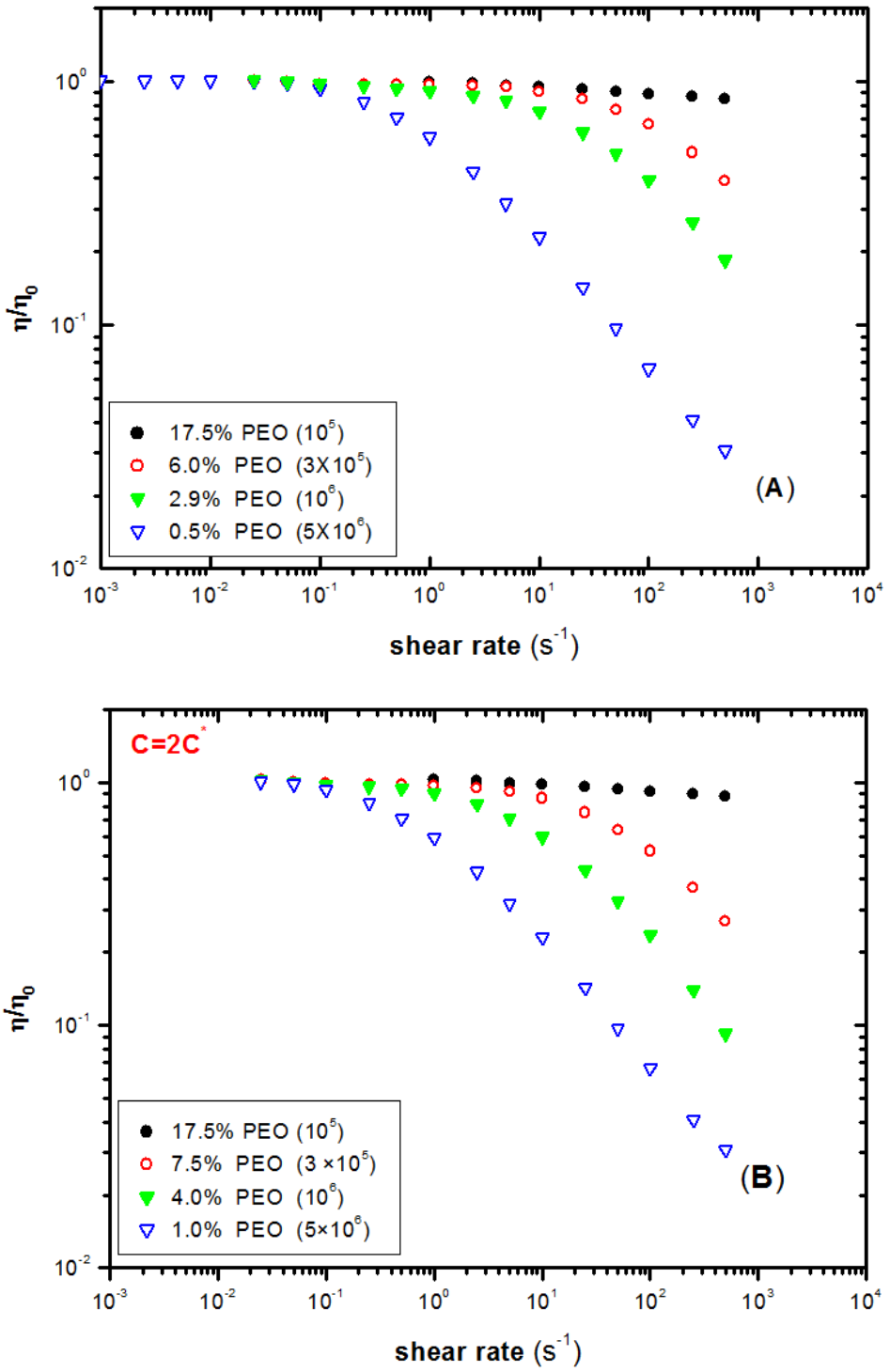

Figure III.1.2: Show the Zero shear viscosity as functions of shear rate: A) represent at η_0 =1 and B) C=2C*

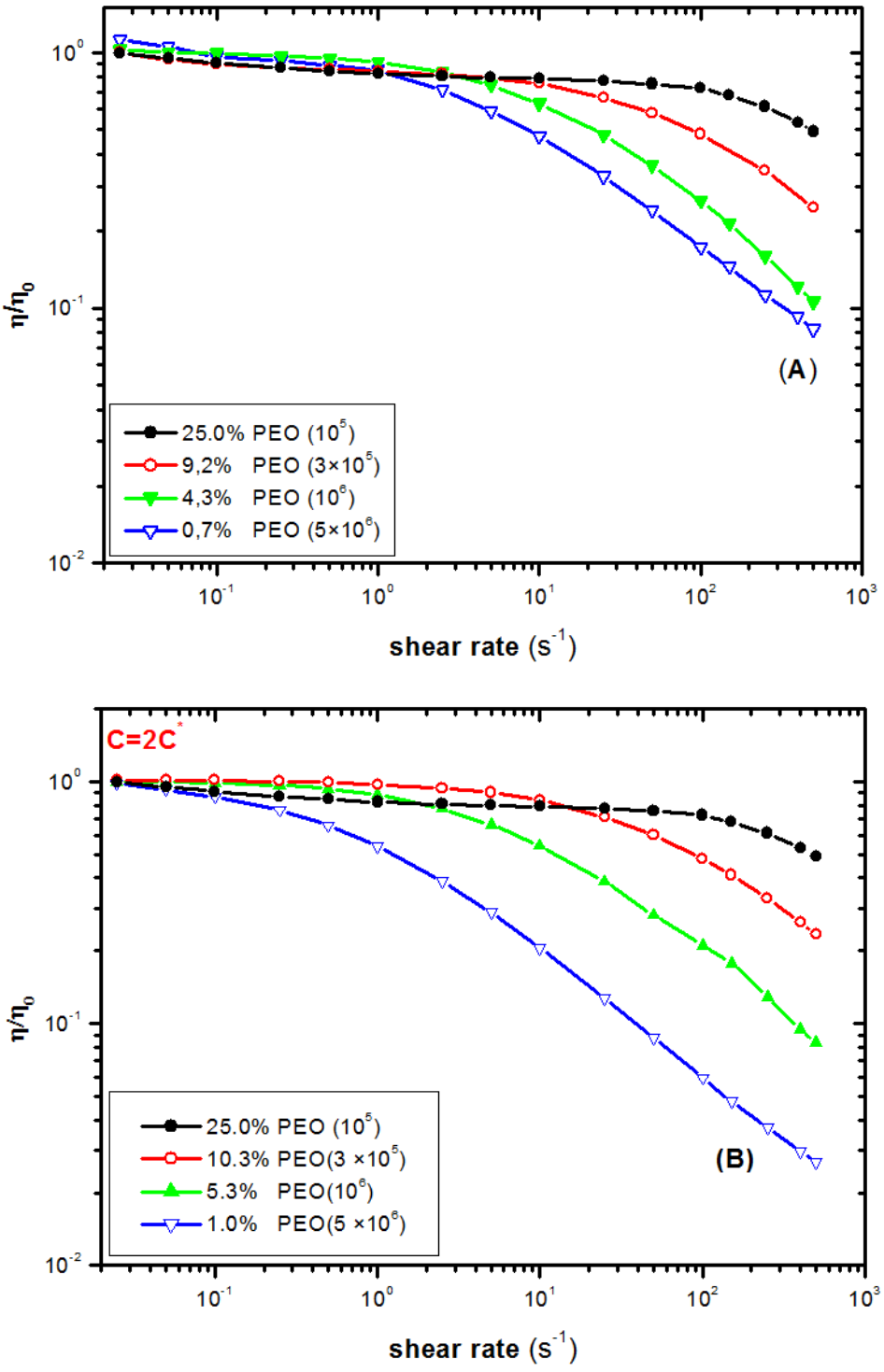

Figure III.1.3: Show the Zero shear viscosity as functions of shear rate: A) represent at η_0 =10 and B) C=2C*

The zero shear viscosities of PEO solutions have been reported in Figure III.1.4 as a function of polymer concentration. For the most concentrated solutions having a non-Newtonian behavior, it may be difficult to measure the value of the zero-shear viscosity. To obtain it, the

experimental data were fitted using the Bird-Carreau model (Equation III.1.1) to extrapolate zero-shear viscosities.

$$\eta = \eta_0 (1 + (\mathrm{K}\dot{\gamma})^2)^{(\frac{n-1}{2})} \qquad \text{eq.(1)}$$

The power law exponent is found to be equal to 0.88, 2.67 and 5.33 for PEO of 1.0×10^5 g/mol, as 1.67, and 4.34 for PEO of 3.0×10^5 g/mol, as 2.05, and 4.53 for PEO of 1.0×10^6 g/mol, and as 4.09, and 4.58 for PEO of 5.0×10^6 g/mol molecular weight. According to de Gennes's scaling concept, the polymer fully solubilized in the solvent can be classified into four regimes with the following exponents: dilute ($\eta \sim C^1$), semi dilute unentangled ($\eta \sim C^{1.25}$), semi dilute entangled ($\eta \sim C^{4.8}$), and concentrated regime ($\eta \sim C^{3.6}$)[135]. The entanglement concentration is the critical concentration between the semi dilute unentangled and the semi dilute entangled regime. Semi dilute unentangled and semi diluted entangled are under the regimes of $\eta \sim C^{1.1 \sim 1.4}$ and $\eta \sim C^{4.25 \sim 4.5}$, respectively[136,137]. In general, the scaling exponents depend on the polymer, polymer conformation, and the interaction between the polymer and the solvent. Factors such as branching or solubility[138, 139] result in different exponents.

In this study, the PEO polymer solutions of 1.0×10^5 g/mol with scales ~ $C^{0.88}$, $C^{2.67}$and $C^{5.33}$ were in the dilute, semi dilute unentangled, and semi dilute entangled regimes, respectively. The PEO polymer solutions of 3.0×10^5 g/mol with scales ~ $C^{1.67}$, and $C^{4.34}$, and of 1.0×10^6 g/mol with scales ~ $C^{2.05}$ and $C^{4.53}$, and of 5.0×10^6 g/mol with scales ~ $C^{4.09}$ and $C^{4.58}$ were under the regimes of semi dilute, unentangled and semi dilute entangled , respectively as shown in the (Figure III.1.4).

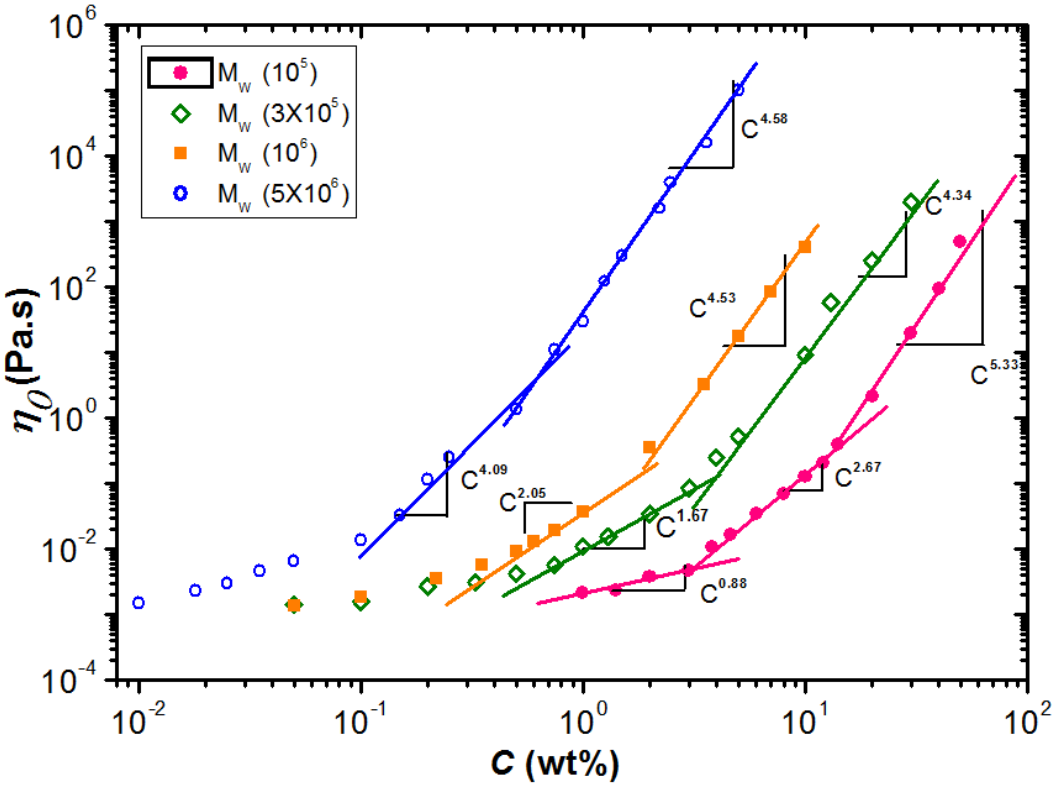

Figure III.1.4: Variation in zero-shear viscosity with concentration for the polymer solutions at different molecular weight (25 ℃)

3.1.1.1 Intrinsic Viscosity and Huggins Coefficient

The reduction of viscosity of PEO (M_w ~ 1.0×10^5) is defined as:

$$\eta_{red} = (\eta_0 - \eta_w)/\eta_w c \qquad \text{eq.(2)}$$

η_{red} : Reduced viscosity

η_0 : Zero-shear viscosity of polymer solutions

η_w : Newtonian viscosity of distilled water (0.97 mPa s) at 21˚C

c : Concentration

The reduced viscosity is illustrated in (Figure III.1.5) as a function of concentration c. The viscosity is defined with η_0 (the zero-shear viscosity of polymer solutions) and $\eta_w = 0.97$ mPa.s

(the Newtonian viscosity) of distilled water at 21°C. In the figure shows that dilute regime, of the reduced viscosity is correlated with nonlinear increasing function of the concentration. On the contrary, the inherent viscosity indicates the linear and slow decrement function. These phenomena are well described by the Huggins equation (1942):

$$\eta_{red} = [\eta] + k_H [\eta]^2 c \qquad \text{eq.(3)}$$

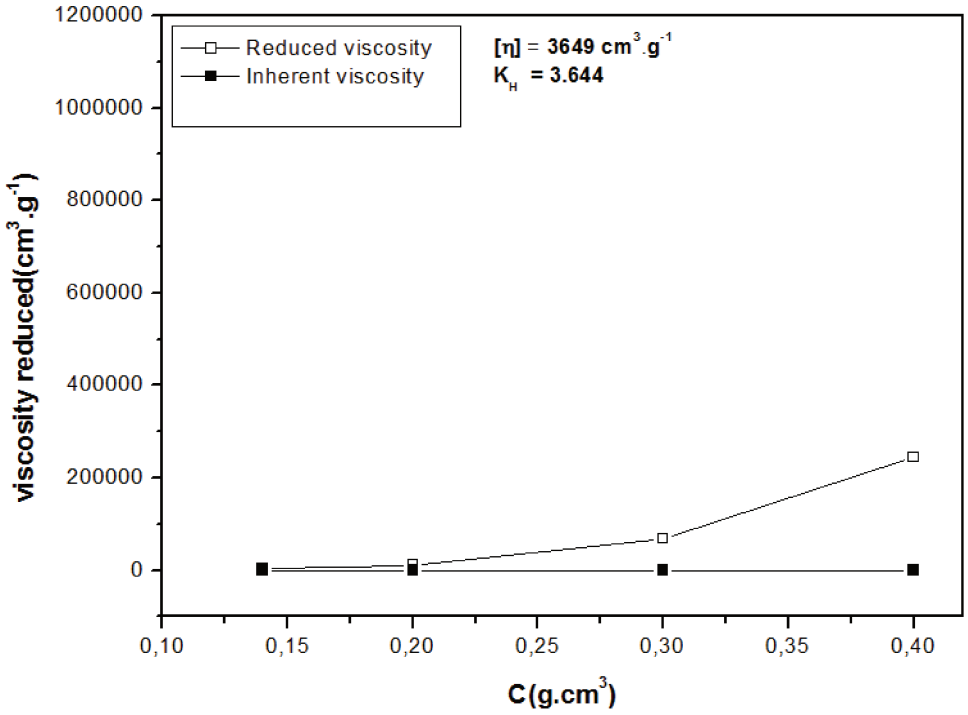

Figure III.1.*5: Reduced viscosity ηred* (□) *and inherent viscosity ln (ηrel)/c* (■) **of PEO (1.0×10^5 g/mol) solutions as a function of concentration. Intrinsic viscosities are the extrapolated values to zero concentration of the reduced viscosity and the inherent viscosity using linear fits

Where $[\eta]$ is the intrinsic viscosity and k_H the Huggins coefficient. The intrinsic viscosity, obtained from Figure III.1.5 by extrapolation of the reduced viscosity at zero concentration, is a unique function of the molecular weight for a given polymer–solvent pair. Alternatively, (η) can be obtained by fitting the inherent viscosity,

$\eta_{inh} = (\ln \eta_{rel})/c$ with the Kraemer equation

$$\frac{\ln \eta_{rel}}{c} = [\eta] - k_K [\eta]^2 c \qquad \text{eq.(4)}$$

Where,η_{rel} is the relative viscosity; $\eta_{rel} = \eta_0/\eta_w$

k_K is the Kraemer coefficient.

The intrinsic viscosity obtained from both Huggins and Kraemer representations is about 3649 $cm^3\ g^{-1}$.The intrinsic viscosity is related to the molecular weight M by the Houwink–Mark–Sakurada (HMS) equation:

$$[\eta] = KM^{\alpha} \qquad \text{eq.(5)}$$

The constant value K= (0.003644) $cm^3\ g^{-1}$ obtained in PEO solutions, with molecular weight ranging from 5.0M to 0.1M g/mol at 25°C[140].

3.1.1.2 Linear Viscoelastic Measurements and Relaxation Time Dynamics

In this dilute regime, where polymer chains are not entangled. However, the elongational stress that induced chain scission during stirring is most likely due to hydrodynamic forces transmitted by the suspending medium through friction. What happens in the concentrated regimes for which polymer chains are entangled? To answer this question, the rheological investigation was performed by linear viscoelastic measurements of PEO solutions at a concentration higher than 0.5 wt%, in order to measure viscoelastic response.

Figure III.6 shows the dynamic storage modulus G′ and loss modulus G″ as functions of angular frequency for the reference solutions of PEO ($M_w \sim 5.0 \times 10^6$) at 0.5 wt% and 1.0 wt%. It is evident that G′ and G″ with the increased angular frequency for all the samples (Figure III.1.6). This increased attributes due to low frequencies of the elasticity of the system dominates over the viscosity. The crossover of G′ and G″ where we obtained at the main relaxation time 0.081s in the system. On the other hands, the higher frequencies (Figure III.1.6) observed at the viscosity dominate region. Where the molecular chains had long enough time to rearrange, the samples behaved as a liquid and the predominant response to the imposed deformation is viscous response. As the shear frequency increased to exceed the frequency scale of molecular chain rearrangements, entanglements were somewhat stable and the samples were more like a solid. The crossover of G′ and G″ at intermediate frequencies (after log10)indicates concentrated solution or viscoelastic fluids or entangled systems[141].The linear viscoelastic

behavior is observed in dense macromolecular systems having a broad relaxation time distribution[142].

For 1.0 wt% PEO solution, the viscoelastic moduli is higher than those reported for 0.5 wt% solutions as shown in the (Figure III.1.6). This observation is valid in the whole explored frequency range (from 0 to 100 rad/s). A significant departure of G ´and G˝ moduli from the terminal zone was observed at lower frequencies of below 10.0 rad/s. Indeed, the pulsation dependence of viscoelastic moduli follows a power law of ω0.43 and ω0.58, respectively. A similar work was reported on the weaker power law dependence of viscoelastic moduli in the terminal zone. It has already been noticed for soft microgel suspensions of commercial associative guar gum[143].The fit of G´ and G ˝data using equations III.1.6 and III.1.7 were performed in order to monitor the concentration dependence of the longest relaxation time, ascribed to the slow dynamics of the longest molecular entities that are individual chains.

The linear viscoelastic behavior can be expressed as a function of a discrete spectrum using the generalized Maxwell model

Where the elastic modulus is defined as:

$$G'(\omega) = \sum_{t=1}^{m} G_i \frac{(\omega\lambda_i)^2}{1+(\omega\lambda_i)^2} \qquad \text{eq.(6)}$$

$$G''(\omega) = \sum_{t=1}^{m} G_i \frac{\omega\lambda_i}{1+(\omega\lambda_i)^2} \qquad \text{eq.(7)}$$

Where the elastic modulus is defined as:

$G'(\omega)$: Storage modulus

$G''(\omega)$: Loss modulus

Gi: Elastic modulus corresponding to a relaxation time

λ_i : Relaxation time

ω : Angular frequency

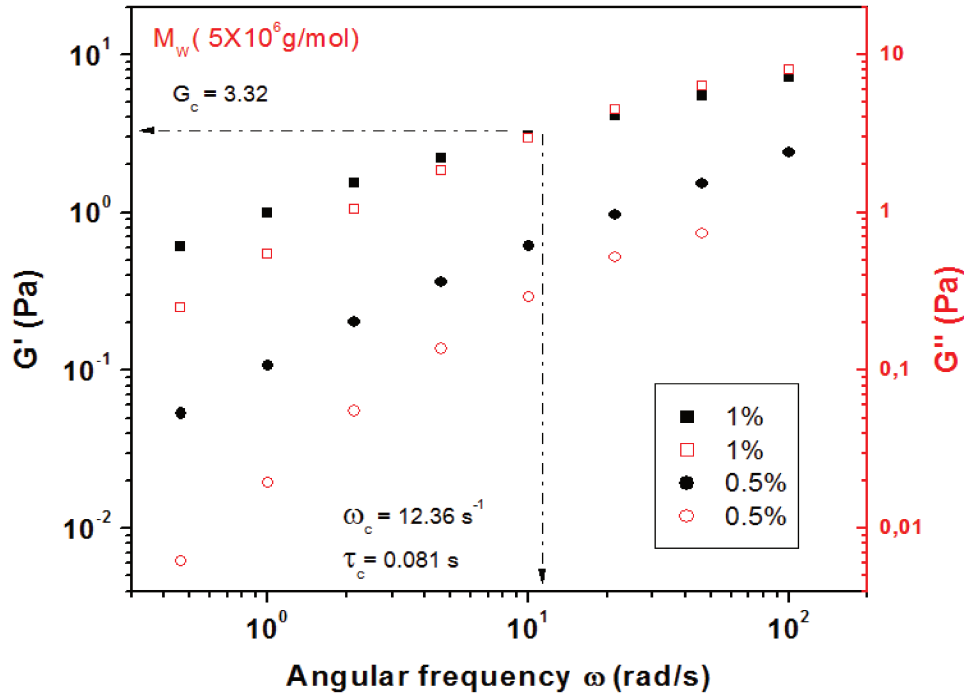

Figure III.1.6: Variation of G´ (■) *and G″*(□) as a function of ω in 0.5 wt% and 1.0 wt% PEO (5.0×10^6g/mole) solutions

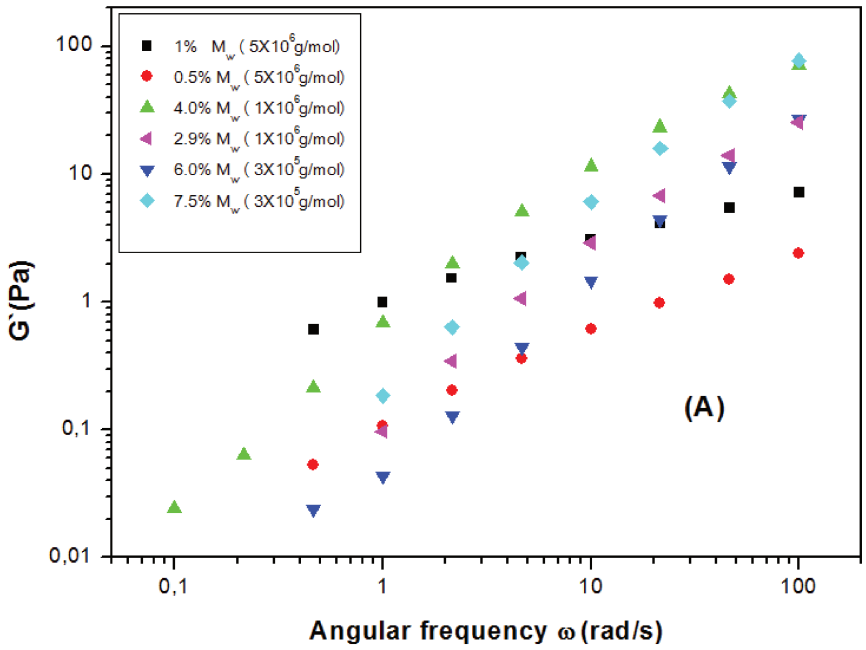

Figure III.1.*7A: Storage modulus G' as a function of* angular frequency for PEO solutions at 25C

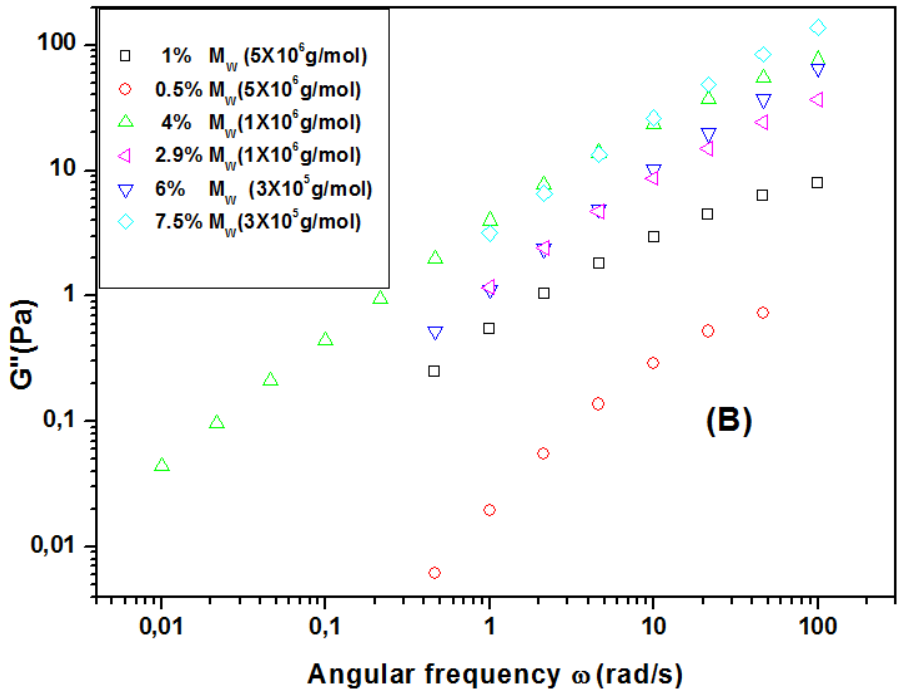

Figure III.1.7.B: loss modulus G″ as a function of angular frequency for PEO solutions at25C

Figure III.1.8 (A,B) use to evaluate the isothermal ,loss modulus and storage modulus data as a function of angular frequency for a 5.0 × 10^6 g/mol and 1.0 × 10^6 g/mol, respectively. In addition, range of temperatures used to exam the PEO melting at narrow distribution[144].The results indicated that the values converged to a single curve by means of a horizontal shift.

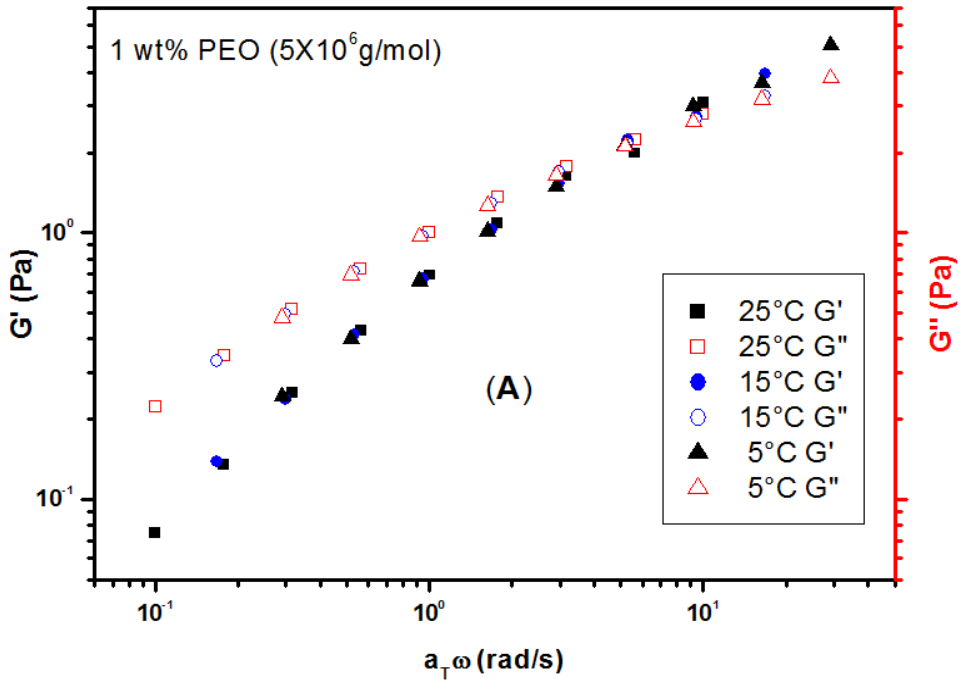

Figure III.1.*8A: Storage modulus G'* and loss modulus *G''* as a function of angular frequency for1.0 wt % (5.0 × 10^6 g/mol) polymer solution PEO at different temperature

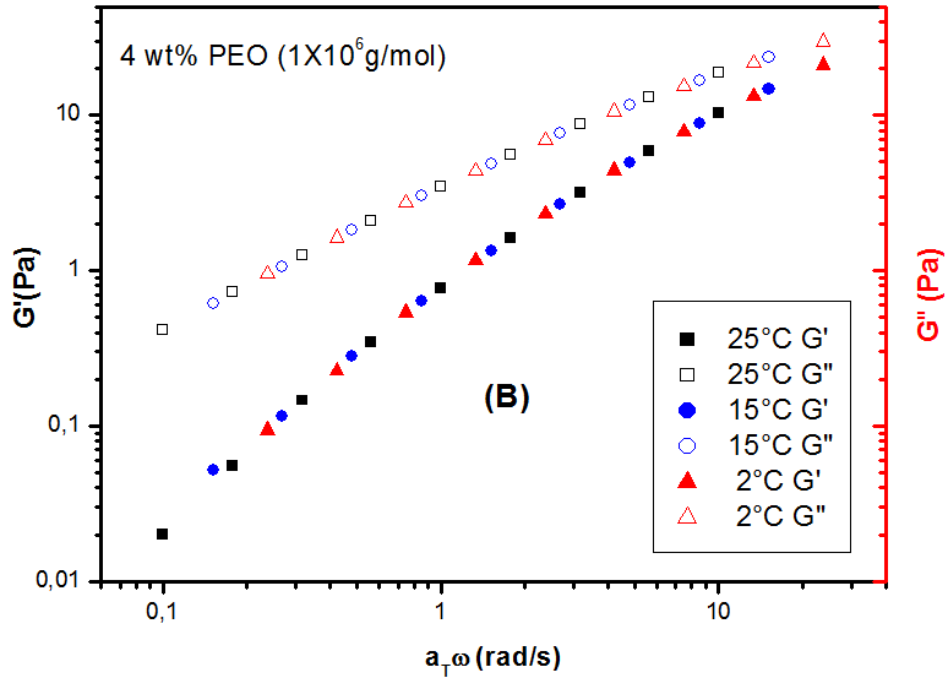

Figure III.1.8B: Storage modulus G *'and loss modulus G''as* a function of angular frequency for 4.0 wt% (1.0 × 10^6g/mol)

3.1.2 Characterization of Nanofibers

3.1.2.1Effect of Concentration and Molecular Weight on the Morphology of Nanofibers (Random deposition)

Studies have shown that the polymer concentration and molecular weight can significantly affect the electrospinning process as well as the diameter and morphology of the resulting fibers[145]. Hence, the effect of these parameters on electrospinning of PEO was systematically investigated as shown in Table III.1.2 and III.1.3. Different molecular weights for poly (ethylene oxide) polymers solutions (1.0×10^5, 3.0×10^5, 1.0×10^6, and 5.0×10^6 g/mol) at different solutions concentrations for each polymer were used to evaluate the effect on fiber formation. (See table III.1.1)

Table III.1.1: Samples preparation used with a different molar weight of PEO.

Molar weight, M_w (g/mol)	Concentration, (w/w) %
1.0×10^5	8.0,10.0,14.0,20.0
3.0×10^5	6.0,7.5,9.2,10.3
1.0×10^6	2.9,4,4.3,5.35,
5.0×10^6	0.5,0.7,1.0

The electrospun PEO SEM images analyses were performed at different concentration of PEO to reveal the change of the morphology of the obtained nanofibrous structure as shown in Figures (III.1.10, III.1.11, III.1.12, and III.1.13).

Figure III.1.10 shows a selected series of scanning electron microscope in order to illustrate the effect of the concentration of PEO solutions on the morphological appearance of obtained nanofibrous materials. At low concentrations (from 8.0 to10.0 wt %) or low viscosities (0.07 to 0.13 Pa.s), a large number of beads were observed (Figure III.1.10 a, III.1.10 b). On the contrary, the PEO solution which have a higher concentration produced nanofibers without beads. Empirical evidence reported by number of authors indicates that by increasing the solution concentration, transitions occur from beads to beaded fibers to homogeneous fibers[50, 62]. As an example, the studies showed that varying the viscosity of polyethylene oxide (PEO) (M_W : 9.0×10^5 g/mol) in water from 13 to 1250 cP by increasing the solution concentration

from 1.0 to 4.0 wt%, transitions from beads to uniform nanofibers could be effectively achieved[146].

The formation of beads along the electrospun fibers could be a result of a number of affecting phenomena. For-instance, it could be a result of the viscoelastic relaxation and the work of the surface tension upon the reduction of the Coulombic force once the fibers are in contact with the grounded target that drives the formation of the beads[146].This phenomenon would only occur when the charged jet was not ‘‘dried” enough prior to its deposition on the target, causing some parts of the partially discharged jet to contract and form beads. As soon as the collected jet is ‘‘dried’’ enough, contraction can no longer occur any more, thus leaving only beaded fibers on the target. The ‘‘dryness’’ of the charged jet is controlled mainly by the amount of solvent that can evaporate during the flight of the charged jet to the target. The amount of evaporating solvent is determined by a number of factors such as the boiling point of the solvent, the initial concentration of the solution, the solution and the ambient temperatures, the diameter of the charged jet which continuously decreases during its flight to the target and the total path length that the charged jet travels from the nozzle to the target which significantly depends on the extent of the bending instability[2, 82] that occurs.

At such low viscosities, the viscoelastic force (a result of the low degree of chain entanglements) in a given jet segment was not large enough to counter the higher Columbic force, resulting in the break-up of the charged jet into smaller jets, which, as a result of the surface tension, were later rounded up to form droplets. This phenomenon has been familiarized in industry as the electro spraying process and has commonly been used in many applications such as paint spraying, ink-jet printing and powder coating[147].

At higher concentrations or higher viscosities, the charged jet did not break up into small droplets. This caused a direct result to increase the chain entanglements, which were sufficient to prevent the break-up of the charged jet and to allow the Columbic stress to further elongate the charged jet during its flight to the grounded target. At end, this make the collected fibers thinned down to nan-scale diameter[50]. An increased in the concentration of the solution from 10.0 wt% to 14.0 wt% (or the viscosity to 0.4 Pa.s) resulted in the reduction disappearance of the beads, leads to produce beads free fibers (Figure III.1.10c). However, the concentration of the solution was increased to 20.0 wt% (or the viscosity to 2.2 Pa.s), the beads disappeared altogether, leaving only smooth ultrafine nanofibers on the target (Figure III.1.10d).

In Figures III.1.11, and III.1.13. We found the form of fibers gradually increased from beads to uniform fibers with increasing of concentration and molecular weight. The average diameter at different concentration and different molecular weight measured by image j.

In the Figure III.1.12, the product of electrospinning varies at the different concentration and molecular weight representing fibers and beads. At 2.9 wt% concentration, may not be enough resulting beadles fibers formation (Figure III.1.12a). A possible reason for such an observation is that at low concentrations and viscosity, fibers will break up into droplets before reaching the collector due to the effects of surface tension[148]. Upon an increase in polymer concentration to 4.0 wt% and thus by an increase in viscosity, the beads decreased, uniform fibers with few elongated beads were observed compared to the lower concentration of 2.9 wt% (Figure III.1.12b). More uniform fibers and the thicker diameters of fibers were formed with the increase of the PEO concentration[80].The fiber diameter of the 5.35 wt% concentration of PEO nanofibers has around 17 nm difference compared to the lower concentration of 4.3 wt% (Figure III.1.12c, III.1.12d) .This may be due to fiber diameter also increased with viscosity. It is widely reported that higher concentrations result in larger fiber diameters[76, 93].

Some of the possible reason of this reduction of beads and formations of fine fibers trends are supported by two instabilities acting on the polymer solution jet. These are axisymmetric varicose instability (Rayleigh instability) and non- axisymmetric whipping instability[149, 150].The former results from the surface tension of the solution, which tends to minimize the surface area by forming individual droplets. The latter is produced due to the presence of the electrostatic field. This causes bending and stretching of the jet through a rapidly spiraling motion, which is required for the development of ultra-fine fibers. Which of these instabilities dominates depends on the factors related to solution properties and operating conditions. These are solution viscosity, conductivity, surface tension, and the strength of the applied electric field[149, 150].

For a given molecular weight, the chain entanglements are increased with polymer concentration[16, 17]. Therefore; an increased in concentration generally results in the following progression in fiber morphology[15, 16, 151] : beads only, beaded fibers, nanofibers, and globular fibers or macro beads. This last result is due to the entanglements being so high that in many regions the chains are not able to slip apart adequately to form uniform fibers. The second key parameter that affects the morphology of the fibers is the solution conductivity[20, 71]. Fluids with high conductivity have high surface charge density. Under a given electric field, this causes

an increase in the elongational force on the jet, as an effect of the self-repulsion of the excess charges on the surface. This inhibits the Rayleigh instability, enhances whipping and leads to finer and more uniform fibers[150].

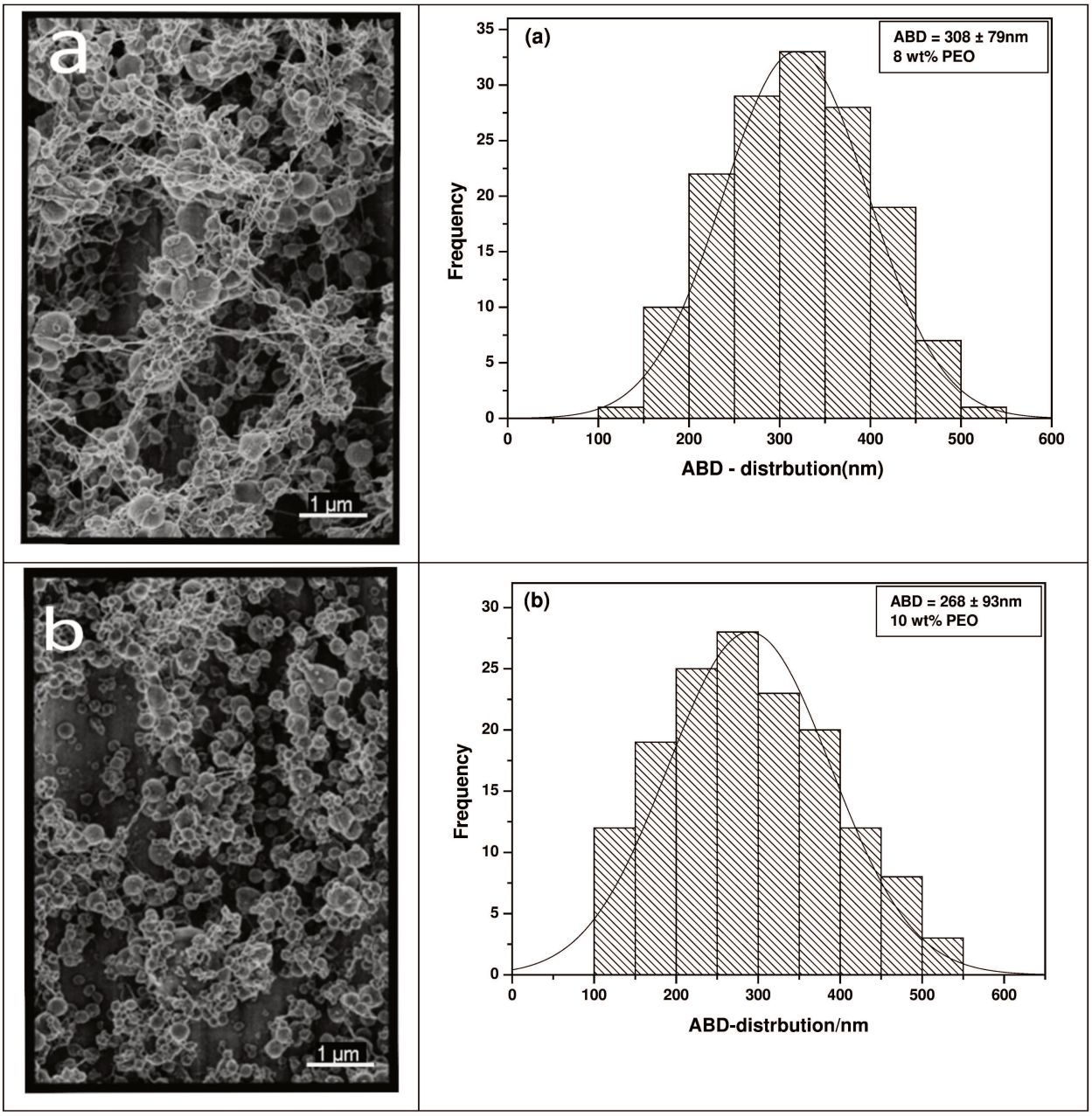

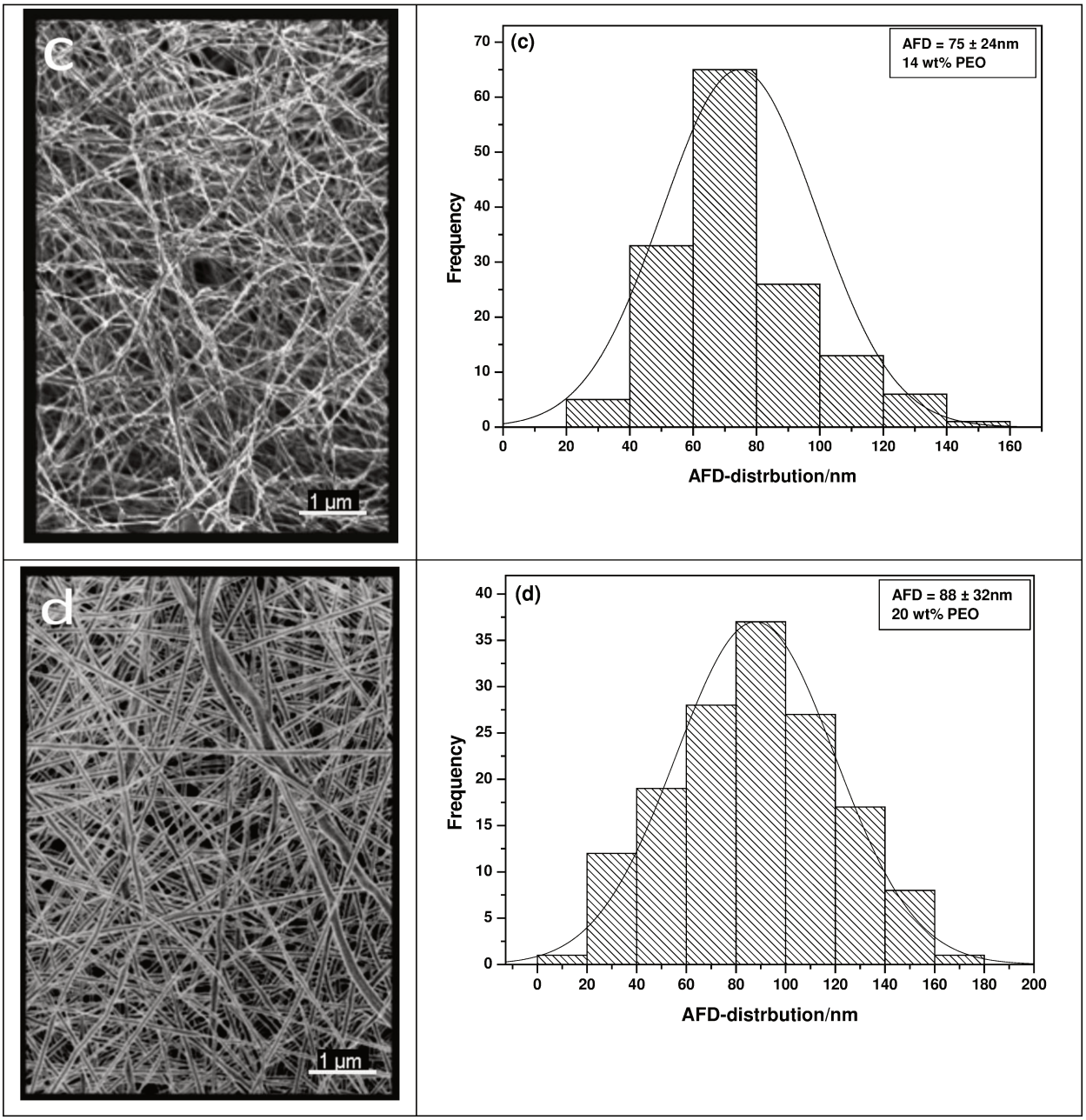

Figure III.1.10: SEM representative images and fibers /beads diameter distributions of the electrospun PEO (Mw ~10^5g/mole): a) Average beads connector fibers diameter [AFD*] = (308 ± 79) nm, b) AFD*= (268 ± 93) nm

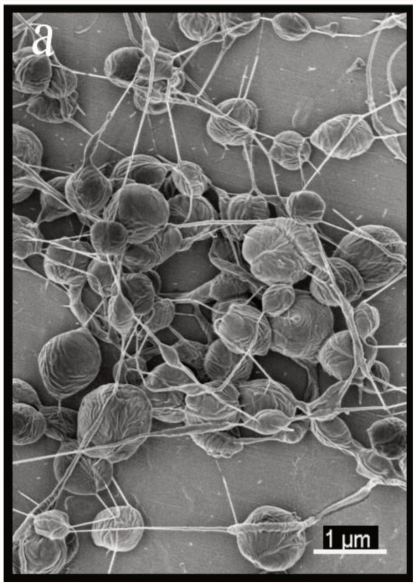
a
1 µm

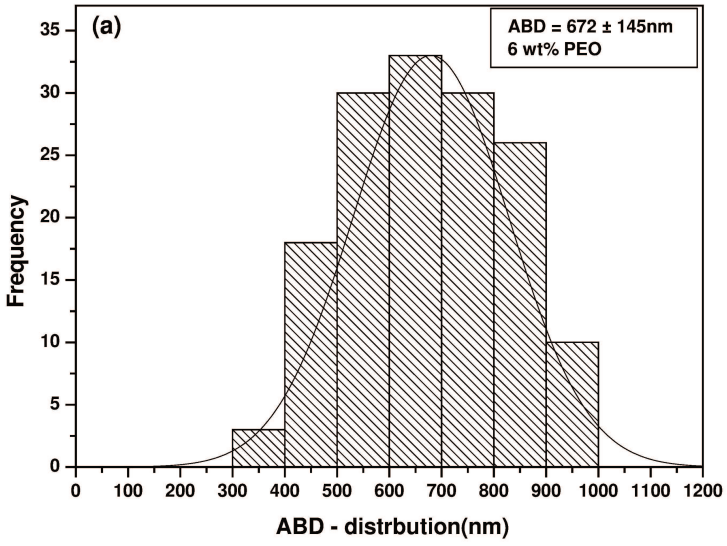
(a)
ABD = 672 ± 145nm
6 wt% PEO
Frequency
ABD - distrbution(nm)

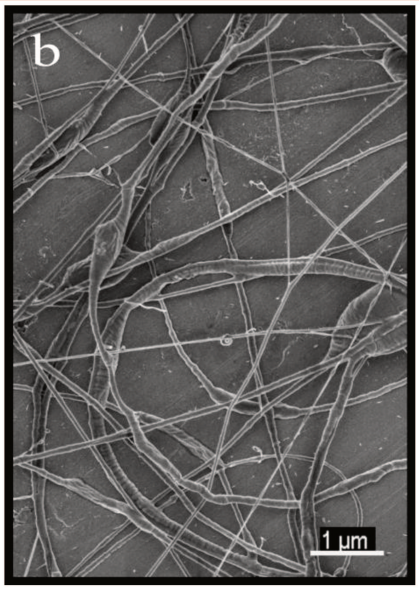
b
1 µm

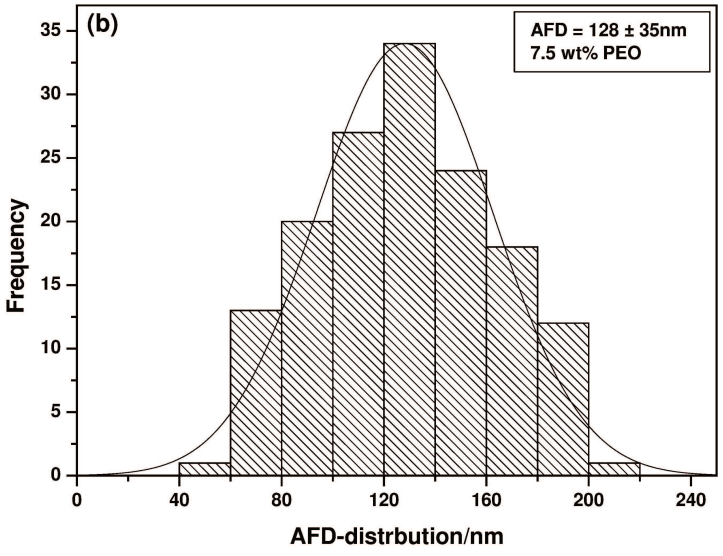
(b)
AFD = 128 ± 35nm
7.5 wt% PEO
Frequency
AFD-distrbution/nm

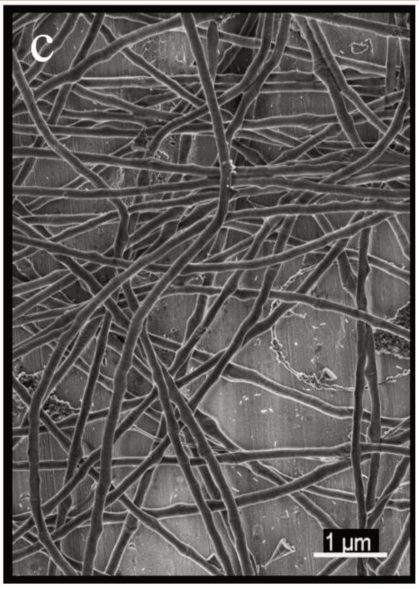
c
1 µm

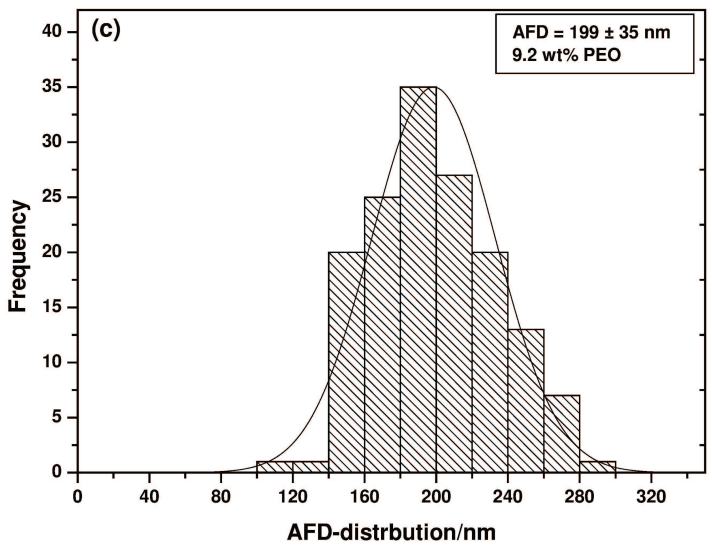
(c)
AFD = 199 ± 35 nm
9.2 wt% PEO
Frequency
AFD-distrbution/nm

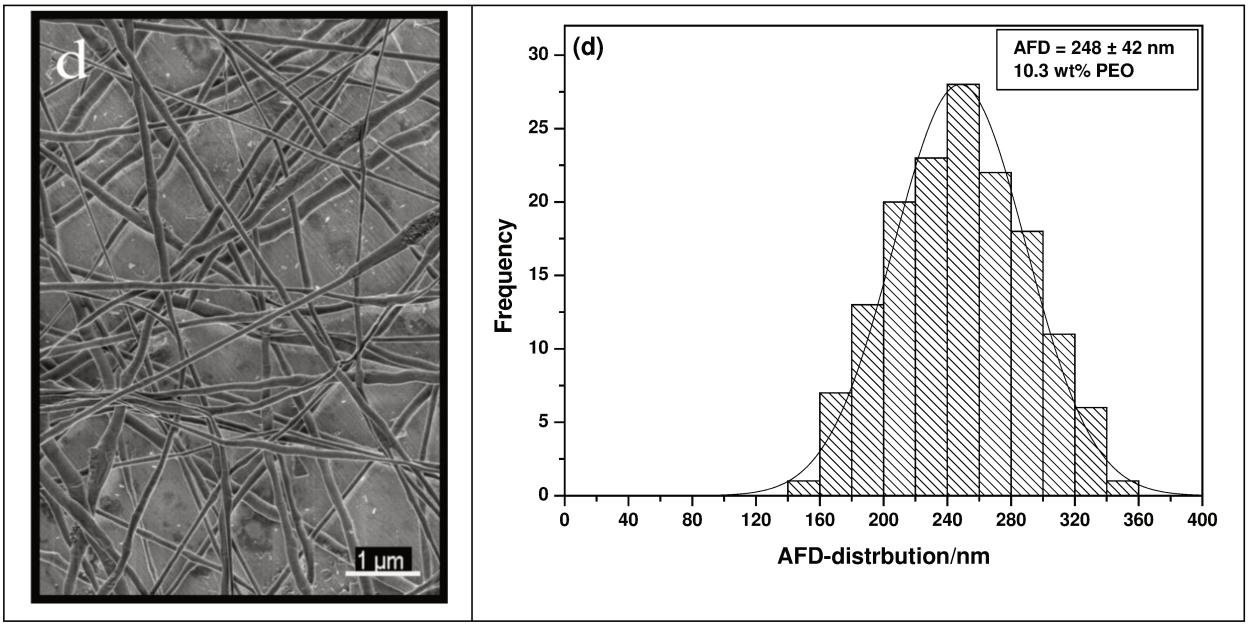

Figure III.1.11: SEM representative images and fiber/beads diameter distributions of the electrospun PEO (Mw ~ 3.0 x 10^5g/mole): a) Average beads connector fibers diameter [AFD*] = (672 ± 145) nm


a
1 µm

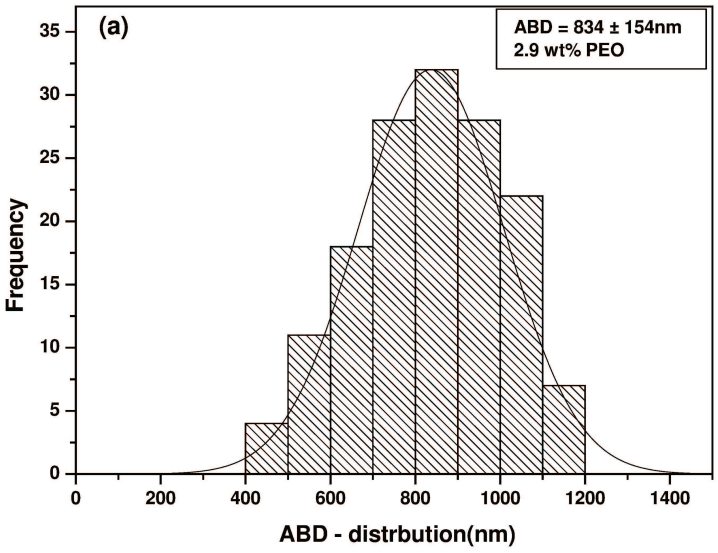
(a)
ABD = 834 ± 154nm
2.9 wt% PEO
Frequency
ABD - distrbution(nm)

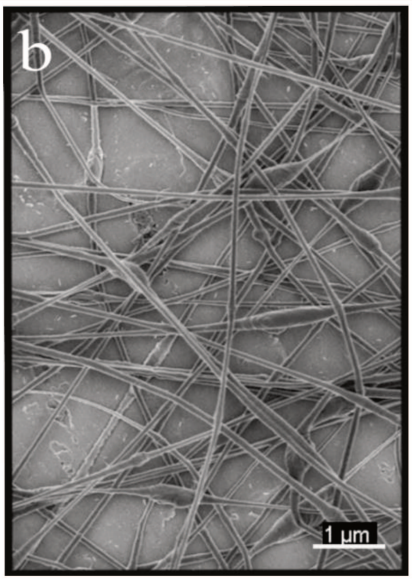
b
1 µm

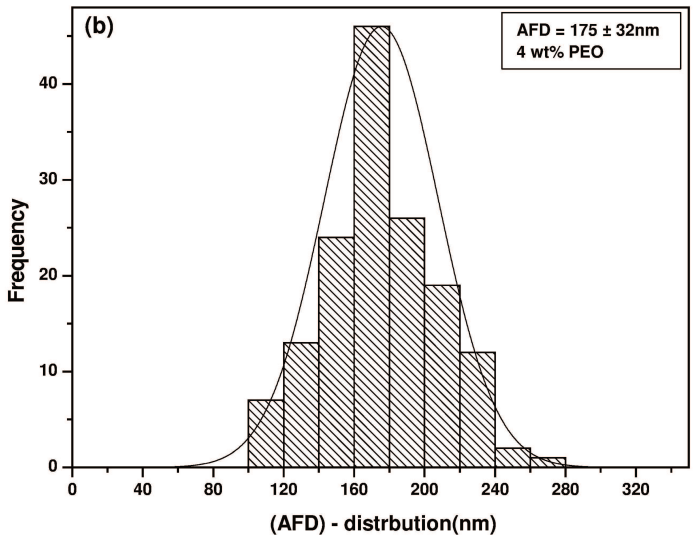
(b)
AFD = 175 ± 32nm
4 wt% PEO
Frequency
(AFD) - distrbution(nm)

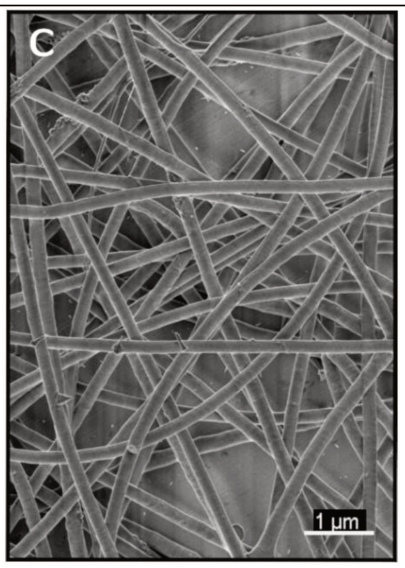
c
1 µm

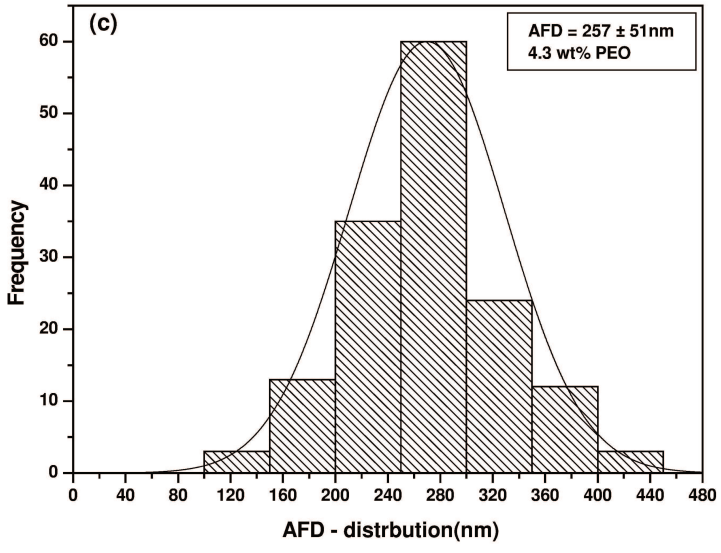
(c)
AFD = 257 ± 51nm
4.3 wt% PEO
Frequency
AFD - distrbution(nm)

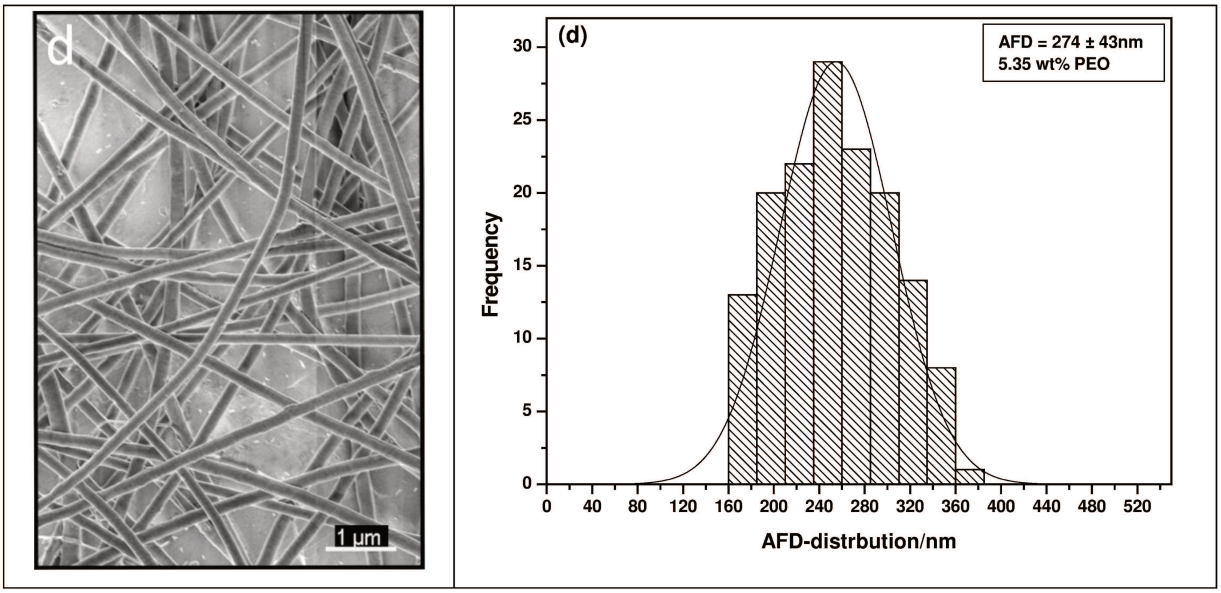

Figure III.1.12: SEM representative images and fibers diameter distributions of the electrospun PEO (Mw ~ 1.0×10^6 g/mol): a) Average beads connector fibers diameter [AFD*] = (834 ± 154) nm

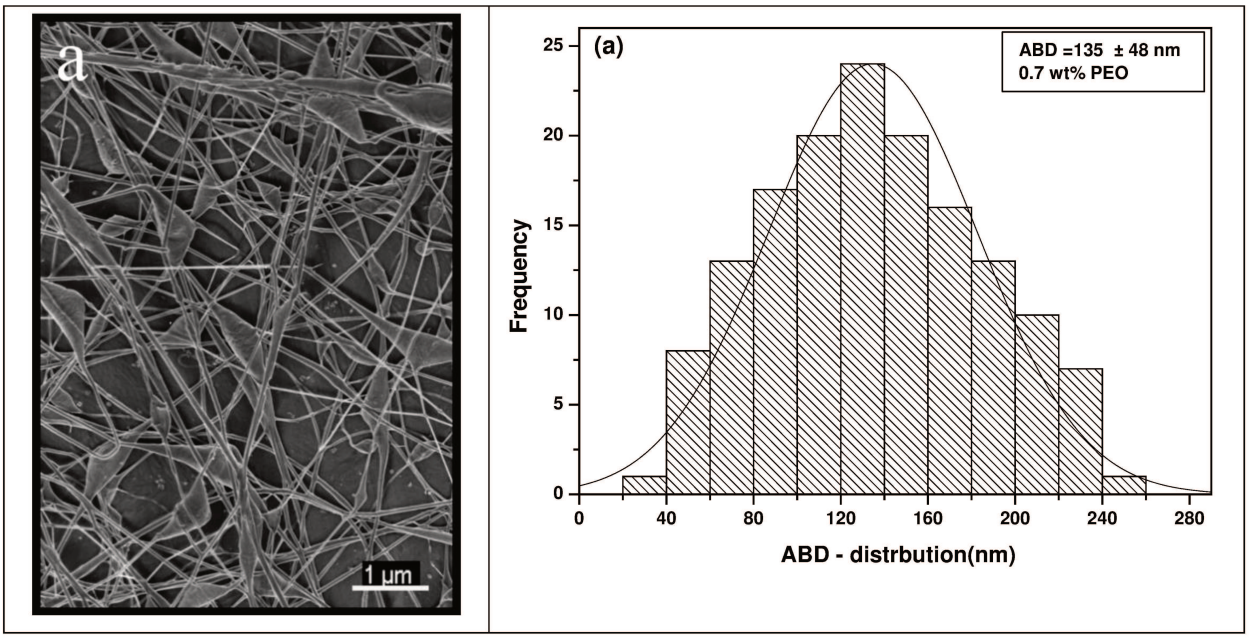

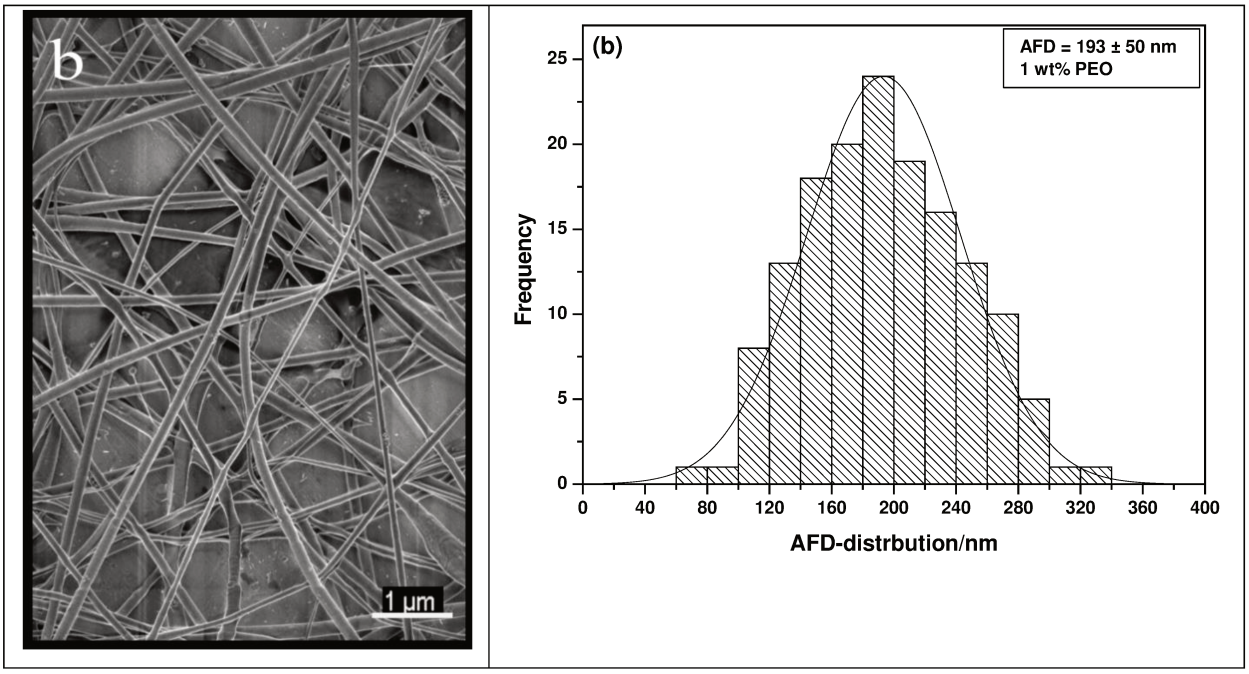

Figure III.1.13: SEM representative images and fiber diameter distributions of the electrospun PEO (Mw ~ 5.0×10^6 g/mole)

3.1.2.2Fibers Diameter Distribution

A single jet ejecting from the Taylor cone can possibly split or break up into beaded fibers or droplets if the entanglement chain is not strong enough to make pure fiber. In the course of electrospinning, the higher concentration solutions does not leads to split the jet due to sufficient chain entanglement. However, it targeted to form larger diameter fibers. Therefore, the different chain entanglement densities ultimately determined whether beaded fibers or a droplets formation at different diameters based on solution concentration. The four PEO (molecular weight 1.0×10^5, 3.0×10^5, 1.0×10^6 and 5.0×10^6 g/mol), have very comparable fiber diameter dependence on the concentration.

The fiber diameter increased from (128 ± 35), (199 ± 35) to (248 ± 42) nm on increasing PEO concentration from 7.5, 9.2 to 10.3 %, respectively (Figure III.1.14).As the concentration of the solution, increases the fiber diameter increased and the diameter range is broadened figures III.1.15 and III.1.16. This behavior can be related to the fact that an increase in polymer concentration causes an increase in viscosity, which in turn causes the splay (formation) of thicker fibers[148]. Higher polymer concentration means there is high viscous force within the solution and there are more molecules aggregated. Because of high aggregation of molecules,

it is difficult to split them. Lower viscous solutions are easy to split and they are much easier to splay to form fibers. Hence, lower polymer solution concentration yields lower diameter fibers[92].

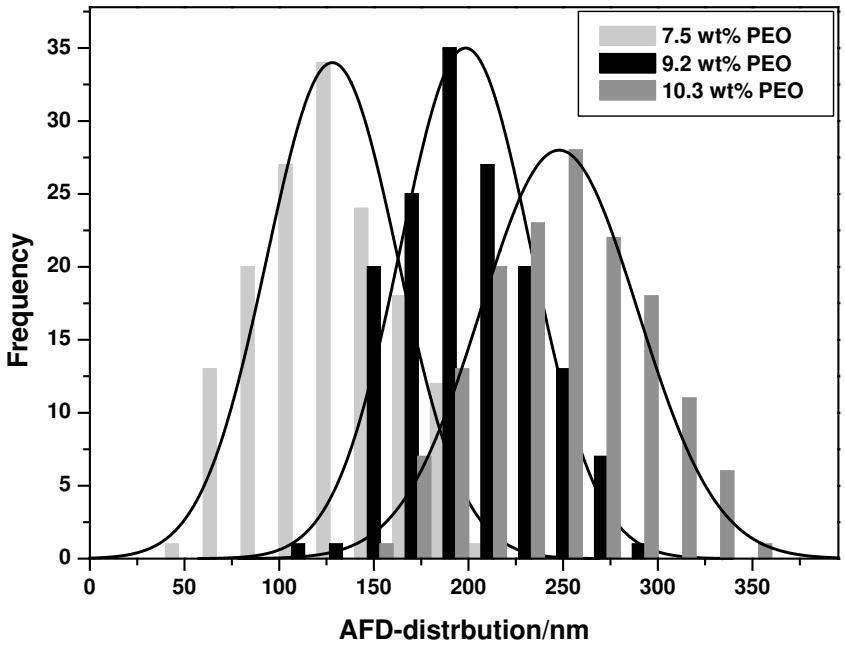

Figure III.1.14: The average of diameter distribution of 7.5 wt%, 9.2 wt% and 10.3 wt% of PEO ~ 3.0×10^5g/mol

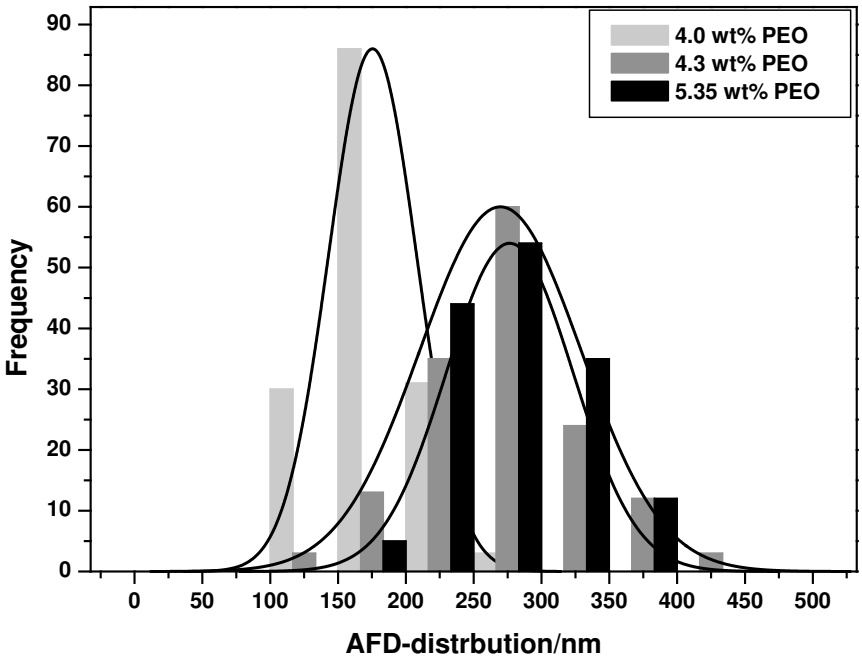

Figure III.1.15: The average of diameter distribution of 4.0 wt%, 4.3 wt% and 5.35 wt% of PEO ~ 1.0×10^6g/mol

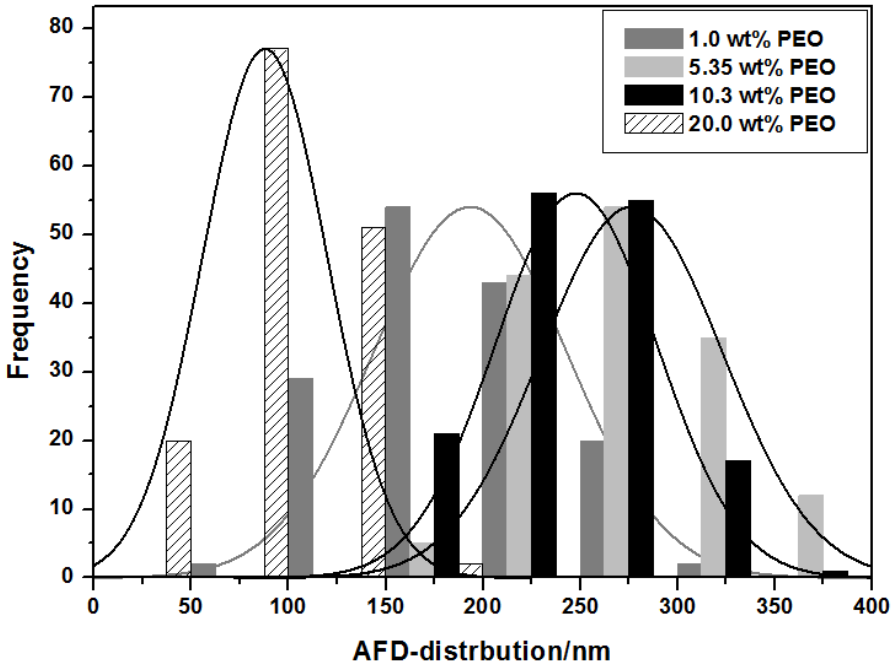

Figure III.1.16: The average of diameter distribution of 20.0 wt%, 10.3 wt%, 5.35 wt%, and 1.0 wt% of PEO ~ 1.0×10^5, 3.0×10^5, 1.0×10^6, and 5.0×10^6 g/mol respectively

3.1.3 Effect of Molar Weight and Concentration on Surface tension and Viscosity

The viscosity, net charge density, and surface tension of solution are key parameters for the formation of the stabilized jets[126].The results in the Table III.1.2 depict the direct relation of concentration and viscosity on the increased AFD of PEO. For instance, increasing of the concentration PEO solutions (1.0×10^5 g/mol) from 17.5 to 25.0 wt% leads increasing of viscosity and AFD from 0.99 to 5.36 Pa.s and 128.0 to 203.0 nm, respectively. In the same case (3.0×10^5 g/mol) from 7.50 to 10.30 wt% increased the viscosity and AFD from 3.17 to 5.92 Pa.s, and 179.0 to 243.0 nm, respectively. PEO solutions (1.0×10^6 g/mol) with concentration increment from 4.0 to 5.35 wt% leads also to increase the viscosity and AFD from 4.59 to 11.93 Pa.s, and 175.0 to 274.0 nm, respectively. For (5.0×10^6 g/mol) at a concentration range from 0.70 to 1.0 wt% possessed the viscosity and AFD from 0.45 to 2.46 Pa.s and 135.0 to 193.0 nm, respectively. These behaviors can be related to the fact that an increase in polymer concentration causes an increase in viscosity, which in turn causes the splay (formation) of thicker fibers[83]. Higher polymer concentration means there is high viscous force within the solution and there are more molecules. Because of high of molecules, it is difficult to split them.

Lower viscous solutions are easy to split and they are much easier to splay to form fibers. Hence, lower polymer solution concentration yields lower diameter fibers.

Surface tension of these concentrations of PEO was measured in order to investigate the influence of the molecular weight. At 3.0×10^5, and 1.0×10^6 g/mol molecular weights, surface tension almost remains constant at a value of 37.0 and 33.0 mN/m with a deviation of 0.74 and 0.67, respectively. However, slight difference was noticed at 1.0×10^5, and 5.0×10^6 g/mol molecular weights (Table III.1.2). The results of Table III.1.2 show that with increasing molecular weight and concentration change in surface tension is insignificant. In general, surface tension has invers related with the increase of molecular weight and concentration of the PEO solutions as shown in the Table III.1.2. This slightly inverse relation has happen due to a drop of polymer on a horizontal surface is flattened rather then spherical. This is due to the force of gravity. Other factors that cause the droplet to flatten on the surface include higher liquid density, decrease in surface tension and increasing the volume of the droplet[152].

Table III.1.2: Molecular weight, concentration, surface tension, viscosity, and average fiber diameter (AFD) of electrospun of PEO at 25°C.

Molecular Weight (g /mol)	Concentration (W/W %)	Surface tension ($mN.m^{-1}$)	Viscosity (Pa.s)	AFD (nm)
1.0×10^5	17.50	35.03 ± 0.4	0.99	128.0 ± 69
	25.00	32.05 ± 0.2	5.36	203.0 ± 73
3.0×10^5	7.50	38.21 ± 1.2	3.17	179.0 ± 73
	9.20	37.76 ± 0.9	3.96	189.0 ± 29
	10.30	37.13 ± 0.8	5.92	243.0 ± 39
1.0×10^6	4.00	33.00 ± 0.4	4.59	175.0 ± 32
	4.30	33.10 ± 0.2	5.75	257.0 ± 51
	5.35	33.81 ± 0.7	11.93	274.0 ± 43
5.0×10^6	0.70	35.38 ± 1.7	0.45	135.0± 48
	1.00	32.26 ± 1.1	2.46	193.0 ± 50

3.1.4 Electrospun Processing Parameters

The most influential spinning parameters are the concentration of polymer solutions, voltage, collector distance and the injecting rate. Each of these parameters significantly influences the morphology of fibers obtained by electrospinning. A proper handling of these parameters provides nanofibers morphology and desired diameter. The parameters used are shown in Table III.1.3.

Table III.1.3: Processing parameters used in the experimental study.

Molecular Weight (g /mol)	Concentration (W %)	Distance (cm)	Voltage (kV)	Flow rate (mL /h)	Observations (with SEM)
1.0×10^5	8.0	24.0	-8.50,+10.85	0.04	Beads
	10.0	27.0	-10.2,+11.49	0.06	Beads
	14.0	30.0	-9.72,+10.32	0.02	Fibers
	20.0	32.0	-8.25,+9.560	0.04	Fibers
3.0×10^5	6.0	24.0	-11.6,+11.60	0.08	Beads
	7.5	24.0	-11.6,+11.56	0.06	Fibers
	9.2	30.0	-10.6,+12.48	0.08	Fibers
	10.3	32.0	-10.5,+12.16	0.08	Fibers
1.0×10^6	2.9	25.0	-10.9,+10.79	0.04	Fibers
	4.0	32.0	-10.0,+11.90	0.06	Fibers
	4.3	32.0	-10.5,+12.15	0.06	Fibers
	5.35	32.0	-9.79,+10.11	0.09	Fibers
5.0×10^6	0.7	32.0	-6.41,+5.24	0.1	Fibers
	1.0	32.0	-3.86,+4.32	0.1	Fibers

The distance between the tip of the capillary and the grounded plate can have a significant impact on morphology of electrospun nanofibers. Four different distances were chosen 24.0, 27.0, 30.0, and 32.0 cm between the tip of the needle and the grounded plate. For a particular molecular weight, other parameters such as concentration, voltage and feed rate were from 0.7 wt% to 20.0 wt%, 11.60 to ± 12.48 kV and 0.02 to 0.1 μL/h respectively. As the distance between the tip and grounded plate increased, more uniform and smaller AFD without beads nanofiber were obtained in all PEO sample. In Table III.1.3 shows, the trend observed for the PEO samples. The distance increased a progressive reduction in bead occurrence and an increase in fiber concentration is observed, applied voltage.

3.1.5 Porosity

One of the key characteristics of membranes for the specific end-use of tissue engineering is the porosity and pore size distribution. A natural phenomenon occurs during cellular proliferation when a fibrous material is present in the cellular culture[153].The cells tend to grow along the fibers. Many researchers believe the structure, shape, and orientation of the fibers can influence the cellular growth and direction.

Because the overall porosity could not be measured directly, indirect calculation was used to determine the theoretical porosity using the density of the polymer and the density of the membrane. The overall porosity was reported as a percentage.

$$\text{Membrane apparent density (dm)} = \frac{Mm/(A \times t)}{dp} \qquad \text{eq.(8)}$$

$$\text{Porosity (P)} = \left(1 - \frac{dm}{dp}\right) x100 \qquad \text{eq.(9)}$$

Where,

dm= Density of the membrane (g/cm^3)
dp = Density of the polymer (g/cm^3)
Mm= Mass of the membrane (g)
A = Area of membrane (length x width) (cm × cm)
t= Thickness of the nanofibrous membranes

The thicknesses of the nanofibrous membranes were measured by a digital micrometer (Mitutoyo IP65, Japan) with an accuracy of ± 0.001 mm. These thickness measurements were used to calculate the membrane apparent density using equation (III.1.8), values of which were used to calculate the membrane porosity according to equation (III.1.9).

The density of the polymer (dp) was found in the literature and reported as 1.13, 1.21 g/cm^3. The mass of the membranes was measured gravimetrically at the time of collection using a scientific balance accurate to ± 0.01mg.The membrane porosity results were calculated as the average ± standard deviation.

TableIII.1.4: Reports the molecular weight, concentration, mass, thickness of the electrospun membranes and the porosity of the membranes.

Molecular Weight (g /mole)	Concentration (W/W %)	Mass (g)	Thickness (cm)	Porosity (%)
1.0×10^5	25.00	0.00053	0.9	93.70
3.0×10^5	7.50	0.00014	0.85	80.00
	10.30	0.00059	0.91	91.70
1.0×10^6	4.00	0.00042	0.92	90.20
	5.35	0.00051	0.95	91.60
5.0×10^6	1.00	0.0005	0.71	92.40

3.1.6 Elongational Rheometry

The earliest determinations of elongational viscosity were made for the simplest case of uniaxial extension. Trouton [154] and many later investigators James and Walters[155] found that for incompressible Newtonian liquids, the elongational viscosity ηE is three times the shear viscosity ηS. Many materials including polymer melts and solutions exhibit shear thinning in shear and strain hardening in uniaxial extension. Even low to medium viscosity solutions may exhibit significant strain hardening effects if they include small amounts of high molecular weight polymer[156].

Several devices for measuring the elongational viscosity of polymer solutions have been developed during the last decades. These techniques are often constrained by the difficulty of establishing and maintaining a uniform elongational flow field for long enough that a steady state can be reached[157]. The review of James and Walters[155] surveys the difficulties inherent with devices such as opposed jet rheometers and contraction geometries. The experimental time and strain windows in the region of strong extension are limited and the path of a typical fluid element does not provide a motion with constant stretch history. Filament stretching devices have their genesis in the work of Matta and Tytus[158] who suggested the use of a small cylindrical mass accelerating freely under gravity to stretch a small liquid bridge connecting the mass to a stationary support.

The technique has been applied to various kinds of complex fluids including carbon nanotube suspensions[159], concentrated emulsions[160], cross linked polymeric thickener solutions [161], or wormlike micellar solutions [162].But over the years, a strong focus was on weakly elastic fluids including aqueous solutions of poly (ethylene oxide) (PEO)[163].

These fluids form uniform, exponentially thinning cylindrical filaments; thus, the elongation rate $\varepsilon$is constant throughout the filament and also in time. These fluids clearly exhibit strain hardening. However, the calculation of an elongational viscosity is not straightforward since the stress in axial direction is not known. Nevertheless, a relaxation time λE characterizing the exponential decay of the filament diameter can be extracted.

PS Boger fluids with concentrations c around the critical over lap concentration c$*$ elongational relaxation times λE close to the longest Zimm relaxation time λZ were found by Bazilevskii et al.[164], and for a PEO solution with c $\approx$ c$*$ Oliveira et al.(2006) report λE $\approx$ λS, were λS is the longest relaxation time obtained from small amplitude oscillatory shear. On the other hand, it has been clearly shown for PEO as well as PS solutions that the elongational relaxation time can vary significantly with concentration even far below c$*$, and values $1 < \lambda E/\lambda Z < 10$ were reported for $0.01 < c/c* < 1$, but also $\lambda E/\lambda Z < 1$ are documented for very dilute solutions down to concentrations of 0.2 ppm[164].

So far, little is known about the relationship between shear and elongational relaxation time (as deduced from CaBER) for semi-dilute and concentrated solutions with c >>c$*$. For wormlike micellar surfactant solutions, $\lambda E/\lambda S \approx 1/3$ has been reported[165], which might be attributed to a breakup of micelles and structural changes in strong flows of these solutions.

It may be either due to flow-induced structural changes like breakup of aggregates/complexes or a limited extensibility of these objects due to internal attractive interactions not present in solutions of linear flexible polymers.

The finding that $\lambda E/\lambda S$ strongly decreases with increasing concentration, and discussed the relationship between λE and λS on the basis of a simple integral constitutive equation using a single relaxation time and a damping function h to account for the effect of the large deformations present in CaBER experiments. Finally, the reporting on the beads-on-a-string instability also occurring in these concentrated solutions prior to filament breakup. For

viscoelastic fluids, this phenomenon has been described first by Goldin et al.[166], and it has been studied intensively since then especially for dilute solutions of PEO.

But high stresses due to the elongation of polymer molecules (strain hardening) lead to a stabilization of filaments and the instability occurs, only when the extensibility limit of the molecules is reached. The formation of beads, the occurrence of satellite drops, and also so-called sub-main drops has been discussed intensively within the framework of fluid mechanics.

The beads-on-a-string structure can be accompanied by a flow-induced phase separation for $c > c*$: the solvent is enriched in the beads, while the filaments connecting them mainly consist of highly extended polymer chains[167]. Here, find that the droplet diameter is essentially independent of concentration and molecular weight of the dissolved polymer over a wide range of viscosities and relaxation times. These results support the earlier finding, that for semi-dilute and concentrated PEO solutions the phenomenon may be controlled by a demixing of polymer and solvent induced by the large elongational strain occurring during capillary thinning.

All solutions investigated here form stable, liquid filament bridges in Caber experiments, and after a short induction time, the filament shape is essentially cylindrical except for the regions close to the endplates. The initial filament midpoint diameter D_0 is mainly controlled by the ratio h_f/h_0 and lies in the range of $D_0 \approx 1.0 - 1.2$ mm. The time evolution of the normalized filament diameter $D(t)/D_0$ for solutions with $M_w \sim 10^5$, 3.0×10^5, 10^6 and 5.0×10^6 g/mol are shown Figure III.1.17 obviously, filament lifetime strongly increases with increasing polymer concentration.

But the filaments break at an essentially constant ratio $D/D_0 \approx 5 \times 10^{-3}$. This is in contrast to the behavior e.g. of the thickener solutions investigated before[168]. For these solutions, a strong increase of the maximum attainable Hencky strain with increasing polymer concentration was observed. Attribute this difference to the fact that filament breakup of the PEO solutions is preceded by the occurrence of a bead-on-a-string instability, which discussed in more detail.

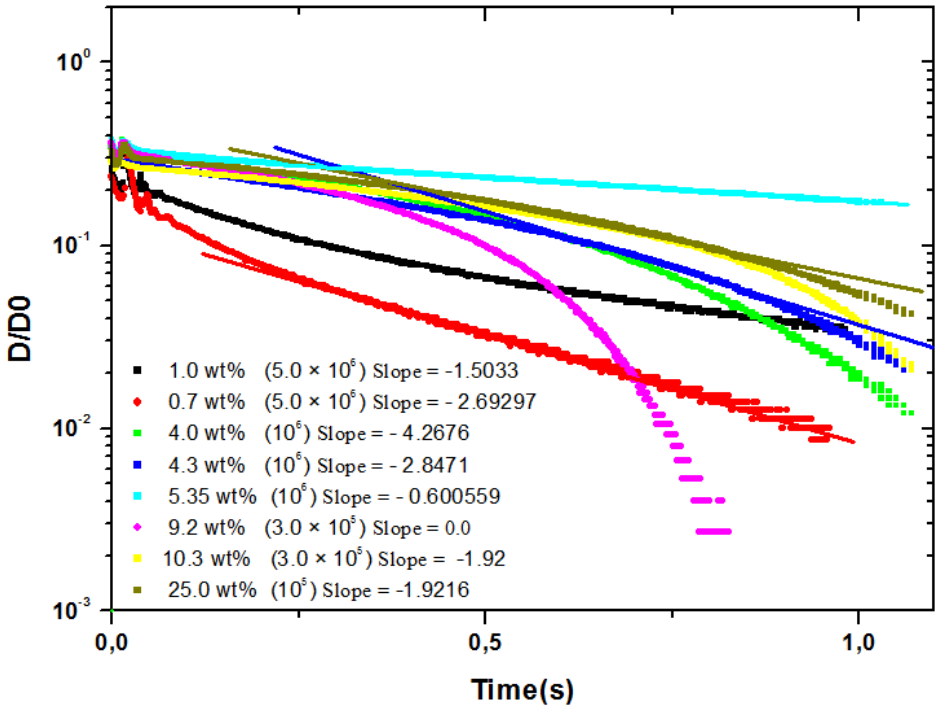

Figure III.1.17: Normalized filament diameter in CaBER experiments for PEO solutions. The time t = 0 is defined as the time at which theupper plate has reached its final position. Mw ~ 10^5, 3.0 × 10^5, $10^6$and 5.0 × 10^6 g/mol and C = 0.7 - 25 wt%

The system at different concentration and molecular weight presents different decays in (Figure III.1.18.A) the decay appears to be linear, Semi-log plot whose function is $Y= a.e^{b.x}$ by the way, Concentration of 9.2 wt% presents a fast decay with time showing a curve that's meaning when the compound need more time that's leads to be more elasticity 0.7 % PEO M_w ~ 5.0 × 10^6 be more elasticity (Figure III.1.18.B).

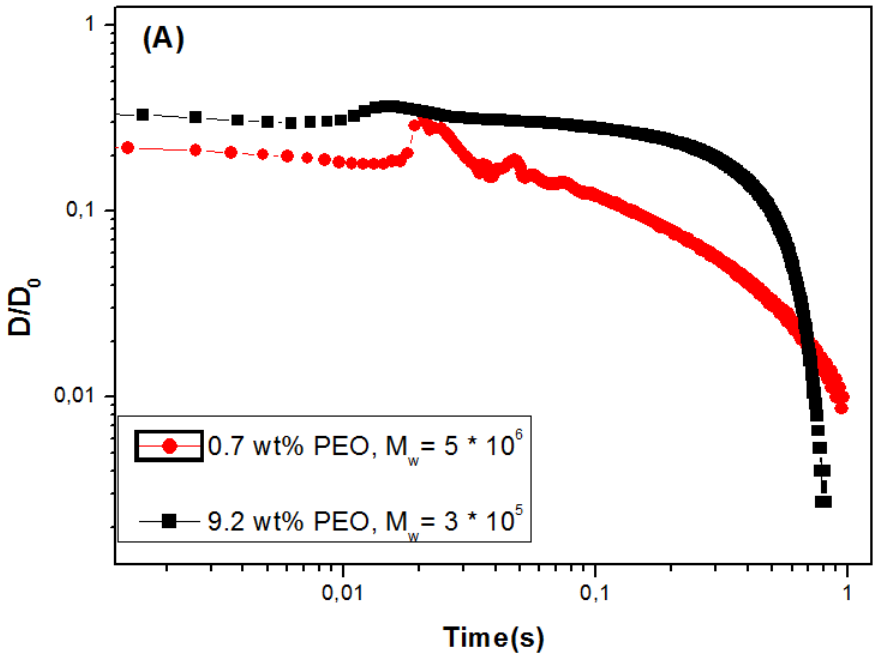

Figure III.1.18.A: Normalized filament diameter in CaBER experiments for PEO solutions. The time t = 0 is defined as the time at which theupper plate has reached its final position. Mw ~ 3.0 × $10^5$and 5.0 × 10^6 g/mol, C = 9.2 wt% and 0.7 wt %.(Diameter as a function of time (Log/Log)

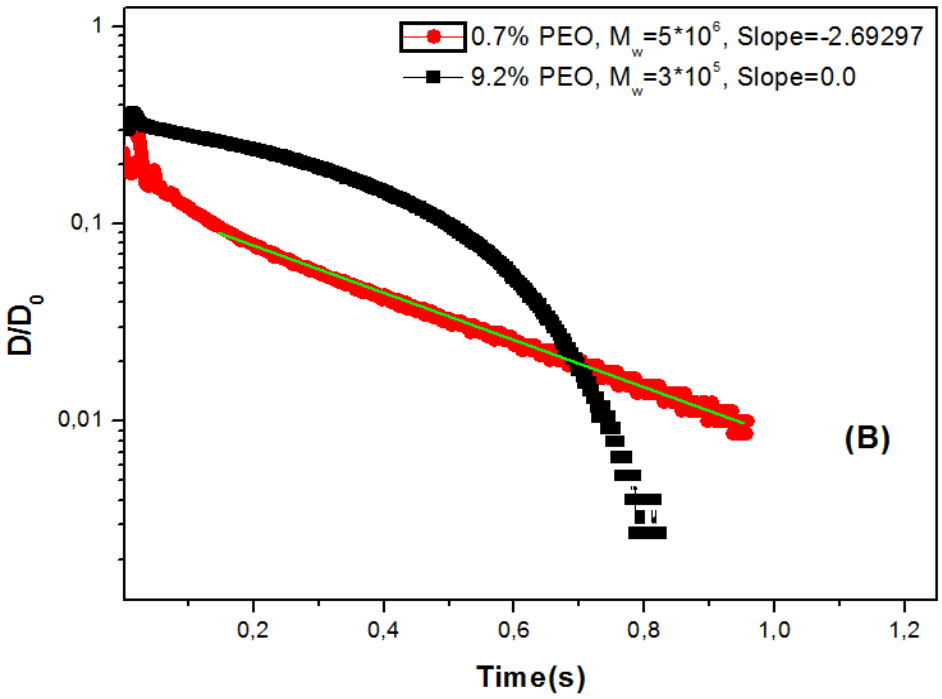

Figure III.1.18. B: Normalized filament diameter in CaBER experiments for PEO solutions. The time t = 0 is defined as the time at which the upper plate has reached its final position. Mw ~ 3.0 × $10^5$and 5.0 × 10^6 g/mol, C = 0.7 wt% and 9.2 wt %. (Diameter as a function of time (log/linear)

The low λE values found in these solutions of linear flexible polymers seem to be due to the strong nonlinear deformation the fluids experience in CaBER experiments. Much lower λE/λS ratios have been found for commercial acrylic thickener solutions[168]. These polyelectrolytes are known to form large aggregates due to hydrophobic interactions and in the cases the low λ_E/λ_S ratios may be due to structural changes induced by the strong elongational deformation during capillary thinning. Understanding the physical meaning of λE is crucial for the interpretation of CaBER experiments and obviously requires careful experimental as well as theoretical investigations.

This phenomenon has been described first by Goldin et al. (1969), and it has been studied intensively since then[167]. For PEO solutions with $c < c*$, the formation of beads has been investigated intensively. For PEO solutions with $c \approx c*$, it has been directly shown, that the beads on- a-string structure is accompanied by a flow-induced phase separation: the solvent is enriched in the beads, while the filaments connecting them mainly consist of highly extended polymer chains[167]. Here, we find that the beads-on-a-string instability is pertinent even at concentrations.

The filament breakup observed in CaBER experiments on acrylic thickener solutions[168] is different in nature. Despite their intermolecular aggregation and high apparent molecular weight, these thickener solutions are not entangled. They thin homogeneously and break at a critical $D(t)/D_0$ ratio which decreases with increasing polymer concentration, but at all investigated concentrations, this critical $D(t)/D_0$ ratio is clearly higher than the value found for the PEO solutions investigated here and no beads-on-a-string instability is observed.

Conclusion

The obtained results confirm the number of deposited nanofibers of PEO has direct correlation with increasing polymer concentration. In addition, the results clearly verified that the viscosity, flow rate and applied voltage have strong influence on the shape and morphology of the fibers. Typically, we demonstrated to control the morphology the fibers and beads presence by monitoring the applied voltage and flow rate. The existance of fibers and beads in the produced electrospinning mats varids with the different molecular weight of PEO at zero shear viscosity (η_0) constant. In addition, Newtonian viscosity of the fluid there were influenced for the morphology of the fibers. The molecular weight of PEO and the solution concentration have a great effect to change the viscosity of the solutions. This effect has also caused the formation of fibers from beads to pure ultra-fibers. The solution properties such as polymer concentration and molecular weight significantly affect fiber/bead formation in compared with surface tension and conductivity.

CHAPTER III

Part II: Mechanical Properties of electrospun membranes

Introduction:

The mechanical properties of bio medically devices are very important to their function. First, the mechanical properties of the substrate affect cell differentiation. Second, the scaffold must have similar properties to the natural tissue it has to replace so that it can perform the function of the tissue. Finally, scaffolds must have the mechanical stability to handle manipulation by the physician during implantation as well as support tissue regeneration and structure degradation.

One important challenge that have to be considered is the ability to control the morphology of the electrospun network. Lavielle et al.[169] have proposed to use simultaneously electrospinning and electrospraying to produce structured composite membranes.

In this work, we are focusing our attention on the conception of structured collector to control the self organization of electrospun fibers. The second task was to investigate the effect of the structuration of the fibrous network on the mechanical properties of membranes. For this purpose, the mechanical property of one structured network is compared with that of randomly oriented network traditional collected one standard collector constituted by an aluminum foil.

3.2.1 Deposition and Architecture Control

The conventional electrospinning process usually leads to non-woven mats by the random deposition of nanofibers. However, the controlling the ways nanofibers are collected in electrospun membranes would provide a great benefit for various applications. Indeed, precise geometric design of multicomponent electrospun membranes or 3D structures with defined porosity and pore sizes are paramount importance to mimic tissue structure and their structural properties for tissue engineering applications[170]. In addition, it has wide range of applications in a specified geometer loaded drug delivery systems and control of its release kinetics[171].

A number of methods have been developed to control the deposition of the nanofibers and prepare regular structured membranes. For example, aligned electrospun fibers have been obtained by electrospinning on a rotating collector[172]. Moreover, one can align nanofibers by modulating the electrostatic field. D. Li and Y. Xia[173] showed that one can influence the nanofibers deposition by using dielectric material to pattern the collector. The geometry and the dielectric constant of the used materials generate a modified electrostatic field guide the deposition of the fibers arranged some certain geometers structures.

Other complex 2D or 3D structured membranes have also been prepared using electrostatic forces[174]. The principle of this approach is the modification of the electrostatic field near the collector, thus guiding the deposition of the charged nanofiber. Deposition control and 3D structures can also be created using 3D structured conductive patterns as a collector (Figure III.2.1)[175].

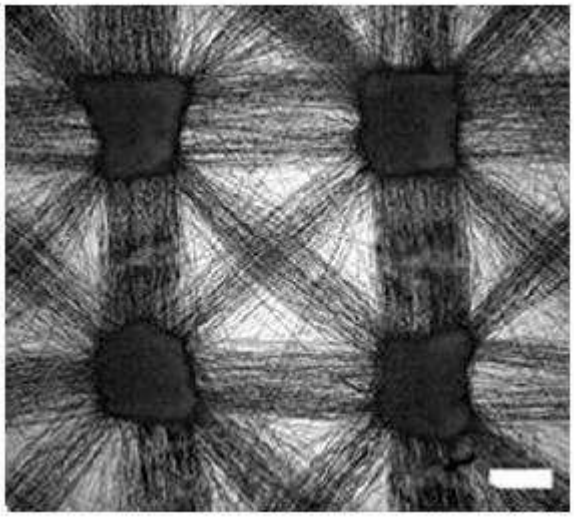

Figure III.2.1: SEM images of patterned architectures (scale bar = *100µm). (adapted from* ref.[175]

Another type of structured membranes can be obtained by the self-organization of electrospun nanofibers. They have been first presented by Deitzel et al.[76] for Poly(ethylene oxide) and then extended the observation for other polymers[176]. It was shown that a bimodal distribution of the fiber diameter is a necessary condition to induce the self-organization. Such irregular fibers, having thick and thin domains, locally impact the electrostatic field and guide the deposition of the fibers into honeycomb-like patterns[176]. In addition, structured membranes were also fabricated using diverse post-electrospinning structuring surface treatments: direct laser machining[177], wetting of porous template[178] or photo patterning of electrospun membranes[179].

We studied two fibers deposition patterns; the first deposition on a sheet of Aluminum (Figure III.2.2) and the second was performed on a micro-structured manifold Copper dimension 3 × 3 cm with 1mm spacing (Figure III.2.3).

Figure III.2.2: The fibers produced by using the aluminum foil

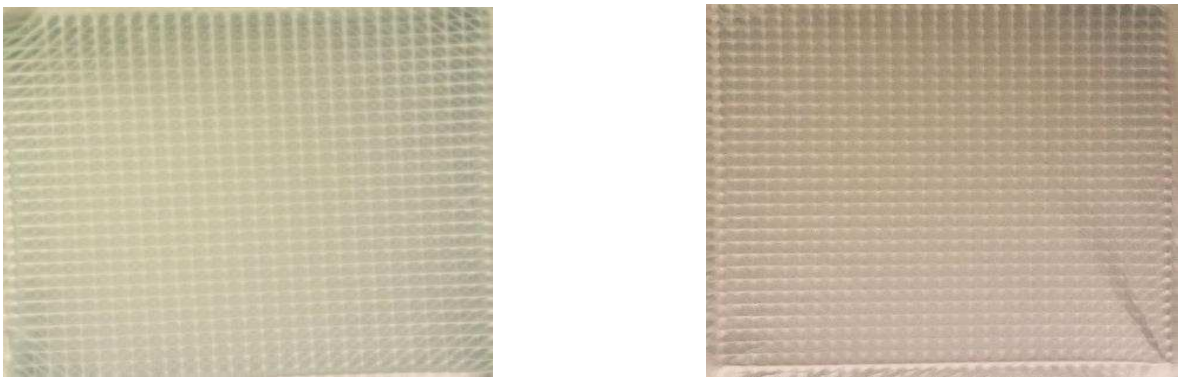

A **B**

Figure III.2.3: The membranes produced by using the microstructure collector: A) represent 4.0 wt% PEO (1.0×10^6) and B) 10.3 wt% PEO (3.0×10^5)

Micro-structured manifold have been used for the deposition of the fibers in order to obtain a well-ordered fiber network as presented In (Figure III.2.4). For better visualisation the distribution of the fibers, zones in the center of the 4 studs, between 2 studs and on the stud itself. Center of the 4 plots between 2 plots (Figure III.2.4) optical microscopy with a

magnification 5 times of a membrane based on PEO 3.0 × 10^5 g/mol collected on a micro-structured collector.

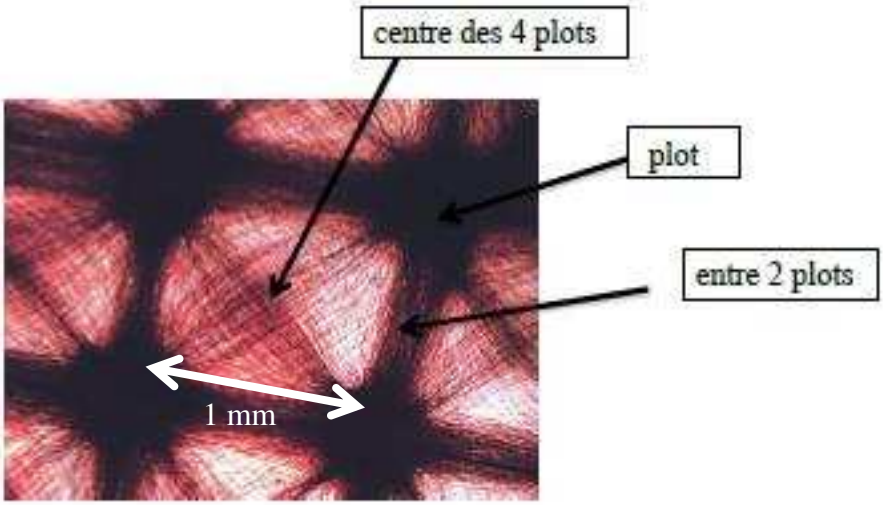

Figure III.2.4: Optical microscopy image of a membrane based on PEO 3.0 × 10^5 g/mol collected on a micro-structured collector

3.2.2 Mechanical Properties of Electrospun Membranes

Despite possessing these unique features, one of the main challenges in this area is to characterize the tensile behavior of the nanofibrous membranes. This could be due to the difficulty in handling the nanofiber network and also due to the low load required for the deformation. Hence, in most cases, the mechanical properties of the fibers and fiber network structures is unsung and it need to be invastigated. Few researchers actively pursued to characterize the mechanical deformation characteristics of the fibers by recording the stress–strain behavior of the electrospun non-woven fabrics. The tensile response of the non-woven are greatly influenced by the fiber diameter and size distribution in the mats, porosity, individual fiber orientation in the mat, fiber–fiber interaction and entanglement of the fibers[(180)]. These parameters cannot be easily isolated and controlled in the non-woven fabrics. Hence, there has been a remarkable growing interest in characterizing the tensile deformation behavior of single fibers and aligned fiber bundles[(181)].

The effect of fiber diameter on the tensile deformation has been invastigated. The tensile response of the fiber was compared with the tensile properties of the bulk polymer system

prepared using injection molding. There is a significant difference in the tensile strength and tensile behavior. The stress–strain curve of the spun sample is consistently found not to display the necking phenomenon whereas the bulk sample shows clear necking. This is attributed to the oriented and stretched polymer chains in the spun fibers[182]. Similar results were obtained by Lu et al.[182].

Another assessment used to determine consistency of the scaffolds was uniaxial tensile testing. Because tissues undergoes important strains it is important that as the scaffold may stretch without important damage. For this purpose, we focus our attention on both the elongation at break and the Young modulus of membranes.

To calculate Young's modulus the relationship defined by Hooke's law was used. Specifically, Hooke's law is the relationship between the stress that a material experiences and the strain that it exhibits. Typically, the initial linear segment of a stress strain curve is characterized by Equation III.2.1. By calculating the strain (ε) and the stress (σ) using equations III.2.2 and III.2.3 respectively, the values can then be used in Equation III.2.1 to find the Young's modulus (E), typically measured in Pascals.

$$\sigma = E\varepsilon \qquad \text{eq. (1)}$$

$$\varepsilon = \frac{L - L_0}{L_0} \qquad \text{eq. (2)}$$

$$\sigma = \frac{\text{Force (N)}}{\text{Sectional Area } (m^2)} \qquad \text{eq. (3)}$$

Figure III.2.5 shows the tensile behavior of three different PEO membranes obtained by extrusion and calendaring, electrospinning on aluminum foil and on the structured collector described in page 65. In case of the extruded membrane, the stress undergoes by the membrane is very important, about 13 MPas, but it breaks at a strain of about 50%. Such kind of membrane are rigid but quite fragile. On the contrary, electrospun membranes exhibit a stress at break of about 6 MPas which is much lower compare to the extruded membrane. Concurrently, they can support higher strain before breaking. The random membrane collected on the aluminium foil breaks at a strain of about 100 % and it reaches more than 400% in case of structured membrane.

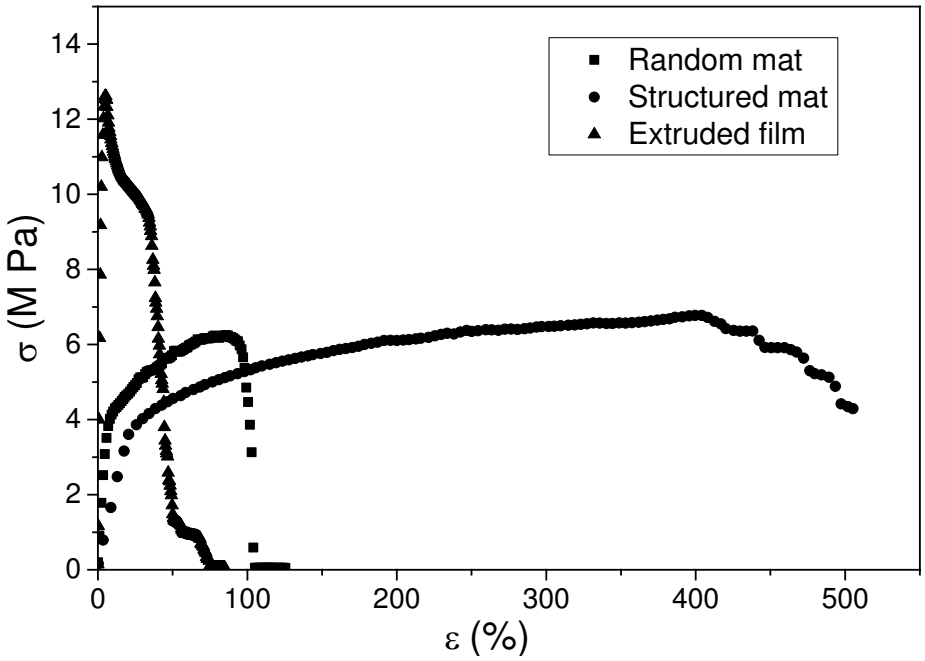

Figure III.2.5: Curve stress-deformation of extuded film, electrospun membranes having a random orientation of fibers and a square like structure. Stretch velocity of 0.25 mm/s

According to the literature[183], the curves obtained for electrospun membranes exhibit a characteristic behavior of non-woven textile structures. Examination of the curves can distinguish three different parts as shown in (Figure III.2.5) of structured mats:

- Part I: This is short deformation range, the stress increases sharply in a linear way. The slop of the stress-strain curve gives the Young modulus of the material. The structured membrane exhibits a Young modulus of about 0.17 MPa will the random membrane has a young modulus of about 0.55 MPa.

- Part II: In this area, the stress gradually level off. This behavior that doesn't exist in the extruded membrane may be attributed to local rearrangements of fibers during stretching.

- Part III: In this area, Fibers no longer undergo stretching and groups of nanofibers break leading to a step profile of the curve, up to the total breakage of the membrane.

To study the relationship between the mechanical property of membrane and the microstructure changes under strain, a camera equipped with microscope lens is placed in front of the

membrane. The camera move up, half the speed of the moving grip to follow the same stretch zone.

Figure III.2.6 shows 4 pictures of the network taken at 10s, 40s, 60s and 90s corresponding respectively to a strain of 1.25%, 50%, 75% and 112% respectively. These pictures point out the effect of the tensile test on the microstructure of the structured membrane. For the first picture corresponding to the part I of Figure III.2.5 the elementary cell of fibers can be easily identify, forming a square of 1 × 1 mm.

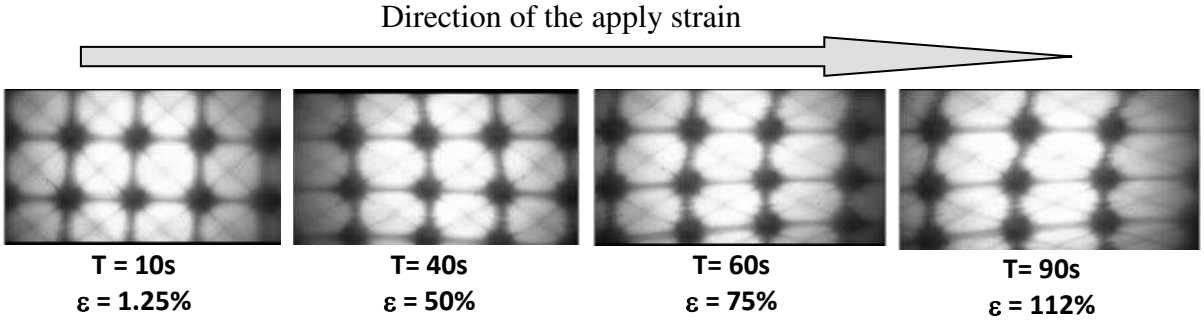

Figure III.2.6: Optical microscopy of the structured membrane observed at different strain. The membrane has been obtained with a PEO solution or 4.0 wt% with a molecular weight of 10^6 g/mol

In this cell, most of the fibers are packed at the edge of the cell connecting tow neighboring picks of the structured collector. In those picks, fibers form knots of strongly connected fibers will some fibers form a cross into the elementary cell.

As the strain increases, the distance between knots increases in the strain direction and decreases in the perpendicular direction of the apply strain. In Figure III.2.7, the two directions have been monitored as a function of time.

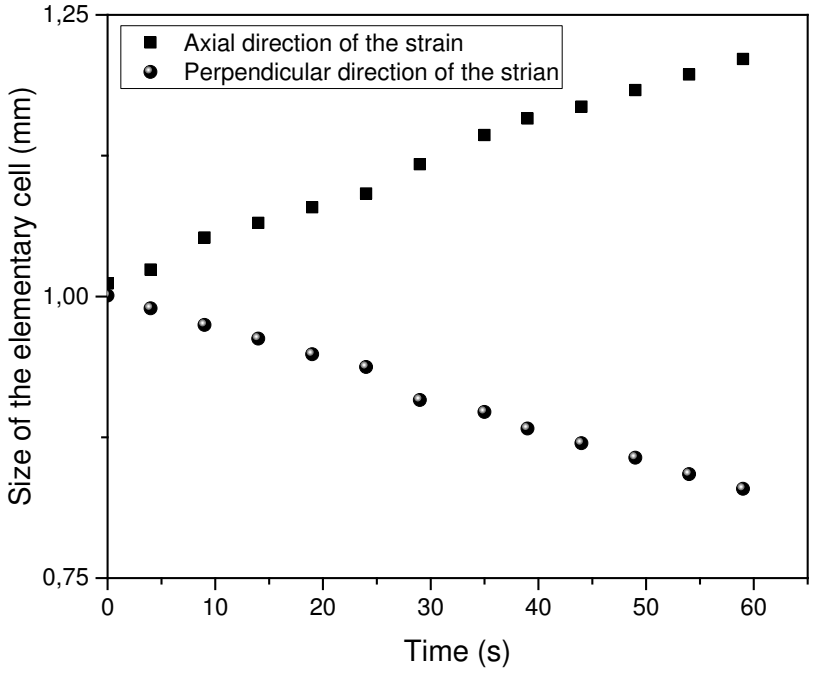

Figure III.2.7: Evolution of the size of the elementary cell in the axial and perpendicular directions of the strain for the structured membrane.

Both sizes change linearly with time. A break in both linear time dependence seams to appear after 25 s corresponding to a strain of about 30% of the membrane. This time evolution of the network morphology can be seen in Figure III.2.8 Showing the aspect ratio of the elementary cell obtained by dividing the size of the elementary cell in the axial direction by that of the perpendicular direction of the strain.

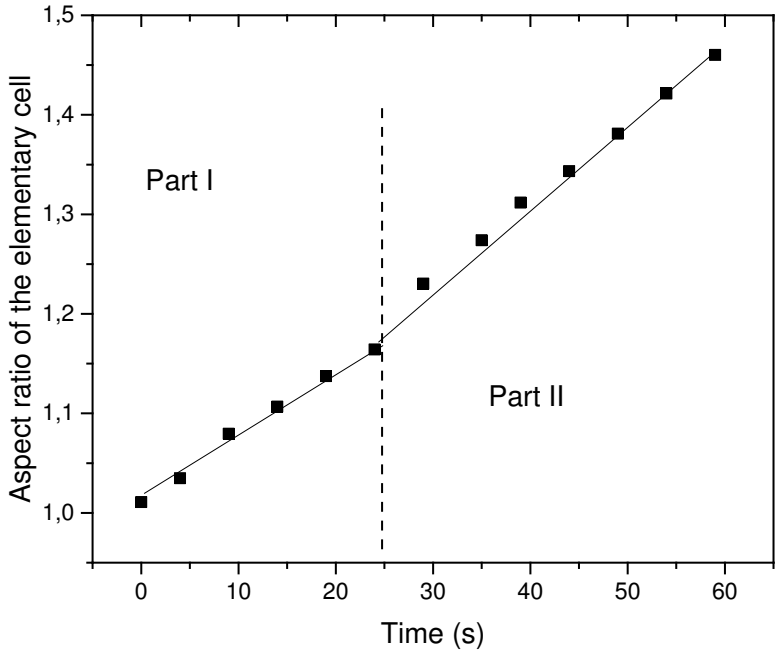

Figure III.2.8: Aspect ratio of the elementary cell as a function of time.

Two strain regimes can be identify, characterized by a change in the slop of line. The first regime corresponds in good approximation to the part I of the stress-strain curve of Figure III.2.5.

This figure suggest that the network is less stretched in the part I. The sharp increase of the stress is probably due to the direct mechanical contribution of fibers aligned in the axial direction of the strain. In the part II of Figure III.2.5, the network is deformed more quickly and the mechanical response of the network is due to local rearrangement of fibers.

What about the random network? For this structure under stretch, the orientation of fibers is rapidly affected as shown by the sketch Figure III.2.9.

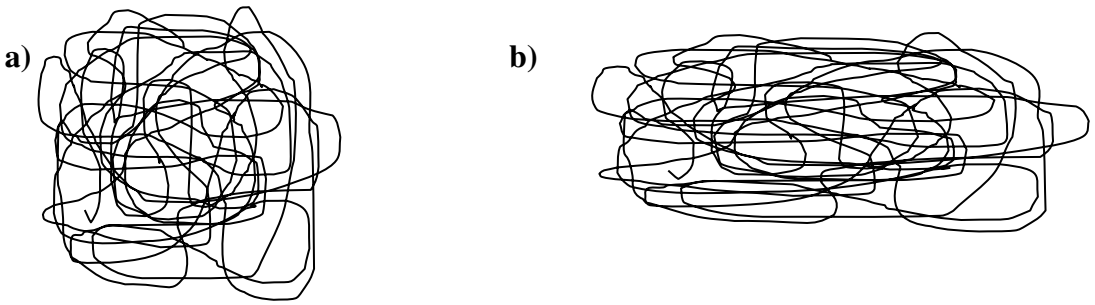

Figure III.2.9: Sketch of the random network a) at rest and b) under stretching

Fibers form a network with a smaller distance between knots. In part I, all fibers are mechanically active in the response of the network that could explain the higher value of the Young modulus in case of random network. But since fibers are more isolated and not packed, strain is more efficient to break them in part II. This organization is more fragile and breaks at a lower strain.

In case of extruded membranes, they are denser so they exhibit a higher Young modulus but they can't modify their structure as electrospun do without ignition of local breakage that rapidly propagate up to the total breakage of the membrane.

Conclusion

This work pointed out on the ability to structure a network of electrospun fibers and the impact of the structuration on the mechanical properties of the membrane.

The use of a structured collector composed of emerging picks favors the deposition of fibers on the top of each peaks leading to the formation of a structured membrane.

The study focused on the mechanical behavior of a square-like structuration of the network. Such organization exhibit a higher strain at break with a similar stress at break compare to network randomly structured. Those mechanical properties are of prim interest in case of application in the development of scaffold dedicated to the reconstruction of soft tissues.

The coming perspective of this work is to develop different topologies of collectors characterized by a distribution of peaks in triangle, hexagons, rectangles, … to initiate various morphologies of network. The influence of those networks in their mechanical response under tensile test will be useful for tissue engineering applications.

CHAPTER IV

General Conclusions and Perspectives

General Conclusions and Perspectives

Electrospinning is a versatile technique used to produce micron and submicron fibers from a wide range of polymers. Using this technique, fiber formation starts when an electrical field is generated on the surface of a polymeric solution and the electrical potential force overcomes the surface tension of the solution, thereby changing the spherical drop to a conical shape, an effect known as the Taylor cone. Electrically charged jets arise from the tip of the cone. Then electrostatic forces create a curled and chaotic movement, or bending instability, driving the jets to the collector. Meanwhile, continuous nanofiber elongation and solidification take place, yielding interconnected fibrous structures with high porosity and expanded surface area. Therefore, collector characteristics strongly influence the electrical field and, consequently, the architectural deposition of the electrospun fibers. Exploring the design of the electrospinning collector can determine the morphology of electrospun fibers, as well as the way fibers are assembled into structures with unique characteristics for specific applications.

The objective of this thesis project was to make non-woven fibrous structures in uncontrolled architecture as well as non-woven with controlled architecture by using the electrospinning process. These fibrous structures are obtained from Poly(ethylene oxide), PEO, solutions with different concentration and molecular weight. The deposit of fibers is made on two types of collectors: a) Aluminum foil, b) micro-structured collector (dimension 3 × 3 cm). The morphological analyses of the membranes were investigated using scanning electron microscopy (SEM) and their mechanical properties were characterized by tensile test using the ARESG2 rheometer. The morphology of the electrospun polymer gradually changes from beads to uniform fibers with increasing polymer concentration and molecular weight. A comparative study of the morphological and mechanical (tensile test) properties, of both fibrous structures is performed. This study showed that it is possible to have a distribution of fiber forming a very uniform primitive cell in a network of dimension 3 × 3 cm. This structured network has a strain at the break more important than that for the network fibers, which are collected on Aluminum foil.

In the present work, the first focus was to develop new biocompatible and bioresorbable materials composed of nanoscale fibers obtained by electrospinning. In addition, this study examined the influence of viscosity, concentration, and surface tension of PEO solutions on the obtained fibers. Further, the flow rate, applied voltage and environmental parameters (temperature and humidity) were also optimized in the course of nanofibers production.

Biocompatible fibers have been obtained by using PEO.

The second major effort of this thesis focused on the control of the mesh fibers. Such research activity is justified by the expected influence of the morphology of the fiber network on the mechanical properties of scaffolds and their biomimetic character that could favor the colonization and growth of the cells of the host tissue. The control of this structure has been achieved through the development of collectors.

Furthermore, the situations envisaged require further study. Indeed, a study of mechanical properties depending on the aging of the membranes is required to determine the influence of moisture and temperature during production. This serves to select the optimal conditions for technical and economic point of view for nonwovens that respond well to the load specifications.

References

References

(1) Ahn ,Y.C.; Park , S.K.; Kim,G.T.; Hwang, Y.J.; Lee, C.G.; Shin, H.S.; Lee , J.K. Development of high efficiency nanofilters made of nanofibers .Current Applied Physics **2006**, 6, 1030 –1035.

(**2**) Renker, D.H.; Chun, I., Nanometre diameter fibers of polymer, produced by electrospinning, Nanotechnology 1996, 7, 216 –223.

(3) Cooley J.F. US patent 692631.

(4) Layman, M.; Kenawy, ER.; Watkins, JR.; Carr, Jr.ME.; Bowlin, G.; Wnek, GE. Polymer **2003**, 44, 94 –5.

(5) Barris, MA. Zelinka, RL. US Patent No. 4,650,506. Issued March 17; 1987 to Donaldson Company, Inc.

(6) Kenawy, ER.; Bowlin,GL.; Mansfield,K.; Layman,J.; Simpson, DG.; Sanders, EH.; et al. J Control Release **2002**, 81, 57– 64.

(7) Gibson, P.; Schreuder-Gibson, H.; Rivin, D. Transport properties of porous membranes based on electrospun nanofibers. Colloids Surf A **2001**, 187, 469 – 81.

(8) Boland, ED.; Matthews, JA.; Pawlowski, KJ.; Simpson, DG.; Wnek,GE.; Bowlin,GL. Front Biosci **2004**, 9, 1422 – 32.

(9) He, CH.; Gong, J. PolymDegrad Stab **2003**, 81,117.

(10) Frenot, A.; Chronakis, IS. CurrOpin .Colloid Interface Sci **2003**, 8, 64 –75.

(11) Liu, HQ.; Kameoka, J. ; Czaplewski, DA.; Craighead, HG. NanoLett **2004**, 4,671,

(12) Wang, M.; Singh, H.; Hatton,TA. Rutledge, GC. Polymer **2004**, 45, 5505.

(13) Ma, ML.; Hill, RM., Lowery, JL., Fridrikh, SV.; Rutledge, GC.Langmuir **2005**, 21, 5549a

(14) Alessandrino, A.; Marelli,B.; Arosio,C.; Fare,S.;Tanzi, M.C.; Freddi, G.Electrospun Silk Fibroin Mats for Tissue Engineering .Engineering in Life Sciences **2008**, 8, 3, 219 –225.

(15) Gupta, P.; Elkins, C.; Long, T.; Wilkes, G. "Electrospinning of linear homopolymers of poly(methyl methacrylate): exploring relationships between fiber formation, viscosity, molecular weight and concentration in a good solvent", Polymer **2005**, 46, 4799 –4810.

(16) Shenoy, S.; Bates, W.; Frisch, H.; Wnek, G. "Role of chain entanglements on fiber formation during electrospinning of polymer solutions: good solvent, non-specific polymer polymer interaction limit", Polymer **2005**, 46, 3372 – 3384.

(17) McKee, M.G.; Wilkes, G.L.; Colby, R.H.; Long, T.E, "Correlations of solution rheology with electrospun fiber formation of linear and branched polyesters", Macromolecules **2004**, 37, 1760 – 1767.

(18) Eda, G.; Shivkumar, S. J.Mat.Sci.**2006**, 41, 5704 –5708.

(19) Tan, S. H. ; Inai, R. ; Kotaki, M. ; Ramakrishne, S. Polymer **2005**, 46, 6128 – 6134.

(20) Fong, H.; Chun, I.; Reneker, D. "Beaded nanofibers formed during electrospinning", Polymer **1999**, 40, 4585 – 4592.

(21) Mit-uppatham, C.; Nithitanakul, M. &Supaphol, P. Ultrafine ElectrospunPolyamide-6 Fibers: Effect of Solution Conditions on Morphology and Average Fiber Diameter .Macromolecular Chemistry and Physics **2004**, 205, 2327 – 2338.

(22) Kenawy, E.; Layman, J.; Watkins, J.; Bowlin, G.; Matthews, J.; Simpson, D.; Wnek, G."Electrospinning of poly (ethylene-co-vinyl alcohol) fibers", Biomaterials **2003**, 24, 907–913.

(23) Taylor, G.Proc R Soc London A, Mat Phys.Sci **1964**, 280, 383 – 97.

(24) Hills Inc. Articles, http://hillsinc.net/Polymeric.shtml, Polymeric nanofibers – Fantasy of future, 05/19/2006.

(25) Guceri , S.; Gogotsi ,Y. G.; Kuznetsov ,V., Nanoengineered Nanofibrous Materials, Kluwer Academic Publishers, **2003**.

(26) Formhals, A. US Patent **1934**, 1, 975 – 504.

(27) Ondarc¸uhu, T.; Joachim, C. "Drawing a single nanofiber over hundreds of microns", Europhys. Lett **1998**, 42, 215 – 220.

(28) Duvail, J. L.; Retho, P.; Garreau, S.; Louarn, G.; Godon, C.; Demoustier-Champagne, S. "Transport and vibrational properties of poly(3,4-ethylenedioxythiophene) nanofibers", Synth. Met **2002**, 131, 123 – 128.

(29) Liu, D.; Zhang, H.; Grim, P. C. M.; De Feyter, S.; Wiesler, U. M.; Berresheim, A. J.; Mullen, K.; De Schryver, F. C. "Self-assembly of polyphenylene dendrimers into micrometer long nanofibers: An atomic force microscopy study", Langmuir **2002**, 18, 2385 – 2391.

(30) Ma, P. X.; Zhang, R. "Synthetic nano-scalefibrousextracellular matrix", J. Biomed. Mater. Res **1999**, 46, 60 – 72.

(31) Ramakrishna, S.; Fujihara, K.; Teo, W E.; Lim, T C. and Ma, Z., An Introduction to Electrospinning and Nanofibers (Singapore: World Scientific), **2005**.

(32) Sedaghat, A. Et al. An Alumina Mat with a Nano Microstructure Prepared by CentrifugalSpinning Method, Department of Materials Science and Engineering, Tarbiat Modares University, published in Journal of Non-Crystalline Solids, **2006**.

(33) Huang, T.; "Centrifugal Solution Spun Nanofiber Process" USPTO Application #: 20090160099 December 17, **2007.**

(34) Weitz, R.T.; Harnau, L.; Rauschenbach, S.; Burghard, M.; Kern, K. Polymer Nanofibers via Nozzle- Free Centrifugal Spinning, Nano Letters **2008**, 8, 4, 1187 –1191.

(35) Url 1 : http://fiberiotech.com/ technology/how-it-works/ **10.05.2012**.

(36) Vasita, R.; Katti, D. S. Nanofibers and their applications in tissue engineering. Int. J. Nanomedicine **2006**, 1, 15.

(37) Xing, X.; Wang, Y.; Li, B., Nanofiber drawing and nanodevice assembly in poly (trimethylene terephthalate), Optics Express **2008**, 16, 14.

(38) Yang, Q.; Jiang, X.; Gu, F.; Ma, Z.; Zhang, J., Limin Tong Polymer Micro or Nanofibers for Optical Device Applications, Journal of Applied Polymer Science **2008**, 110, 1080 – 1084.

(39) Ondarçuhu, T.; Joachim, C. Europhysics Letters (EPL) **1998**, 42, 215 – 220.

(40) Cao, G.; Liu, D. Advances in Colloid and Interface Science **2008**, 136, 45 – 64.

(41) Yang, Z.; Niu, Z.; Cao, X.; Yang, Z.; Lu, Y.; Hu, Z.; Han, C. C. Angewandte Chemie International Edition **2003**, 42, 4201 – 4203.

(42) Thurn-Albrecht, T.; Schotter, J.; Kästle, G. A.; Emley, N.; Shibauchi, T.; Krusin-Elbaum, L.; Guarini, K.; Black, C. T.; Tuominen, M. T.; Russell, T. P. Science **2000**, 290, 2126 – 2129.

(43) Lakshmi, B. B.; Dorhout, P. K.; Martin, C. R. Chemistry of Materials **1997**, 9, 857 – 862.

(44) Lei, B.; Shin, K.-H.; Noh, D.-Y.; Jo, I.-H.; Koh, Y.-H.; Kim, H.-E.; Kim, S. E. Materials Science and Engineering: C **2013**, 33, 1102 – 1108.

(45) Sharma, M. K.; Ambolikar, A. S.; Aggarwal, S. K. Journal of Nanoparticle Research **2012**, 14, 1–10.

(46) Hulteen, J. C.; Chen, H. X.; Chambliss, C. K.; Martin, C. R. Nanostructured Materials **1997**, 9, 133 –136.

(47) Grimm, S.; Martín, J.; Rodriguez, G.; Fernández-Gutierrez, M.; Mathwig, K.; Wehrspohn, R. B.; Gösele, U.; Roman, J. S.; Mijangos, C.; Steinhart, M. Journal of Materials Chemistry **2010**, 20, 3171– 3177.

(48) Vasita, R., Katti, D, S., "Nanofibers and their applications in tissue Engineering" InternationalJ Nanomedicine **2006,** 1, 15 – 30.

(49) MacDiarmid, A. G.; Jones, Jr., W. E.; Norris, I. D.; Gao, J.; Johnson, Jr, A. T.; Pinto, N. J.; Hone, J.; Han, B.; Ko, F. K.; Okuzaki, H.; Llaguno, M. Synthetic Metals **2001**, 119, 27.

(50) Buchko, C. J.; Chen, L. C.; Shen, Y. & Martin, D. C. Processing and microstructural characterization of porous biocompatible protein polymer thin films. Polymer **1999**, 40, 7397 –7407.

(51) Formhals, A. US Patent **1940**, 2187306.

(52) Formhals, A. US Patent **1939**, 2160962,568 SUBBIAH ET AL.

(53) Baumgarten, P. K. Journal of Colloid Interface Science **1971**, 36, 71.

(54) Larrondo, L.; Mandley, R. St. J. J Polym Sci: Polymer Physics Edn **1981**, 909.

(55) Thompson, C.J.; Chas, G.G; Yarin,A.l.; Reneker,D.H.Effects of parameters on nanofiber diameter determined from electrospinning model. Polymer **2007**, 48, 6913 – 6922.

(56) Bueche, F. "Viscosity of polymers in concentrated solution*" J. Chem. Phys*. **1956**, 25, 599 – 600.

(57) Bhardwaj, N. &Kundu, S. C. Electrospinning: a fascinating fiber fabrication technique. Biotechnology Adv. **2010**, 28, 325 – 347.

(58) Koski, A.; Yim, K.;and Shivkumar, S., Materials Letters **2004**, 58, 493.

(59) Feng JJ. J Non-Newtonian Fluid Mech. **2003**, 116, 55 – 70.

(60) Keller A. Faraday Discuss **1995**, 1 – 49.

(61) Reneker, DH.; Yarin, AL.; Zussman, E., Xu, H. Electrospinning of nanofibers from polymer solutions and melts. Advances in Applied Mechanics **2007**, 41, 43–195.

(62) Gupta, P., PhD thesis, Virginia Polytechnic Institute and State University, **2004**.

(63) Bolgen, N.; Menceloglu, Y.Z.; Acatay, K.; Vargel, I.; Piskin, E. In vitro and in vivo degradation of non-woven materials made of poly (ε -caprolactone) nanofibers prepared by electrospinning under different conditions. J. Biomater. Sci. Polymer **2005**, 16, 1537–1555.

(64) Megelski, S.; Stephens, J.S.; Chase, D.B.; Rabolt, J.F.Micro-and nanostructured surface morphology on electrospun polymer fibers. Macromolecules **2002**, 35, 8456–8466.

(65) Lancuski, A; Bossard , F..Processing and characterization of click-Functionalized Electrospun Nano-Fibers toward tissue Engineering Applications, PhD thesis **2013**.

(66) Han, S. O.; Son, W. K.; Youk, J. H.; Lee, T. S., and Park W. H., Materials Letters **2005**, 59, 2998.

(67) Bognitzki, M.; Czado, M.; Frese, T.; Schaper, A.; Hellwig, M.; Steinhart, M.; Greiner ,A., and Wendorff, J. H., Advanced Materials **2001**, 13, 70.

(68) Lee, K. H.; Kim, H. Y.; La, Y. M.; Lee, D. R.; Sung, N. H. J. Polym. Sci. Part B: Polym. Phys. **2002**, 40, 2259.

(69) Yarin, AL.; Koombhongse, S.; Reneker, DH. On Bending instability in electrospinning of nanofibers. J Appl Phys. **2001**, 89, 3018–26.

(70) Zhenxin Zhong , .Polymer **2007**, 48 , 5742 – 5746.

(71) Zuo, W.; Zhu, M.; Yang, W.; Yu, H.; Chen, Y.; Zhang, Y. "Experimental Study on Relationship between Jet Instability and Formation of Beaded Fibers during Electrospinning", Polym. Eng. Sci. **2005**, 45, 704 –709.

(72) Magarvey, R.; Outhouse, L. "Note on the break-up of a charged liquid jet", J. Fluid Mech.**1962**, 13, 151 – 157.

(73) Haghi, A.K.; Akbari, M. Trends in electrospinning of natural nanofibers .physical status solide **2007**, 204, 6, 1830 – 1834.

(74) Zhang, C.; Yuan, X.; Wu, L., Study on morphology of electrospunpoly (vinyl alcohol) mats - European Polymer Journal **2005**, 41, 423 – 432.

(75) Yao, L.; Haas, T.; Guiseppi-Elie, A., Bowlin, G.; Simpson, D.; Wnek, G. "Electrospinning and Stabilization of Fully Hydrolyzed Poly (Vinyl Alcohol) Fibers", Chem. Mater **2003**, 15, 1860 – 1864.

(76) Deitzel, J.; Kleinmeyer, J.; Harris, D.; Beck Tan, N. "The effect of processing variables on the morphology of elecrospun nanofibers and textiles", Polymer **2001**, 42, 261–272.

(77) Mo, X.M.; Xu, C.Y.; Kotaki, M. Electrospun P(LLA-CL) nanofiber: a biomimetic extracellular matrix for smooth muscle cell and endothelial cell proliferation, Biomaterials **2004**, 25,1883 – 1890.

(78) Jacobs, V.; Anandjiwala, R. D. &Maaza, M. The influence of electrospinning parameters on the structural morphology and diameter of electrospun nanofibers. Journal of Applied Polymer Science **2009**, 115, 3130 –3136.

(79) Larrondo, L. & St. John Manley, R. Electrostatic fiber spinning from polymer melts. I. Experimental observations on fiber formation and properties. Journal of Polymer Science: Polymer Physics Edition **1981**, 19, 909 – 920.

(80) Yuan, X.; Zhang, Y.; Dong, C. & Sheng, J. Morphology of ultrafine polysulfone fibers prepared by electrospinning. Polymer International **2004**, 53, 1704 –1710.

(81) Wannatong, L.; Sirivat, A. &Supaphol, P. Effects of solvents on electrospun polymeric fibers: preliminary study on polystyrene. Polymer International **2004**, 53, 1851 –1859.

(82) Reneker, DH.; Yarin, AL.; Fong, H., Koombhongse S. Bending instability of electrically charged liquid jets of polymer solutions in electrospinning. J. Appl Phys. **2000**, 87, 4531– 47.

(83) Demir, M.M; Yilgor, I.; Yilgor, E.; Erman, B.. Electrospinning of polyurethane fibers. Polymer**2002**, 43, 3303 –3309.

(84) Casper, C. L.; Stephens, J. S.; Tassi, N. G.; Chase, D. B. &Rabolt, J. F. Controlling Surface Morphology of Electrospun Polystyrene Fibers: Effect of Humidity and Molecular Weight in the Electrospinning Process. Macromolecules **2004**, 37, 573 – 578.

(85) Srinivasarao, M.; Collings, D.; Philips, A., and Patel, S., Science **2001**, 292, 79.

(86) Bhattarai, S. R. et al. Novel biodegradable electrospun membrane: scaffold for tissue engineering. Biomaterials **2004,** 25, 2595 – 2602.

(87) Dosunmu, O. O.; Chase, G. G.; Kataphinan, W. &Reneker, D. H. Electrospinning of polymer nanofibers from multiple jets on a porous tubular surface. Nanotechnology**2006**, 17, 1123 – 1127.

(88) Chen, Z.; Mo, X. & Qing, F. Electrospinning of collagen chitosan complex.MaterialsLetters **2007,** 61, 3490 – 3494.

(89) Li, D.; Wang, Y.; Xia, Y., Electrospinning of Polymeric and Ceramic Nanofibers as Uniaxially Aligned Arrays, Nano Letters **2003**, 3, 8, 1167 –1171.

(90) Boland, E.D.; Wnek, G.E. Simpson D.G .Tailoring tissue engineering scaffolds using electrostatic processing techniques: a study of poly (glycolic acid) electrospinning. Journal of Macromolecular Science Part A, **2001**, 38, 12, 1231 – 1243.

(91) Rho, K.S.; Jeong, L.; Lee G., Electrospinning of collagen nanofibers: Effects on the behavior of normal human keratinocytes and early-stage wound healing, Biomaterial **2006**, 27, 1452 –1461.

(92) Theron, A.; Zussman, E.; Yarin, A. L. Nanotechnology **2001**, 12, 384.

(93) Li, D.; Wang, Y.; Xia, Y. Electrospinning Nanofibers as Uniaxially Aligned Arrays and Layer by Layer Stacked Films, Advanced Materials **2004**, 16, 4, 361–366.

(94) Lyons, J.; Li, C.; Ko, F.Melt-electrospinning part I: processing parameters and geometric properties Polymer **2004**, 45, 7597–7603.

(95) Yogeshwar, Velu. Structure and Formation of Meltblown 3D Fabrics Using Robotic Fiber Assembly and Control System (RFACS). Doctoral Dissertation, North Carolina State University, **2002**.

(96) Koombhongse, S.; Liu, W. and Reneker, D.H. Flat Polymer Ribbons and Other Shapes by Electrospinning. Journal of Polymer Science: Part B: Polymer Physics **2001**, 39, 2598 –2606.

(97) Jaeger R; Schonherr H;Vancso J. Chain packing in electrospun poly (ethylene oxide) visualized by atomic force microscopy. Macromolecules **1996**, 29 (23), 7634 –7636.

(98) Jaeger, R.; Bergshoef, M.M; Batlle, C.M.;Schonherr, H., Vancso, GJ. Electrospinning of ultra-thin polymer fibers. Macromolecular Symposium**1998**, 127, 141 – 150.

(99) Yarin, AL. Free liquid jets and films: hydrodynamics and rheology. New York:Wiley, **1993**.

(100) Entov,VM; Shmaryan, LE. Numerical modeling of the capillary breakup of jets of Polymer liquids. Fluid Dynamics **1997**, 32, 5, 696 –703.

(101) Bergshoef, MM;Vancso, GJ. Transparent Nanocomposites with Ultrathin Electrospun nylon-4, 6 Fiber Reinforcement. Advanced Materials **1999,** 11, 16, 1362 –1365.

(102) Dullien FAL. Porous Media: Fluid Transport and Pore Structure, 24, Second edition, Academic press, New York, **1992.**

(103) Xu, B. Measurement of Pore Characteristics in Nonwoven fabrics Using Image Analysis. Clothing and Textiles Research Journal**1996**, 14, 1, 81– 88.

(104) Bear, J.; Buchlin, J-M.. Modelling and applications of transport phenomena in porous media. Dordrecht, Boston, **1991**.

(105) Bear, J. Dynamics of fluids in porous media. Environmental Science Series, **1972**.

(106) Bhatia, SK.; Smith, JL.; Christopher, BR. Geotextile Characterization and Pore Size Distribution: Part III. Comparison of methods and application to design. Geosynthetics International, **1996**, 3, 3, 301–328.

(107) Bhatia, SK.; Smith, JL.. Comparative Study of Bubble Point Method and Mercury Intrusion Porosimetry Techniques for Characterizing the Pore-Size distribution of Geotextiles. Geotextiles and Geomembranes, **1994**, 13, 679 –702.

(108) Malkan, SR. and Wadsworth, LC. Process-Structure-Property Relationships in MeltBlowing of Different Molecular Weight Polypropylene Resins part I – Physical Properties. INDA Journal **1991**, 3, 2, 21–34.

(109) Pourdeyhimi, B; Dent R. Measuring Fiber Diameter Distribution in Nonwovens. Textile Research Journa l**1999**, 69 (4), 233–236.

(110) Pourdeyhimi, B; Dent R; Jerbi A; Tanaka S; Deshpande A. Measuring Fiber Orientation in Nonwovens. Part V: Real Webs. Textile Research Journal **1999**, 69, 3, 185–192.

(111) Khenoussi, N.; Schacher, L.; Adolphe, D.; Lehuu ,T.; Balard ,H.; Hekmati , A.H. Structural observation of nanofibre surface by AFM - Materials Technology **2010**, 25, 2, 89–92.

(112) W.D. Callister, Materials Science and Engineering: An Introduction, 7th ed., John Wiley & Sons, Inc., New York, NY, **2007**.

(113) ASTM, Standard Test Method for Tensile Properties of Thin Plastic Sheeting, ASTM Int. D882-12 (2012) 1–12. doi : 10.1520/D0882-12.

(114) Huang, Z. M.; Zhang, Y. Z.; Kotaki, M.; Ramakrishna, S., A review on polymer nanofibers by electrospinning and their applications in nanocomposites, Composites Science and Technology **2003**, 63, 2223–2253.

(115) Tsaia, P.P.; Schreuder-Gibsonb, H.; Gibson, P. Different electrostatic methods for making electrets filters .Journal of Electrostatics **2002**, 54, 333–341.

(116) Graham, K.; Ouyang, M.; Raether, T. Polymeric Nanofibers in Air Filtration Applications, Fifteenth Annual Technical Conference & Expo of the American Filtration & Separations Society-Galveston – Texas - **April 9-12, (2002)**.

(117) Groitzsch et al. – US patent 4618524

(118) Salem D., Structure Formation in Polymeric Fibers, Hamser Gardner Publications, Cincinnati, Ohio, **2001.**

(119) Kwoun, SJ.Lec, RM.; Han, B.;Ko, FK. Polymer nanofiber thin films for biosensor applications, Proceedings of the IEEE 27th Annual Northeast Bioengineering Conference **2001**, 9–10.

(120) Chakraborty, S.; Liao, I.; Adler, A.; Leong, K.W. Advanced drug delivery Reviews **2009,** 61, 1043–1054.

(121) Hu, J.; Wei, J.; Liu , W.; Chen, Y. Journal of Biomaterials Science , Polymer Edition 2013, 24, 972–985.

(122) Mickova, A.; Buzgo, M.; Benada, O.; Rampichova, M.; Fisar, Z.; Filova, E.; Tesarova, M.; Lukas, D.; Amler, E, Biomacromolecules **2012**, 13, 952–962.

(123) Dasaratha, M.; Vema, K.; Jayakumar, R.; Vamsadhara, C. International Journal of pharmaceutiques **2003**, 268, 23 – 29.

(124) Dasaratha, M.; Gopinath, D.; Rafiuddin Ahmed, M.; Jayakumar, R.; Vamsadhara, C .Journal of Biomedical Materials Research Part A **2006**,76A,63–72.

(125) Brydson, J. A.; Plastics Materials, 5th Ed., Butterworths, Boston **1989**, 513.

(126) Daoust, H. St Cyr D Microcalorimetric. Macromolecules **1984**, 17, 596 – 601.

(127) Bekiranov, S.; Bruinsma, R.,Pincus,. Solution behavior of poly (ethylene oxide) in water as a function of temperature and pressure. Phys. Rev. E. P. **1997**, 55, 577.

(128) Hammouda, B.; Ho, D. L.; Kline, S. Insight into clustering in poly (ethylene oxide) solutions. Macromolecules **2004**, 37, 6932.

(129) B. Le Neindre, "Tensions superficielles et interfaciales," Tech. Ing. - TI K475, Oct.**1993**.

(130) Billmeyer, F. W. Textbook of Polymer Science, Singapore, John Wiley & Sons, Inc. **1984**.

(131) Chuenjitkuntaworn, B.; Supaphol, P.; Pavasant, P. & Damrongsri, D. Electrospun poly (L-lactic acid)/hydroxyapatite composite fibrous scaffolds for bone tissue engineering. Polymer International **2010**, 59, 227–235.

(132) Riley W.F.; Sturges, L. D.; Morris, D. H. "Mechanics of Materials, 5th eds., John Wiley & Sons Inc. **1999**, 350–365.

(133) Geng, X.; Kwon, O.; Jang, J. "Electrospinning of chiosan dissolved in concentrated acetic acid solution", Biomaterials **2005**, 26, 5427–5432.

(134) Kopperud, HM.; Hansen, FK. and Nystrom, B. Effect of surfactant and temperature on the rheological properties of aqueous solutions of unmodified and hydrophobically modified Poly (acrylamide). Macromolecular Chemistry Physics **1998**, 199, 2385–2394.

(135) Caturla, F.; Sabio, M. M., and Reinoso, F. R., Carbon, **1991**, 29, 999.

(136) Addoun, A.; Dentzer, J., and Ehrburger, P., Carbon, **2002**, 40, 1140.

(137) Sabio, M.M.; Gonzalez, M. T.; Reinoso F. R., and Escribano, A. S., Carbon, **1996**,34, 505.

(138) Endo, M.; Kim, Y. J.; Takeda, T.; Maeda, T.; Hayashi, T.; Koshiba, Hara, K., H., and Dresselhaus, M. S., Journal of the Electrochemical Society **2001**, 148, A1135.

(139) Alonso, A. ; Ruiz, V. ; Blanco, C. ; Santamaría, R. ; Granda, M. ; Menéndez, R., and de Jager, S.G. E., Carbon, **2006**, 44, 441.

(140) Khan, MS. Aggregate formation in poly (ethylene oxide) solutions. J ApplPolymSci. **2006**, 102, 2578–2583.

(141) Zhang, Y.; Xu, X., Xu, J. and Zhang, L. Dynamic viscoelastic behavior of triple helical Lentinan in water: effects of concentration and molecular weight. Polymer **2007**, 48, 6681–6690.

(142) De Gennes, PG.Scaling concepts in polymer physics.Cornell University Press, Ithaca**1979**.

(143) Aubry, T.; Bossard, F.and Moan, M.Rheological study of compositional heterogeneity in an associative commercial polymer solution. Polymer**2002**, 43, 3375–3380.

(144) Metzner, A.B. Flows of polymeric solutions and emulsions through porous mediacurrent status.In:D.O.Shah, R.S.Schcchter, cds, Improved Oil Recovery by Surfactant and polymer flooding .Academic Press, New York, **1977**, 439– 451.

(145) Lee, K. H.; Kim, H. Y.; Khil, M. S.; Ra,Y. M.; Lee, D. R., Polymer **2003**, 44, 1287–1294.

(146) Kroschwitz, J. I., Polymers: fibers and textiles: a compendium, Wiley – Interscience Publication, New York, Wiley, **1990.**

(147) Cross, J., ‘‘Electrostatics: Principles, Problems, and Applications’’, AdamHilger, Bristol **1987**.

(148) Fong, H.; Liu, W.; Wang, C. and Vaia RA. Generation of electrospun fibers of nylon 6 and nylon 6-montmorillonite nanocomposite. Polymer **2002**, 43, 775–780.

(149) Shin, Y.; Hohman, M.; Brenner, M.; Rutledge, G. “Electrospinning: A whipping fluid jet generates submicron polymer fibers”, Appl. Phys. Lett.**2001**, 78, 1149–1151.

(150) Hohman, M.; Shin, Y.; Rutledge, G.; Brenner, M. “Electrospinning and electrically forced jets. II. Applications”, Phys. Fluids **2001**, 13, 2221–2236.

(151) Zong, X.; Kim, K.; Fang, D.; Ran, S.; Hsiao, B. S.; Chu, B. “Structure and process relationship of electrospum bioabsorbable nanofiber membranes”, Polymer **2002**, 43,4403–4412.

(152) Reid, R. C, Prausnitz, J. M. and Poling, B. E. The Properties of Gases and Liquids, McGraw-Hill Book Company, Singapore, Fourth Edition. 1998.

(153) Theron, SA.; Zussman, E.; Yarin, AL. Experimental investigation of the governing Parameters in the electrospinning of polymer solutions. Polymer **2004**; 45:2017–2030.

(154) Trouton FT On the coefficient of viscous and its relation to that of viscosity. Proc R SocLond, **1906, A** 77(Iss 519):426– 440.

(155) James, DF; Walters, K A. critical appraisal of available methods for the measurement of extensional properties of mobile systems. Techniques in Rheological Measurements. Elsevier, London, **1993**, 33–53.

(156) Solomon, MJ.; Muller, SJ. The transient extensional behavior of polystyrene-based Boger fluids of varying solvent quality and molecular weight. J Rheol. **1996**, 40(5), 837–856.

(157) Stelter, M.; Brenn, G.; Yarin, AL., Singh RP, Durst F Validation and application of a novel elongational device for polymer solutions. J Rheol. **2000**, 44, 595–616.

(158) Matta, J.; Tytus, RP. Liquid stretching using a falling cylinder.Non-Newtonian Fluid Mech. **1990**, 35, 215–229.

(159) Tiwari, MK.; Bazilevsky, AV.;Yarin, AL.; Megaridis,CM. Elongational and shear Rheology of carbon nanotube suspensions. RheolActa. **2009**, 48, 597– 609.

(160) Niedzwiedz, K.; Arnolds, O.; Willenbacher, N.; Brummer,R. How to characterize yield stress fluids with Capillary Breakup Extensional Rheometry (CaBER) ApplRheol.**2009**, 19:41969–1–41969–10.

(161) Kheirandish, S.;Guybaidullin, I. et al .Shear and elongationalflow behavior of acrylic thickener solutions, Part II: effect of gel content. RheolActa.**2009**, 48, 397–407.

(162) Rothstein, JP. Strong flows of viscoelastic wormlike micelle solutions. In: Binding DM, Walters K. (Eds) Rheology review. The British Society of Rheology, Aberystwyth **2009,** 1–42.

(163) Rodd, LE. Scott, JJ.et al .Capillary break-up rheometry of low-viscosity elastic fluids. ApplRheol.**2005**, 15, 12–27.

(164) Bazilevskii, AV.; Entov, VM.et al .Failure of polymer solution filaments. PolymSci. A, **1997**, 39, 316–324.

(165) Yesilata, B.; Clasen, C.; McKinley,GH. Nonlinear shear and extensional flow dynamics of wormlike surfactant solutions. J Non-Newton Fluid Mech. **2006**, 133, 73–90.

(166) Goldin, M.;Yerushalmi, J.; Pfeffer, R.; Shinnar, R. Breakup of laminar capillary jet of a viscoelastic fluid. J Fluid Mech. **1969**, 38, 689–711.

(167) Sattler, R.; Wagner, C.; Eggers,J.Blistering pattern and formation of nanofibers in capillary thinning of polymer solutions. Phys Rev Lett. **2008**, 100, 164502.

(168) Kheirandish, S.; Gubaydullin, I.; Willenbacher, N.Shear and elongational flow behaviour of acrylic thickener solutions, Part I: effect of intermolecular aggregation. RheolActa. **2008**, 49, 397–407.

(169) Lavielle, N.; Hébraud, A. ; Schlatter, G.; Thöny-Meyer, L.; Rossi, R. M.; Popa, A. M.Simultaneous electrospinning and electrospraying: A straightforward approach for fabricating hierarchically structured composite membranes, ACS Appl. Mater. Interfaces **2013**, 5, 10090-10097.

(170) Szentivanyi, A.; Chakradeo, T.; Zernetsch, H.; Glasmacher, B., Electrospun cellular microenvironments: Understanding controlled release and scaffold structure. Adv Drug Deliver Rev **2011**, 63 (4-5), 209 –220.

(171) Bonani, W.; Motta, A.; Migliaresi, C.; Tan, W., Biomolecule Gradient in Micropatterned Nanofibrous Scaffold for Spatiotemporal Release. Langmuir **2012**, 28 (38), 13675–13687.

(172) Katta, P.; Alessandro, M.; Ramsier, R. D.; Chase, G. G., Continuous electrospinning of aligned polymer nanofibers onto a wire drum collector. Nano Lett. **2004**, 4 (11), 2215–2218.

(173) Li, D.; Ouyang, G.; McCann, J. T.; Xia, Y. N., Collecting electrospun nanofibers with patterned electrodes. Nano Lett. **2005**, 5 (5), 913–916.

(174) Lavielle, N.; Hébraud, A.; Mendoza-Palomares, C.; Ferrand, A.; Benkirane-Jessel, N.; Schlatter, G., Structuring and Molding of Electrospun Nanofibers: Effect of Electrical and Topographical Local Properties of Micro-Patterned Collectors. Macromol Mater Eng. **2012**, 297 (10), 958–968.

(175) Zhang, D. M.; Chang, J., Electrospinning of Three-Dimensional Nanofibrous Tubes with Controllable Architectures. Nano Lett. **2008**, 8 (10), 3283–3287.

(176) Ahirwal, D.; Hebraud, A.; Kadar, R.; Wilhelm, M.; Schlatter, G., From self-assembly of electrospun nanofibers to 3D cm thick hierarchical foams. Soft Matter **2013**, 9 (11), 3164–3172.

(177) Huaqiong Li, Y. S. W.; Feng Wen, Kee Woei Ng, Gary Ka Lai Ng, Subbu S. Venkatraman, Freddy Yin Chiang Boey, Lay Poh Tan, Human Mesenchymal Stem-Cell Behaviour On Direct Laser Micropatterned Electrospun Scaffolds with Hierarchical Structures. Macromol Biosci. **2013**, 13, 299–310.

(178) Chen, J. T.; Chen, W. L.; Fan, P. W., Hierarchical Structures by Wetting Porous Templates with Electrospun Polymer Fibers. Acs Macro Lett. **2012**, 1 (1), 41– 46.

(179) Sundararaghavan, H. G.; Metter, R. B.; Burdick, J. A., Electrospun Fibrous Scaffolds with Multiscale and Photopatterned Porosity. Macromol Biosci. **2010**, 10 (3), 265 – 270.

(180) Wei, X.; Xia, Z., Wong, SC., Baji, A. Modelling of mechanical properties of electrospun nanofibre network. Int J Exp Comp Biomech **2009**, 1, 45 – 57.

(181) Wong, SC.; Baji, A.; Leng, SW. Effect of fiber diameter on tensile properties of electrospun poly(ε-caprolactone). Polymer **2008**, 21, 4713–22.

(182) Lu, JW.; Zhang, ZP.; Ren, XZ.; Chen, YZ.; Yu, J., Guo, ZX. High-elongation fiber mats by electrospinning of polyoxymethylene. Macromolecules **2008**, 41, 3762 – 4.
(183) N. Khenoussi, Contribution to the study and characterization of nanofibers obtained by electro-spinning: Application to medical and composite domains, **Thesis 2012**, 142 – 146.

Abstract

Electrospinning is a widely used technique for the development of nonwoven nanofibrous membranes. The electrospun membranes have a high porosity and a high surface to volume ratio. Those material has a potential interest in many applications such as sensors, tissue engineering or drug delivery. Current research aims to have fibrous membranes with a controlled architecture using various types of collectors. The research study of this thesis focused on making non-woven fibrous structures in uncontrolled architecture as well as non-woven with controlled architecture by using the electrospinning process. These fibrous structures are obtained from polyoxyethylene PEO solutions with different molecular weight. The deposit of fibers is made on two types of collectors: a) Aluminum foil, b) micro-structured collector (dimension 3 × 3 cm). The rheological properties of the polymer solutions under elongational and shear flows were characterized in relation to their electospinnability. Concurrently, the morphology of both fibers and fibrous networks have been analyzed using scanning electron microscopy (SEM). A comparative study, of the morphological and mechanical (tensile test) properties, of both fibrous structures has been performed. This study showed that it is possible to have a distribution of fiber forming a very uniform primitive cell in a network of (dimension 3 × 3 cm). This structured network has a strain at the break more important than that for the random fibrous network obtained conventionally with an Aluminum foil.

Résume

L'électrospinning est une technique largement utilisée pour la fabrication de membranes nanofibreuses non tissées. Les membranes electrospinnées ont une forte porosité et un rapport surface / volume élevé. Ces matériaux ont un intérêt potentiel pour de nombreuses applications telles que les capteurs, l'ingénierie des tissus ou la diffusion de principes actifs pour les médicaments. La recherche actuelle vise à avoir des membranes fibreuses avec une architecture contrôlée utilisant différents types de collecteurs. L'étude menée dans cette thèse a porté sur la fabrication de structures fibreuses non tissées aléatoire et structurée en utilisant le procédé d'électrospinning. Ces structures fibreuses sont obtenues à partir de solutions de polyoxyéthylène PEO à différentes masses moléculaires. Le dépôt de fibres est réalisé sur deux types de collecteurs: a) Feuille d'aluminium, b) Collecteur microstructuré (dimension 3 × 3 cm). Les propriétés rhéologiques des solutions de polymère sous écoulement élongationnel et sous cisaillement ont été caractérisées par rapport à leur électosinabilité. Parallèlement, la morphologie des fibres et des réseaux fibreux a été analysée à l'aide d'une microscopie électronique à balayage (SEM). Une étude comparative, des propriétés morphologiques et mécaniques (test de traction), des deux structures fibreuses a été réalisée. Cette étude a montré qu'il est possible d'avoir une distribution de fibres formant une cellule primitive très uniforme dans un réseau de (dimension 3 × 3 cm). Ce réseau structuré a une contrainte à la rupture plus importante que celle du réseau fibreux aléatoire obtenu conventionnellement avec une feuille d'aluminium.